ERDA/JPL-1012-77/1

LSSA
LOW-COST SILICON SOLAR ARRAY
PROJECT

Project QUARTERLY REPORT-2

FOR THE PERIOD JULY 1976 – SEPTEMBER 1976

5101-10

DISCLAIMER

This work was performed by the Jet Propulsion Laboratory, California Institute of Technology, under National Aeronautics and Space Administration Contract NAS7-100, for the U. S. Energy Research and Development Administration (ERDA), Division of Solar Energy.

The Low-Cost Silicon Solar Array Project is funded by ERDA and forms part of the ERDA Photovoltaic Conversion Program to initiate a major effort toward the development of low-cost solar arrays.

LSSA
LOW-COST SILICON SOLAR ARRAY PROJECT

Project QUARTERLY REPORT-2

FOR THE PERIOD JULY 1976 – SEPTEMBER 1976

5101-10

THIS PAGE

WAS INTENTIONALLY

LEFT BLANK

CONTENTS

CONTENTS (contd)

CONTENTS (contd)

CONTENTS (contd)

Figures

CONTENTS (contd)

CONTENTS (contd)

CONTENTS (contd)

CONTENTS (contd)

CONTENTS (contd)

LIST OF ABBREVIATIONS

General

AM0	air mass zero
AM1	air mass one
CAST	capillary action shaping technique
CVD	chemical vapor deposition
DPESA	Development, Procurement, and Evaluation of Solar Arrays
EFG	edge-defined film-fed growth
EPDM	ethylene propylene diene monomer
ERDA	Energy Research and Development Administration
IST	Inverted Stepanov Technique
JPL	Jet Propulsion Laboratory
LASS	Large Area Silicon Sheet Task
LeRC	Lewis Research Center
LSSA	Low-Cost Silicon Solar Array Project
NASA	National Aeronautics and Space Administration
NSF	National Space Foundation
PA&I	Project Analysis and Integration Task
PFR	Problem/failure report
PIM	Project Integration Meeting
RFP	Request for Proposal
RTR	ribbon-to-ribbon
SAMICS	Solar Array Manufacturing Industry Costing Standard
SAMIS	solar-array manufacturing industry simulation
SSMS	spark-source mass spectroscopy
USES	Utility-Owned Solar Electric Systems

Chemical Symbols

Al	aluminum	Mn	manganese
Ar	argon	N	nitrogen
B	boron	Na	sodium
C	carbon	Ni	nickel
Cl	chlorine	O	oxygen
Cu	copper	P	phosphorus
Cr	chromium	Si	silicon
F	fluorine	Sn	tin
Fe	iron	Ti	titanium
H	hydrogen	V	vanadium
He	helium	Zn	zinc
I	iodine	Zr	zirconium
Mg	magnesium		

PART I

SUMMARY

The potential for future widespread use of photovoltaic systems for the generation of electric power was the motivation for the establishment, in January 1975, of the Photovoltaic Conversion Program by ERDA's Division of Solar Energy. The Program's activities are planned to develop and to promote the use of photovoltaic systems to such an extent that the private sector will produce and utilize cost-competitive photovoltaic systems. As part of the ERDA Program, the Low-Cost Silicon Solar Array Project (LSSA) was established in January 1975.

The Project objective is:

- To develop the national capability to produce low-cost, long-life photovoltaic arrays at a rate greater than 500 megawatts per year and a price of less than $500* per kilowatt peak by 1986. The array performance objectives include an efficiency greater than 10% and an operating lifetime in excess of 20 years.

The approach is to reduce the cost of solar cell arrays by improving solar array manufacturing technology and by increasing solar array production capacity and quantity. Forty-three contracts have been awarded to date, to industrial firms and university and independent laboratories (Tables 1-1 and 1-2) for experimental work, process development and analysis, technology assessment, and the production of solar-array modules. Approximately 42 kW of state-of-the-art modules have been delivered; contracts have been issued and design development has begun for 130 kW of moderately advanced modules.

Efforts of the LSSA Project are organized into an Analysis and Integration Task, four Technology Development Tasks — covering the areas of Silicon Material, Large Area Silicon Sheet, Encapsulation, and Automated Array Assembly — and a Large Scale Procurement Task, an Engineering Task, and an Operations Task.

*In 1975 dollars.

Table 1-1. Technology development contractors

	Contractor		Technology Area
TASK 1. SILICON MATERIAL (11 contracts)			
	Semiconductor-Grade Silicon Production Processes		
1.	Battelle Memorial Institute	Columbus OH	Si from $SiCl_4$
2.	Union Carbide	Sistersville WV	Si from SiH_4
3.	Motorola	Phoeniz AZ	Si using SiF_4 transfer
	Solar-Cell-Grade Specifications		
4.	Westinghouse Electric	Pittsburgh PA	Investigation of effects of impurities on solar cell performance
5.	Monsanto Research	St. Louis MO	Investigation of effects of impurities on solar cell performance
	Solar-Cell-Grade Silicon Production Processes		
6.	Dow Corning	Hemlock MI	Si from pure source materials using arc furnace processing
7.	Stanford Research Institute	Menlo Park CA	Si by duplex vapor-electrochemical conversion of SiF_4
8.	Texas Instruments	Dallas TX	Si from C reduction of SiO_2 using plasma processing
9.	Westinghouse Electric	Pittsburgh PA	Si by plasma-arc-heater reduction of $SiCl_4$ with H_2 and alkali metals as reducing agents
10.	AeroChem Research	Princeton NJ	Si by use of a nonequilibrium plasma jet
	Commercial Potential of Processes		
11.	Lamar University	Beaumont TX	Evaluate relative commercial potentials of Si production processes developed under Task 1.
TASK 2. LARGE AREA SILICON SHEET (11 contracts)			
	Ribbon Growth Processes		
1.	Mobil-Tyco	Waltham MA	Edge-defined, film-fed growth
2.	IBM	Hopewell Junction NY	Edge-defined, film-fed growth
3.	RCA	Princeton NJ	Inverted Stepanov growth
4.	University of S. Carolina	Columbia SC	Web-dendritic growth
5.	Motorola	Phoenix AZ	Laser zone ribbon growth
	Sheet Growth Processes		
6.	Honeywell	Bloomington MN	Dip-coating of low-cost substrates
7.	Rockwell International	Anaheim CA	Chemical vapor deposition on low-cost substrates
8.	General Electric	Schenectady NY	Chemical vapor deposition on floating silicon substrate
9.	University of Pennsylvania	Pittsburgh PA	Hot-forming of silicon
	Ingot Growth		
10.	Crystal Systems	Salem MA	Heat-exchanger ingot casting*
	Ingot Cutting		
	Crystal Systems	Salem MA	Multiple-wire sawing*
11.	Varian	Lexington MA	Breadknife sawing

*Crystal systems contract provides for both ingot casting and multiple-wire sawing.

Table 1-1. (contd)

Contractor		Technology Area
TASK 3. ENCAPSULATION (4 contracts)		
1. Battelle Memorial Institute	Columbus OH	Encapsulant experience and definition of environment; encapsulant test methods and capabilities
2. Rockwell International	Anaheim CA	Accelerated/abbreviated testing
3. Simulation Physics	Burlington MA	Bonded integral glass covers
4. DeBell and Richardson	Enfield CT	Polymeric properties and aging studies
TASK 4. AUTOMATED ASSEMBLY OF ARRAYS (5 contracts)		
1. Motorola	Phoenix AZ	Manufacturing processes assessment
2. RCA	Princeton NJ	Manufacturing processes assessment
3. Texas Instruments	Dallas TX	Manufacturing processes assessment
4. Simulation Physics	Burlington MA	Electron-beam solar cell fabrication
5. Texas Instruments	Dallas TX	Czochralski growth and wafering improvements

Table 1-2. Large-scale procurement contractors (8 contracts)

46-Kilowatt Solar Array Procurement		Kilowatts
Sensor Technology	Chatsworth CA	8
Solar Power	Wakefield MA	15
Solarex	Rockville MD	10
Spectrolab	Sylmar CA	10
130-Kilowatt Solar Array Procurement		
Sensor Technology	Chatsworth CA	40
Solar Power	Wakefield MA	15
Solarex	Rockville MD	30
Spectrolab	Sylmar CA	40

A. PROJECT ANALYSIS AND INTEGRATION

The Project Analysis and Integration Task supports Project planning, integration, and decision-making through a planning and integration function, a technology cost-analysis function, and economics/industrialization analysis, using analytical tools developed for these purposes.

During the quarter, the Task provided planning and support in connection with the third Project Integration Meeting held in July, and performed goals-analysis studies for the Photovoltaic Program Planning Group, making presentations to the July and August Group meetings.

Development of the Solar Array Manufacturing Industry Cost Standards procedure continued during the quarter, with development of preliminary design and planning of initial programming and tests. This procedure is intended to provide the basis for uniform cost analysis of different processes and process chains by contractors. The SAMIS industry simulation program, from which the Standards effort has derived, continued its development, as did the Design Evaluation Model. A preliminary installation, operations, and maintenance model was developed, and cost goal allocations to the Technology Development Tasks were reviewed.

B. SILICON MATERIAL TASK

The objectives of the Silicon Material Task are (1) to develop a process for producing silicon suitable for solar cells at a market price of less than $10 per kg and (2) to establish an information base relating the effects of impurities and processing steps to the properties of silicon and to the performance of solar cells. This task has three principal subtasks: further development of cost-effective processes for semiconductor-grade silicon, the establishment of an information base for the effects of impurities and processing steps on material and solar-cell properties, and the development of processes for solar-cell-grade silicon.

Semiconductor-grade silicon processes include the zinc reduction of $SiCl_4$, being examined under contract by Battelle Memorial Institute; the redistribution

of chlorinated silanes to produce SiH_4, being developed by Union Carbide; and silicon refinement through SiF_4/SiF_2 transport reactions, being studied under contract by Motorola. During the quarter, the Battelle and Union Carbide efforts reached the stage of miniplant construction and evaluation. The Battelle plant was operated and evaluated over about a dozen runs, of which five yielded useful production data; the production goal is about 200 gm/hr. The Union Carbide miniplant was in construction; its yield is expected to be 10 pounds of silane per day. The Motorola effort during the quarter was concerned with determining the factors affecting transport rate and product purity and with studying elemental-analysis methodology.

The study of the effects of impurities and processing continued to be carried out under contract by Westinghouse and Monsanto, while the Project continued preparations to add other contractors to this research effort. The Westinghouse effort considered both slow (Czochralski ingot) and fast (dendritic-web) silicon crystal-growth processes during the quarter, and found some distinct impurity effects in web growth. The Monsanto experimental program, including ingot preparation, material characterization and metallographic testing, lifetime measurements, and fabrication and measurement of solar cells, was completed.

Development of solar-cell-grade silicon processes depends on the completion of chemistry and chemical engineering studies, the building of an experimental data base for process modeling, and appropriate economic and process analyses. Contract efforts to study the submerged-arc (AeroChem), and an arc-heater plasma process (Westinghouse) were begun in this quarter. Processes for the carbon reduction of SiO_2 using an induction plasma (Texas Instruments) and the use of Na_2SiF_6 in a two-step, sodium-reduction, SiF_4/SiF_2 transport process (Stanford Research Institute) were under continued study during the period. Considerable data on the difficulties of the carbon reduction process have been gathered, leading to modification of the plan. The sodium reduction process investigation developed an apparatus for the first step and ran temperature and pressure curves.

The Lamar University economic analysis effort concentrated on the Battelle $Zn/SiCl_4$ process during this quarter, producing an estimate of $10 million for a 1000 metric ton/year plant, assuming 72% conversion efficiency and recovery of the zinc.

C. LARGE AREA SILICON SHEET TASK

Research and development on ribbon, sheet and ingot growth plus ingot cutting has shown various degrees of progress during the past quarter. Basic aspects of the individual technologies are still being studied (e.g., crystal growth conditions such as pull rates, etc.). However, these developmental investigations are in some instances beginning to substantiate economic models upon which cost (price) predictions are being made. Such predictions must still be "hedged" because of the general lack of data regarding the quality of solar cells prepared from the forms of crystalline silicon being developed. Such data are forthcoming in a highly disparate fashion owning to the varied states of development of the individual processes. Significant advances in the "economic predictability" and "solar cell qualification" of the processes under investigation are expected during the next quarter's activities.

Ribbon growth has undergone an evolution in both width and pull rate. Ribbon widths have advanced from 25 to 38 mm for CAST (capillary action shaping technique) and 46 mm for EFG (edge-defined film-fed growth). The pull rate for 13 mm wide, stress-free RTR (ribbon-to-ribbon) ribbons has increased roughly ten-fold, to 25 mm/min through the use of auxiliary heating. Stress-free EFG ribbon growth has been demonstrated at a 50 mm/min pull speed using an active after-cooling head. For the IST (inverted Stepanov technique) process, thermal control and silicon feed problems have prevented stable ribbon growth from a fused silica die. The pressure differential applied to the molten silicon is being examined to rectify the feed problem. Thermal analyses have shown functional relationships between critical growth velocity and ambient temperature, die temperature and ribbon geometry (e.g., thickness). Attempts at web-dendrite ribbon growth have been largely unsuccessful because of thermal control problems. Thermal analyses have been made for the crucible (melt), meniscus and ribbon regions in order to predict growth rates. Electrical and structural characterization of ribbon (EFG, CAST, RTR) has generally shown that not all defect boundaries affect local resistivity, and that linear boundaries which show no resistivity effects may act as effective recombination sites.

Sheet growth on low-cost substrates by dip-coating and CVD (chemical vapor deposition) differ substantially in their ability to achieve large grains.

Whereas dip-coating can provide 0.5 by 10 mm grains with great regularity on mullite substrates, CVD on either ceramic or glass substrates is limited to the substrate grain size (polycrystalline alumina) or $\gtrsim$10 μm (glass). The use of two-step CVD growth has not yet been successful in demonstrating grain size enhancement compared to a one-step deposition. Photodiodes fabricated on dip-coated layers of 25-30 μm thickness have shown 16 ma/cm^2 short-circuit current densities and 0.405 volt open-circuit voltages for 100 mW/cm^2 (effective) AM1 illumination. The role of substrate impurities in the limitation of photocurrent generation is now being investigated. Work on the Si/Sn floating substrate process has shown that, although surface solidification can be sustained, surface contamination has all but completely negated the seeded growth of single crystalline material. Even though the use of H_2 instead of N_2 as a purging/transport gas has shown significant improvement in reducing surface contamination, sustained single-crystal surface growth appears to be a formidable problem. Hot-forming studies of polycrystalline silicon are continuing to give new data on the deformation and recrystallization behavior of silicon.

In the heat-exchanger-method ingot growth studies, increasing the seed (heat-exchanger) temperature and decreasing the melt (crucible) superheat has led to good nucleation and growth of ingots. Although impurity contamination is evident at the seed/ingot interface, crystallinity can be maintained, and ingot growth across the entire crucible diameter has been obtained. Ingot cracking due to tensile stress from the crucible/silicon bond is a problem which must be solved.

Multiple-blade slurry sawing with up to 225 grams/blade force has yielded "controlled" cutting (no wandering) with 0.02 cm thick blades. Severe blade distortion and wandering has been observed with 0.01 cm thick blades, even with only 30 grams/blade force. Investigations involving variations in slurry composition and application are being made to improve the cutting efficiency. Surface damage due to cutting is also being investigated. Multiple-wire cutting systems are potentially advantageous over multiple-blade systems when fixed abrasive is used. Multiple-wire cutting rates of 0.0100 cm/min have been achieved using 115 grams/wire force with copper-plated wires impregnated with

45 μm diameter diamond fines. Higher cutting forces have been shown to cause diamond pullout and wire wear. Diamond density, uniformity and impregnation (to minimize pull-out) are being investigated.

In-house activities during the last quarter included (1) electrical and structural characterization of ribbon, sheet, and wafers cut from ingots, (2) ingot (Czochralski) growth-defect studies, (3) silicon sessile drop experiments on refractory materials, and (4) economic analyses of crystal growth and ingot cutting.

D. ENCAPSULATION TASK

Battelle has completed work on Studies 1 and 2 (respectively the identification of encapsulant materials from worldwide experience, and the definition of environmental conditions). Drafts of the final reports have been approved for both studies. These reports are scheduled to be released in late October (Study 1) and late November (Study 2).

Rockwell International has designed a Universal Test Specimen and fabricated specimens. Outdoor exposure of test samples has been initiated. An accelerated-weathering chamber has been completed and the exposure of samples is to begin in the next quarter. DeBell and Richardson has started the exposure of samples to aging environments consisting of combinations of heat, humidity and ultraviolet light.

Simulation Physics has constructed a preliminary electrostatic bonder apparatus. Live 2 in. diameter silicon solar cells have been successfully attached to sheets of Corning 7740 and 7070 glass. Dr. W. Knauss of Caltech has started work to evaluate delamination using a fundamental fracture mechanics approach.

Work was begun in-house to develop a test module for the purpose of identifying various material relationships such as synergisms, compatibilities, and causes of "systems" failures. A program has also been initiated to investigate delamination in modules.

The work of all Encapsulation Task contractors is on schedule with exception of Battelle Study 3 (the evaluation of encapsulant materials properties and test methods), which is approximately 2 months behind schedule. This behind-schedule status is primarily due to the change in emphasis in materials testing philosophy described in the previous quarterly report. Efforts are currently being made to improve the behind-schedule status.

Phase IA and Phase II efforts are proceeding as planned.

E. AUTOMATED ASSEMBLY TASK

The objective of the Array Automated Assembly Task is to develop and demonstrate process and equipment technology for the mass production of low-cost solar arrays. The plan is to study and assess present and potential production processes and techniques that are adaptable to solar array production; design automated production equipment; and stimulate expansion of solar array production facilities. Three companies are assessing the current state-of-the-art technology to identify those areas of solar cell technology which require development to achieve low-cost high-volume production.

During this report period, Motorola has chosen a process sequence for initial fabrication of solar cells. The process includes texture etching, ion implantation, silicon nitride (antireflection coating), and plated contacts. Reliability considerations for solar cell modules dictate a moisture-resistant cell metallization and a redundant, parallel-oriented interconnection scheme. A protective coating for steel makes it competitive with stainless steel with respect to corrosion. A stress test to study moisture ingression into modules has been developed and is currently being investigated for effectiveness.

RCA's technology assessment phase has been completed. Based upon all analyses conducted by RCA, screen-printed silver contacts appear to be the most cost-effective. The specific process approach studied includes gas-diffusion junction formation technology, screen-printed silver contacts, spin-on anti-reflective coating, gap welding for interconnects, and a glass plate/conformal coating/metal foil moisture barrier panel.

The efforts of Texas Instruments were concentrated on demonstrating process elements that appear to offer the lowest-cost approaches, and on identifying the most effective approaches to higher cell efficiency. The techniques utilized for the implementation of these efforts were device modeling and device characterization.

Device modeling was used to assess the impact of changes in single parts of the cell model on the cell output. Modeling was achieved by using computer simulation of a "best fit" model for a 7.6 cm hexagonal cell. Results to date indicate that an improved solar cell design must strive to minimize series resistance in order to minimize power loss.

F. LARGE SCALE PROCUREMENT TASK

The objective of the Large Scale Procurement Task, in the development, procurement, and evaluation of solar arrays, is to stimulate industry to produce larger quantities of improved, less expensive silicon solar arrays. This involves the periodic purchase of increasing quantities of solar arrays at decreasing unit prices, using the latest state-of-the-art technology, for use in numerous and diverse ERDA tests and demonstrations.

Contracts to procure 46 kW of terrestrial state-of-the-art silicon solar cell modules were awarded to five contractors in early 1976. The objective of the procurement was to purchase production quantities of existing solar cell module designs for use in practical demonstration programs of photovoltaic solar arrays. During this quarter, four of the contractors completed delivery of modules on their contract; one was unable to manufacture modules at a reasonable production rate because of technical difficulties. The contractors produced modules with a total power capacity slightly in excess of 43 kW. An add-on of 15 kW was negotiated with one of the contractors, to provide spares and support additional system-test needs.

In a competitive procurement, contractors were selected (prior to this quarter) and placed under contract for a second phase of production, this time for a total of 130 kW. Preliminary design reviews were held with each of the

four contractors, Sensor Technology, Solar Power Corporation, Solarex, and Spectrolab. After the design requirements had been met, each contractor was instructed to start production of prototype modules.

G. ENGINEERING TASK

This task is concerned with coordinated and evolutionary design and testing requirements for near- and mid-term array module procurements as well as future designs.

During this quarter various evaluation test programs were completed, using state-of-the-art module hardware delivered under the Large-Scale Procurement Task, but directed toward generalized concepts of design. These include thermal evaluation and structural cyclic load testing. Evaluation testing of a low-cost electrical convector was also conducted.

In addition, the Engineering Task was involved in design reviews and other start-up activities associated with the second (130 kW) block procurement of array modules, and with initiation of the development of requirements for the third large-scale procurement block.

H. OPERATIONS TASK

This task is responsible for environmental qualification testing in connection with the block array module procurements, exploratory and field testing associated with longer-term test and performance definitions, performance and failure analyses, the standardization of performance measurement, and module control.

During this quarter, the Operations Task continued qualification testing of modules produced in the first block, initiated program of exploratory tests which will simulate a broad spectrum of environmental conditions (such as humidity/freezing, initiated during the quarter). Testing of design variations and of special modules also began. Test facility planning to accommodate the larger second procurement block was also conducted, and fixtures and equipment

were designed. The first prototype modules from the new procurement arrived for testing at the end of the period.

Design work for the JPL Pasadena, Table Mountain, and Goldstone Field Test sites was completed, and construction and installation of test stands and data-collection systems began. The design and development of a test data processing system were virtually completed.

The module problem/failure reporting system was implemented during the quarter. This system is derived from those employed by JPL flight projects, providing problem data to concerned Project elements, including vendors and user/application centers, maintaining records, and yielding summaries of various kinds. During this quarter, high-voltage-breakdown problems were reported and analyzed among others.

A cooperative effort with NASA Lewis Research Center to assess module-performance measuring procedures and experience resulted in joint statements on standards for the next procurement block and analysis of the previous measurement processes. Standard-cell characteristics, processes, and responsibilities were formulated, and regular coordination meetings on this issue were established.

PART II

PROJECT OVERVIEW

The period of July, August, and September 1976 was a Transition Quarter for the Federal Government's Fiscal Year, and it served as a key transition and assessment period for the LSSA Project. The first complete Fiscal Year of Project activity and the first year of the earliest technology development contract work had just concluded, and the first phases of most technical Task activities were drawing to a close. The singular emphasis upon initiating technology development was evolving into a broad focus which included economic and process analyses, module and array design, engineering, test, and operational coordination, and technology selection and development. Profound albeit preliminary, conclusions were beginning to emerge and to affect planning and decisions regarding the extension or redirection of existing efforts and the initiation of new ones. In brief, the exploratory stage of Project work was ending, and the integrated, advanced development, feasibility, and industrilization phase was beginning to take form.

Specific planning for the FY 77 effort, on the basis of preliminary technical conclusions from the Tasks and of strong interaction with the Program Office and other Projects in the solar photovoltaic area, was carried forward during this quarter. Evolutionary changes in the Project structure, reflecting planned broadening of the focus of attention, were implemented. Project Integration Meetings conducted during and just after the end of the quarter demonstrated the growing interaction and mutual understanding among the Tasks of the Project and between ERDA/JPL and industrial/university contractor participants, as well as revealing and reviewing technical progress.

Tentative technical conclusions reached during the quarter, and studied in the light of their effect on future plans, included the following:

- Silicon material was recognized as a major cost driver in the manufacturing of arrays; the cost of semiconductor-grade silicon remained high, as did the losses in its use in solar-cell production. Achievement of interim cost-reduction goals would require intensified near-term efforts in material cost reduction.

- Improvements in the technology of ingot crystal growth and processing which may provide interim cost reduction and the potential for further improvements in the long-term, were encouraging enough to suggest increased emphasis.
- Glass was perceived as an increasingly promising material for protecting solar cells in the terrestrial environment, and efforts to characterize its more applicable forms and the relevant cost relationships were increased.
- Solar-cell contacts and interconnects were recognized as a significant problem area, as to cost and reliability, and were slated for greater attention.
- The project high costs of material for installing arrays, on site, prompted the assignment of increased effort to improve array and cell efficiency, to reduce the area per unit power and therefore the installation material and installed cost of arrays in the field.

These conclusions were coupled with the recognition of significant progress made during recent months:

- Demonstration of state-of-the-technology module production at significantly increased production rate and reduced prices.
- Improved fundamental understanding of silicon refining processes, some offering near-term and others major long-term price-reduction potential.
- Increased understanding of the character and potential for improvement of a variety of crystal-growth and sheet-processing techniques, including ingot growth and slicing, several ribbon processes, and sheet-growth investigations.
- A new perspective on glass vs. polymers as encapsulant materials, and enhanced understanding of the characteristics of encapsulant systems.
- The identification of limiting technologies in array manufacturing and of some new options.
- Progress toward the establishment of uniform cost-collection and price-analysis methodologies for array production and utilization.

PART III

PROJECT ANALYSIS AND INTEGRATION TASK

The Project Analysis and Integration (PA&I) Task supports the planning, integration, and decision-making activities of the project. To provide this support, the PA&I Task is organized into three highly interrelated functional areas: planning and integration; array technology cost analysis; and economics and industrialization. Most of the PA&I activities are backed up by analytical tools developed for those activities.

A. PLANNING AND INTEGRATION

During the quarter, plans were generated and support was provided for the third Project Integration Meeting (PIM), July 27-29. A presentation at the PIM by PA&I summarized the current status of the developing uniform costing methodology.

A considerable amount of analysis relating to the 1986 industry production goal of 500 peak megawatts (MW_{pk}) per year was presented to Photovoltaic Program Planning Group meetings on July 14 15 and August 12-13.

Responses by the utility industry regarding the USES methodology ("The Cost of Energy from Utility-Owned Solar Electric Systems," J.W. Doane, et al., ERDA/JPL-1012-76/3) have started to come in. These responses generally agree that the methodology is consistent with utility practices. Several copies of the pocket calculator program for its use have been distributed.

In response to a request from the project manager, the task managers were asked to assess whether there have been any changes in the likelihood of achievement of the project goals. The results of this survey were published in an internal memorandum. The major concern expressed was that potential manufacturers would not perceive a large enough market, prior to achievement of the project price goal, to risk building enough facilities to achieve the project quantity goal.

A procedure was also developed by which the learning-curve concept could be applied to estimating the actual, potential, or possible impact of the LSSA Project on the nation's total cost of photovoltaic silicon solar power. Companion research on the character of the learning curve was also performed.

B. ARRAY TECHNOLOGY COST ANALYSES

1. Costing Standards

Development of Solar Array Manufacturing Industry Costing Standards (SAMICS), a uniform procedure for the preparation of manufacturing cost estimates, continued during the quarter. The preliminary design contains the following steps:

1) Each manufacturing process is described in terms of the characteristics of that process: its cycle time (or flow rate) and yields, equipment costs and lifetime, personnel and facilities requirements, and supplies and materials.
2) A standardized process model is used to determine the annual direct requirements (number of machines, personnel, floor space, supplies and materials, and so on) implied by a spectrum of industry production rates.
3) The indirect requirements (walls, parking lots, supervisors, guards, etc.) associated with a factory performing these processes are estimated by a standardized procedure, using standardized data, taking into account economies and diseconomies of scale.
4) Capital requirements will be estimated from the combined direct and indirect requirements, using a standardized type of construction and prices inflated to the year of manufacture.
5) Operating costs will be estimated by multiplying requirement quantities by standardized costs associated with those quantities and inflated to the year of manufacture.
6) Overhead costs will be estimated by applying a financial model of the firm, and will include taxes, insurance, replacement of capital, interest on debt, return on equity, and other factors. Markup (as

a fraction of direct costs) and profit (as a fraction of price) will be calculated. (The rate of return on equity will be a standardized input.)

7) The total cost of doing business is then divided by the production quantity and deflated back to base year dollars to obtain the price.

This methodology will be described at the Photovoltaics Specialists Conference during the next quarter, and published in the Proceedings of that conference. An explicit delineation of the SAMICS Process Description input is expected to be published in January 1977. An appropriate contractor is being sought to assist in development of the values of the standardized data.

2. Industry Simulation

The Solar Array Manufacturing Industry Simulation (SAMIS) activity, from which the costing standards have been developing, has also continued during the quarter. Industry Description 4 (an improved description of an industry based on Czochralski ingots) and Industry Description 7 (an industry based on a ribbon process) have been prepared and entered into the computer. The results of sensitivity studies, using the SAMIS II computer program, will be reported next quarter.

Design of the SAMIS III computer program, based on the SAMICS methodology described above, has been started.

3. Evaluation of Array Designs

Development of the Project Alternative Design Evaluation Model (PADEM) continued during the quarter. This model will permit examination of the effects of different design trade-offs on the desirability of the resultant systems.

The life cycle cost of the array subsystem is a vital component of the comparison, and a crucial component of the life cycle cost is the cost of installation, operations, and maintenance (IOM) of the arrays. The preliminary IOM model developed during the quarter can be summarized as follows:

1) Installation cost is the product of the amounts of installation manpower, materials, and so forth with the cost rates of those factors. Further development is required to relate the amounts of the factors to the characteristics of array designs.

2) Operations costs result from daily operations activities, and can be estimated in a straightforward manner after some "typical" operations plans have been formulated. An effort to develop such plans was initiated during the quarter.

3) Maintenance costs include both scheduled and unscheduled maintenance activities. Their estimation requires optimization of the scheduled maintenance period. The data requirements and the optimization procedures were identified during the quarter.

4. Cost Goal Allocation

The allocation of manufacturing price goals for each of the technology development tasks at 2-year intervals throughout the life of the project was reviewed. Project goals for 1980 and 1982 were changed from $\$5/W_{pk}$ and $\$3/W_{pk}$, respectively, to $\$4/W_{pk}$ and $\$2/W_{pk}$ to achieve consistency with interim ERDA goals. The corresponding revision to the task goals is expected during the next quarter.

C. ECONOMICS AND INDUSTRIALIZATION

Considerable attention was given during this quarter to a reconsideration of the project 1986 production quantity goal of 500 MW_{pk}/year. Other (non-LSSA) studies within the ERDA Photovoltaics Program indicate that there will be no significant market for photovoltaic systems until array prices near the project 1986 price goal of $\$0.50/W_{pk}$ have been attained. Even if this technology were available in 1981 or 1982, the very short time interval to 1986 would imply an extremely rapid development of the new technology. Earlier development of large-scale manufacturing capability would be viewed by potential manufacturers as highly risky, owing to the possibility that the LSSA Project would render the manufacturing equipment obsolete. Further, large investments could work against the achievement of the price goal, because of the resultant inertial resistance to change. In consequence, it is being suggested that the

production objective be reformulated along the lines of providing demonstration plants of a scale and character such that potential manufacturers will perceive little risk in building full scale production facilities to manufacture arrays that will sell at $\$0.50/W_{pk}$ or less.

To arrive at these conclusions, a number of studies were performed:

1) Linear and exponential growth rates implied by current ERDA Photovoltaic Program goals, and the sensitivities of goal-attainment to modifications in those growth rates, were calculated.
2) Empirical studies of the growth rates achieved by eight manufacturing industries and by six segments of the electric utility industry were performed for a variety of time periods.
3) Three studies examined the interrelationships of technological change and output growth of an industry undergoing extensive governmental encouragement from the point of view of economic theory. These studies resulted in approaches to the development of revised program goals and an identification of further studies that would improve the understanding of this complex area.

The critical requirement appears to be the development and demonstration of the technology required to produce photovoltaic arrays on a large scale at a price of $\$0.50/W_{pk}$ or less. The risk associated with scaling the results of a demonstration plant to a full scale operation is extremely important; operational use of the standardized costing methodology (SAMICS) is expected to reduce that risk to a minimum. In addition, the minimum size of the demonstration plant, and consequently the cost to the government of building that plant, will be reduced to the extent that the scaling relationships are better understood.

PART IV

TECHNOLOGY DEVELOPMENT TASKS

TASK 1. SILICON MATERIAL

The objective of the Silicon Material Task is to establish by 1986, an installed plant capability for producing silicon suitable for solar cells at a rate equivalent to 500 megawatts (peak) of solar arrays per year at a price of less than $10 per kilogram. The program formulated to achieve this objective is based on the conclusion that the price goal can not be reached if the process used is essentially the same as the present commercial process for producing semiconductor-grade silicon. Consequently, it is necessary that either a different process be developed for producing semiconductor-grade silicon or a less pure and less costly silicon material (i.e., a solar-cell-grade silicon) be shown to be utilizable.

A. TECHNICAL BACKGROUND

Solar cells are presently fabricated from semiconductor-grade silicon, which has a market price of about $65 per kilogram. A drastic reduction in price of material is necessary to meet the economic objectives of the LSSA Project. One means for meeting this requirement is to devise a process for producing a silicon material which is significantly less pure than semiconductor-grade silicon; the price goal for this material is less than $10 per kilogram. However, the allowance for the cost of silicon material in the overall economics of the solar arrays for LSSA is dependent on optimization trade-offs, which concomitantly treat the effects of the price of silicon material and the effects of material properties on the performance of solar cells. Accordingly, the program of the Silicon Material Task is structured to provide information for the optimization trade-offs concurrently with the development of high volume and low cost processes for producing different impurity-grades of silicon.

B. ORGANIZATION AND COORDINATION OF THE TASK 1 EFFORT

The Task 1 effort is organized into five phases. As Table 4-1 indicates, Phase I is divided into four parts. In Part I the technical feasibility and practicality of processes for producing semiconductor-grade selicon will be demonstrated. In Part II the effects of impurities and of various processing procedures on the properties of single-crystal silicon material and the performance characteristics of solar cells will be investigated. This body of information will serve as a guide in developing processes (in Part III) for the production of solar-cell-grade silicon. The process developments in Parts I and III will be accomplished through chemical reaction, chemical engineering, energy-use, and economic studies. In Part IV of Phase I, the relative commercial potentials of the various silicon-production processes developed under Parts I and III will be evaluated. Thus, at the end of Phase I a body of information will have been obtained for optimization trade-off studies and the most promising processes will have been selected.

Phase II will be initiated to obtain scale-up information. This will be derived from experiments and analyses involving mass and energy balances, process flows, kinetics, mass transfer, temperature and pressure effects, and operating controls. The basic approach will be to provide fundamental scientific and engineering information from which valid extrapolations usable for plant design can be made; applicable scale-up correlations will also be used. This body of scale-up information will then provide the necessary basis for the design, construction, and operation of a large-scale production plant.

Since the installation and operation of a commercial chemical process plant that incorporates a new process involves high risks, experimental plants will be used to obtain technical and economic evidence of large-scale production potential. In the experimental plant phase (i.e., Phase III) there will be opportunities to correct design errors; to determine energy consumption; to establish practical operating procedures and production conditions; and to more realistically evaluate the requirements for instrumentation, controls, and on-line analyses.

Table 4-1. Organization of the Task 1 effort

	Objective
Phase I	Demonstrate the technical feasibility and practicality of processes for producing silicon.
Part I	Establish the practicality of a process capable of high volume production of semiconductor-grade silicon at a markedly reduced cost.
Part II	Investigate the effects of impurities and of various processing procedures on the properties of single-crystal silicon material and the performance characteristics of solar cells.
Part III	Establish the practicality of a process capable of high volume production of solar-cell-grade silicon at a price of less than $10 per kilogram.
Part IV	Evaluate the relative commercial potentials of the silicon-production processes developed under Phase I.
Phase II	Obtain process scale-up information.
Phase III	Conduct experimental plant operations to obtain technical and economic evidence of large-scale production potential.
Phase IV	Design, install, and operate a full-scale commercial plant capable of meeting the production objective.

In the final phase of Task 1 (i.e., Phase IV), a full-scale commercial plant capable of meeting the production objective will be designed, installed, and operated. The experimental plant and the commercial plant will be operated concurrently so as to permit the use of the experimental plant for investigations of plant operations, i.e., for problem solving and for studies of process optimization.

Additional basic chemical and engineering investigations to respond to problem-solving needs of Task 1 will be conducted in supporting efforts. These supporting subtasks will be accomplished under contract and by an in-house JPL program.

C. TASK 1 CONTRACTS

Eleven contracts are in progress: three for Part I, two for Part II, five for Part III, and one for Part IV. These contracts were negotiated after careful evaluations of responses to a Request for Proposal (RFP) and of unsolicited proposals. The contracts are listed in Table 4-2. Additional contractors for subsequent phases will be selected from unsolicited proposals and from future RFPs.

D. TASK 1 TECHNICAL ACTIVITY

The objectives of Phase I of Task 1 are as follows:

- Part I — Establish the practicality of a process capable of the high volume production of semiconductor-grade silicon at a markedly reduced cost.
- Part II — Investigate the effects of impurities and process-steps on the properties of single-crystal silicon material and the performance characteristics of solar cells.
- Part III — Establish the practicality of a process capable of the high volume production of solar-cell-grade silicon at a price of less than $10 per kilogram.
- Part IV — Evaluate the relative commercial practicality of the silicon-production processes developed under Phase I of Task 1.

Table 4-2. Task 1 contractors

Contractor	Technology Area
SEMICONDUCTOR-GRADE PRODUCTION PROCESSES (Part I of Phase I)	
Battelle Memorial Institute, Columbus, Ohio	Si from $SiCl_4$ reduction by Zn
Union Carbide, Sistersville, W. Virginia	Si from SiH_4 derived by redistribution process
Motorola, Phoenix, Arizona	Si using SiF_4 reaction with metallurgical grade Si and SiF_2 transfer
SOLAR-CELL-GRADE SPECIFICATIONS (Part II of Phase I)	
Westinghouse Electric, Pittsburgh, Pennsylvania	Investigation of effects of impurities on solar cell performance
Monsanto Research, St. Louis, Missouri	Investigation of effects of impurities on solar cell performance
SOLAR-CELL-GRADE PRODUCTION PROCESSES (Part III of Phase I)	
Dow Corning, Hemlock, Michigan	Si from purer source materials using arc furnace processing
Stanford Research Institute Menlo Park, California	Si by Na reduction of SiF_4
Texas Instruments, Dallas, Texas	Si from C reduction of SiO_2 using plasma processing
Westinghouse Electric Pittsburgh, Pennsylvania	Si by plasma-arc-heater reduction of $SiCl_4$ with H_2 and alkali metals as reducing agents
AeroChem Research Laboratories, Princeton, New Jersey	Si by use of a non-equilibrium plasma jet
COMMERCIAL POTENTIAL OF PROCESSES (Part IV of Phase I)	
Lamar University, Beaumont, Texas	Evaluate relative commercial potentials of Si-production processes developed under Task 1

1. Processes for Producing Semiconductor-Grade Silicon

The approach for Part I incorporates theoretical studies involving thermodynamics, reaction chemistry, and chemical engineering; chemical reaction investigations consisting of the experimental determinations of reaction kinetics yields, and suitable process conditions; a chemical engineering effort for securing an experimental data base for preliminary process modeling; and energy-use and economic calculations for preliminary process models. In each case the contract requires a demonstration of technical feasibility and a projection of commercial practicality, involving the preliminary analysis of suitability for a scale-up study. The processes for the Phase II scale-up studies will be selected over a period of time, the decision point for each process-development being dependent upon the maturity of that process. The scale-up studies for the most mature processes will begin in early FY 1977.

a. Semiconductor-Grade Si Production by Zn Reduction of $SiCl_4$ - Battelle Memorial Institute

The objective of this contract is to develop the Zn reduction of $SiCl_4$ as a process for producing semiconductor-grade Si. The operation of a miniplant, designed to prepare Si at a rate of over 200 gm/hour in 4 to 6 hour runs, is being evaluated. The objective of the evaluation is to obtain operating data for the design of a large production plant, for iterations of economic analyses, and for the identification and correction of operating problems. Ten of the 22 runs were terminated by equipment failures; suitable data were obtained from the remaining 12 runs. On 5 of the runs that provided meaningful data, the time of operation was limited only by the amount of Zn available in the batch; the other 7 runs were terminated because of constrictions caused by the condensation of Si product in the exit section or by premature Si deposition in the inlet orifices of the reactor. These problems can be solved with proper design based upon continued experiments to define the proper condensation conditions for the free flow of Zn and the segregation of Zn and $ZnCl_2$.

Runs were made at a fluidized bed temperature of 1200°K to avoid the condensation problems which had occurred at 1123°K. Near-stoichiometric reactant compositions, together with a small amount of diluent gas, were used. The Si deposited on the bed averaged about 65% of that predicted from thermodynamic calculations. In addition, Si powder, amounting to from 10 to 20% of that deposited in the bed, was collected downstream of the bed; this powder may have been elutriated in part from the gas phase nucleation reaction in the bed. The Si production rates were as high as 188 gm/hour.

b. Production of SiH_4 by Redistribution of Chlorinated Silanes - Union Carbide Corporation

The preparation of SiH_4 by the disproportionation of chlorinated silanes in a bed of a tertiary amine·HCl resin is the basis of a section of a development program now under contract to Union Carbide. The deposition of Si from the SiH_4 will also be developed. Laboratory investigations are under way in these areas: the disproportionation of SiH_2Cl_2 to SiH_4, the disproportionation of $SiHCl_3$ to SiH_2Cl_2, the purification of SiH_4, the hydrogenation of $SiCl_4$ to $SiHCl_3$, the direct synthesis of SiH_2Cl_2, and the stability of $SiHCl_3$. Efforts under the miniplant phase have been concerned with construction of the unit, a study of SiH_4 storage, process design calculations, calibration of the on-line chromatograph, and initial segments of an economic analysis of the process for producing SiH_4.

A study of the effect of extended reaction times on the activity of the resin was undertaken to examine a decrease in SiH_4 production rate which had been observed to occur after a succession of runs. The data, which are rather limited, indicate that there were no appreciable decreases in rate or yield when the SiH_2Cl_2 feed rate was low, at 250 cm^3/min. At a feed rate of 500 cm^3/min, however, significant decreases in rate and yield occurred. Assuming the loss in activity to be due to a loss of HCl (the free amine is inactive in this reaction), it was shown that a substantial reactivation was obtained by treating the depleted resin with HCl. However, the original activity was not reinstituted, the loss being especially noted at high feed rates. A tentative conclusion is that a loss of lower molecular weight

amine·HCl has taken place by elution from the resin bed. The physical characteristics of the resin and the mechanism of the disproportionation reactions will be studied in an effort to optimize the conditions for operation while minimizing the loss of activity.

Comparisons of the rates of vapor and liquid phase disproportionations of $SiHCl_3$ to SiH_2Cl_2 and of the relative rates of disproportionation of $SiHCl_3$ and SiH_2Cl_2 were made. The vapor phase conversion of $SiHCl_3$ to SiH_2Cl_2 was found to be much faster than the liquid phase reaction, the ratio of residence times to reach the equilibrium concentration of 10% SiH_2Cl_2 being about 1:6. However, since the throughput in the liquid phase is much greater than for the vapor phase, the reaction is carried out most advantageously in the liquid phase. It was also shown in a series of experiments at 60°C and atmospheric pressure that the rate of disproportionation of $SiHCl_3$ is much slower than for SiH_2Cl_2; in a 1.8 second residence time, for example, 50% of the SiH_2Cl_2 had reacted, but only 5% of the $SiHCl_3$. These data will be useful in sizing the equipment for recycling.

The use of carbon as an adsorbent for the removal of the trace amounts of chlorosilanes which remain in the SiH_4 product after the purification steps of distillation, condensation in cold traps, and scrubbing is being studied. In the experiments, the mixture fed to the carbon contained chlorosilanes in larger proportion than is anticipated for the actual plant operation. The activated carbon removed the chlorosilanes to beyond the detection limit of 5 ppm. The adsorption capacity was calculated to be about 11% by weight. Attempts to regenerate the carbon showed that only one-half of the original capacity could be restored by heating at 350°C for 1 hour. It was also found that the carbon should be heated before use to desorb H_2O and perhaps other impurities. Efforts to achieve reversibility will continue so as to prevent a serious problem from arising if this purification process is used in large scale operations.

The assumption that the hydrogenation of $SiCl_4$ to $SiHCl_3$ over a Cu/Si mass in a fluidized bed reactor proceeds via a two-step reaction seemed to fit data obtained for the reaction. The temperature profile, which was measured in the reactor, can be explained as the result of a slightly endothermic

hydrogenation step ($3SiCl_4+3H_2 \xrightarrow{Cu} 3SiHCl_3+3HCl$) in the lower part of the bed followed by a fast exothermic reaction in the upper section of the bed ($3HCl+Si \xrightarrow{Cu} SiHCl_3+H_2$).

The construction of the miniplant is nearly completed; only the lines for the SiH_2Cl_2 feed, the SiH_4 product, and the safety vent remain to be installed. All of the instruments have been calibrated and aligned. Equipment design calculations have included determinations of the theoretical plate and reflux ratio requirements of the SiH_4/SiH_2Cl_2 still and of the expected efficiency of the absorber of SiH_3Cl and SiH_2Cl_2.

In the case of the still it was calculated that a unit with 12.6 stages operating at a 1.55 reflux ratio would achieve a separation of 90% recovery of SiH_2Cl_2 in the distillate and 95% recovery of $SiHCl_3$ in the distilland. A 44% recovery of SiH_4 at a purity of 67.6 mole % can be obtained at -5°C using a SiH_2Cl_2 condenser. At higher temperatures, increased recoveries with the penalty of less purity would occur. The distillation unit designed for the miniplant is 1 inch by 54 inches, is packed with steel gauze and is calculated to have about 22 theoretical stages.

A unit containing 2.4 mole % SiH_3Cl in $SiCl_4$ will be used to absorb the traces of SiH_3Cl and SiH_2Cl_2 remaining in the SiH_4 product. The goal is to obtain a SiH_4 purity greater than 99 mole %. Using assumptions of ideal vapor and liquid behaviors, it was calculated that the use of one mole of liquid $SiCl_4$ per 5 moles of SiH_4 raw product and 10 theoretical stages would result in a SiH_4 purity of 99.1 mole %. The absorber to be used in the miniplant is more than adequate to achieve this purity goal.

A material balance has been calculated as a step in the economic analysis. The assumptions for the recycle streams were as follows: 100% efficiency in the redistribution reactions, 2% loss of H_2 per pass in the hydrogenation unit, 90% Si reaction efficiency, and complete separation of $SiHCl_3$ from SiH_4 in the SiH_2Cl_2 reactor section. The resultant material balance is shown in Fig. 4-1. An energy balance using a computer modeling of the various stills is under way.

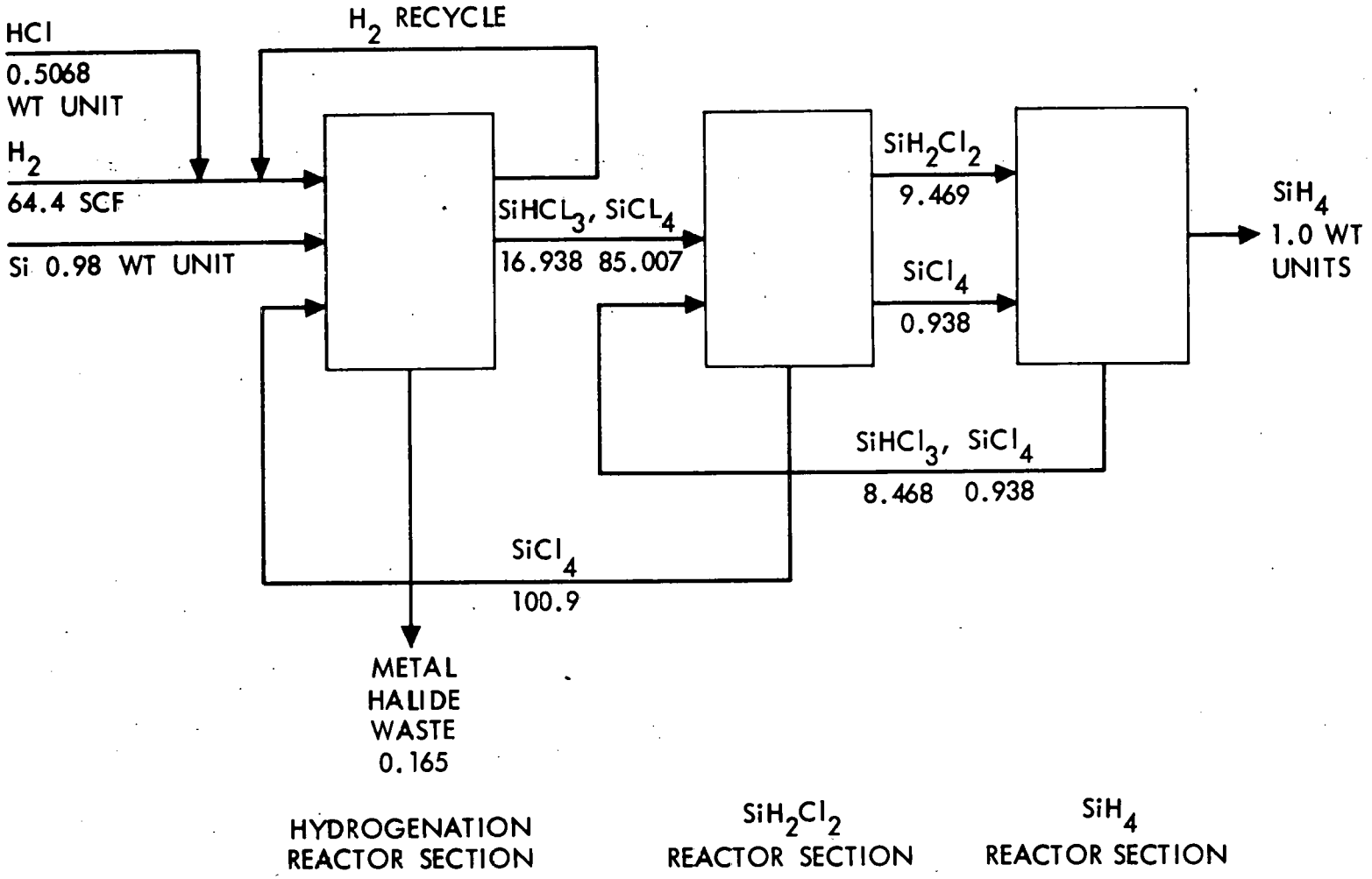

Fig. 4-1. Material flow chart for production of 1.0 weight unit of SiH_4

The objective of the operation of the miniplant is to demonstrate the economic and production potential of the redistribution reactor process for the preparation of SiH_4. The unit is to be capable of yielding 10 pounds of SiH_4 per day.

c. Semiconductor-Grade Si Production by SiF_4/SiF_2 Transport - Motorola Corporation

This contract is for the development of a process for converting metallurgical-grade Si into semiconductor-grade Si using SiF_4/SiF_2 transport reactions. The objectives during this quarter were to determine the factors affecting Si transport rate and product purity and to establish a reliable elemental-analysis method using the spark-source mass spectrometer.

The following results and conclusions were reported:

1) In the baffle area of the apparatus, particulates are removed from the gas stream, and major amounts of Al and other impurities are eliminated by prepolymerized SiF_2 forming at ambient temperatures.
2) A quartz liner in the high temperature zone is necessary to prevent reactions with the mullite tube and the concomitant addition of impurities to the stream.
3) The spark-source mass spectrometer data obtained so far are not reliable enough to allow determinations of the impurity concentrations in the product.
4) Values of residence times in the high temperature zone and of rates of cooling of the SiF_2 gas mixture were obtained for different flow rates.
5) Transport rates of 40 gm/hour for short runs have been obtained.
6) A cold trap at -78°C collects all of the SiF_2-polymer in one pass even at the highest flow rates used so far.
7) SiF_4 is incorporated in the SiF_2-polymer under conditions of increased flow rates without increased furnace temperature.

8) Although some of the physical properties of Si, SiF_2, and SiF_4 were calculated or obtained from the literature, there is a lack of data at the low temperatures of interest.

Efforts continue to determine the impurity concentrations in the product and to further characterize reaction conditions.

2. Determination of the Effects of Impurities and Process-Steps on Properties of Silicon and the Performance of Solar Cells

The Phase I approach for Part II involves setting up a matrix of impurities and concentrations; preparing crystals, using techniques for Czochralski, float zone, and dendritic-web crystals, which contain the baseline dopant B and selected concentrations of specific elements; performing a series of chemical, microstructural, and electrical tests; and analyzing the data for the purpose of correlating the impurities and concentrations with material properties and solar cell performance. The conclusions from the Phase I investigations will form a preliminary description upon which the more comprehensive, detailed plan for Phase II will be structured.

a. Effects of Impurities and Process-Steps on Silicon Properties and Solar Cell Performance - Westinghouse Electric Corporation

All of the Czochralski-grown ingots, which were doubly doped, as well as all doubly doped web samples, with exception of those containing Zn and Mg, have been prepared. The groups, which were multiply doped to determine possible synergistic effects, included Mn/Cu, Cr/Cu, Cr/Mn, Zr/Ti, Cr/Ni, Ni/Cr/Cu, Fe/Ti, Cr/Fe/Ti, Fe/V, Cu/Ni/Zr, Ti/V, and Cu/Ti in the Czochralski ingots, and Cr/Cu, Mn/Cu, Cr/Mn, Ni/Mn, Zr/Ti, and Cu/Ti in the web samples. All of the preparations contain B at 3.5×10^{15} atoms/cm^3 concentration. The segregation coefficients, calculated from data obtained in the course of the ingot preparations, differed from the literature values in some instances. The most extreme variations were for Mg, Ti, V, and Zr. The data for the effective coefficients are shown in Table 4-3. A general observation was that single crystal growth was difficult to secure when the melt concentrations were

Table 4-3. Characteristics of dopant impurities

Dopant	Form	Purity %	Melting Point (°C)	Temperature for 1 mm Vapor Pressure (°C)	Segregation Coefficient*
Aluminum**	Wire	99.99	659	1284	1.6×10^{-3} ($2.8 \times 10^{-3}/3 \times 10^{-2}$)
Chromium	Pellets	99.999	1900	1504	10^{-5} (0.95×10^{-5})
Copper	Zone refined ingot	99.9997	1083	1628	4×10^{-4} (4×10^{-4})
Iron	Sponge/ ingot	99.999/ 99.999	1535	1783 -	0.8×10^{-5} (--)
Magnesium	Ingot	99.99	651	605	$\sim 10^{-3}$ (1×10^{-5})
Manganese	Flake	99.99	1244	1251	10^{-5} (1.35×10^{-5})
Nickel	Sponge/ wire	99.999/ 99.97	1455	~1884	0.8×10^{-5} (3.2×10^{-5})
Titanium	Crystal	99.95	1668	~2500	10^{-5} (0.36×10^{-5})
Vanadium	Dendrite	99.9	2190	2550	10^{-5} (0.45×10^{-5})
Zinc	Rod	99.999	419	487	10^{-5} (--)
Zirconium	Foil	99.99	2127	2450	10^{-5} ($<0.45 \times 10^{-5}$)

*The segregation coefficients shown are best values obtained from a review of the literature on impurities in silicon. The quantity in parentheses represents calculated segregation coefficients based on this work.

**Two segregation coefficients are shown for aluminum. The first value is based on electrically active aluminum as determined by resistivity measurements; the second value is based on total aluminum content in the ingot as determined by mass spectrometer.

greater than about 1%; multiply doped ingots could be grown if the melt concentration was decreased to less than 0.5%. The presence of C and O did not seem to adversely affect crystal growth.

The spark-source mass spectrometer was used for the analyses of impurity concentrations. The performance characteristics of the instrument used are illustrated in Table 4-4. The analyses for Zr and Fe were difficult owing to the need for relatively low concentrations to prevent polycrystalline formation. The data for Al, Mg, and Zn are not adequate for similar assessments of the spark-source mass spectrometer measurements. Complementary data are being obtained using neutron activation analysis.

Table 4-4. Performance characteristics achieved with spark-source mass spectrometer

Impurity Element	Limit of Detection (ppba)	Mean (ppba)	Standard Deviation (ppba)
Cr	3	26(13)	10
Cu	3	32(9)	19
Fe	30	ND	--
Mn	3	29(6)	16
Ni	30	64(10)	19
Ti	3	8.5(6)	1.6
V	3	8.8(5)	6.2
Zr	10	12.3(6)	5.4

The effects of impurities on the properties of single crystal materials and solar cells for crystals grown at substantially faster rates than in the case of the Czochralski crystals are being studied using dendritic web crystals; the rates for these experiments were greater by about 10-fold. The effect of rate on the segregation coefficients was considered in the calculations of the melt concentrations which would be required to attain the desired crystal concentrations. Estimates of the ratios of effective segregation coefficients for Cr, Ni, and Cu were calculated to be $k_{web}/k_{Cz} = 1 \times 10^2$, 0.3×10^2, and 0.2×10^2, respectively.

No major differences in metallurgical characteristics were found to occur with B-doped Si. However, the addition of impurity elements caused breakdowns, which are formations of irregular, ridged patches along the web surface. Breakdowns were most common in webs grown with V, Ti, Zr, Cr, Mn, and Fe at concentrations of 10^{18} atoms/cm^3 in the melt. The incorporation of Cu, N, or Al rarely affected the web structure. A tentative explanation of these observations is that the elements causing breakdowns are those with relatively small segregation coefficients and solid solubilities and hence the surface structure defects may precede a breakdown of the solid-liquid interface.

Measurements of minority carrier recombination lifetimes were continued in attempts to correlate these data, as functions of impurity concentrations and processing parameters, with cell performance characteristics. In the first attempt the relationship $I_{sc} = I_o \tau^n$ was assumed, and a linear regression curve fit was applied to the experimental data. The curve is given in Fig. 4-2. There is a scattering of the data, which for most cases results from shallow trapping effects. The value of $n = 0.145$ was derived from the curve-fitting whereas the expected value was 1/2, since the diffusion length is proportional to $\tau^{1/2}$.

The theoretical relationship between I_{sc} and τ_r was then derived using a series of simplifying assumptions, which included: (1) τ_r is a constant, (2) the electric fields in an operating cell are negligible, (3) the junction and backside contacts are infinite sinks for the minority carriers, (4) surface recombination can be neglected, and (5) each absorbed quantum generates an electron-hole pair. The resulting equation was then used to plot I_{sc} vs L, the diffusion length, as given in Fig. 4-3. There is a reasonable agreement between the experimental and theoretical curves, and the decrease of I_{sc} below $L_n \sim 150\,\mu m$ is apparent; for a resistivity of 4 ohm-cm the corresponding value of τ_r is 6.16 μsec.

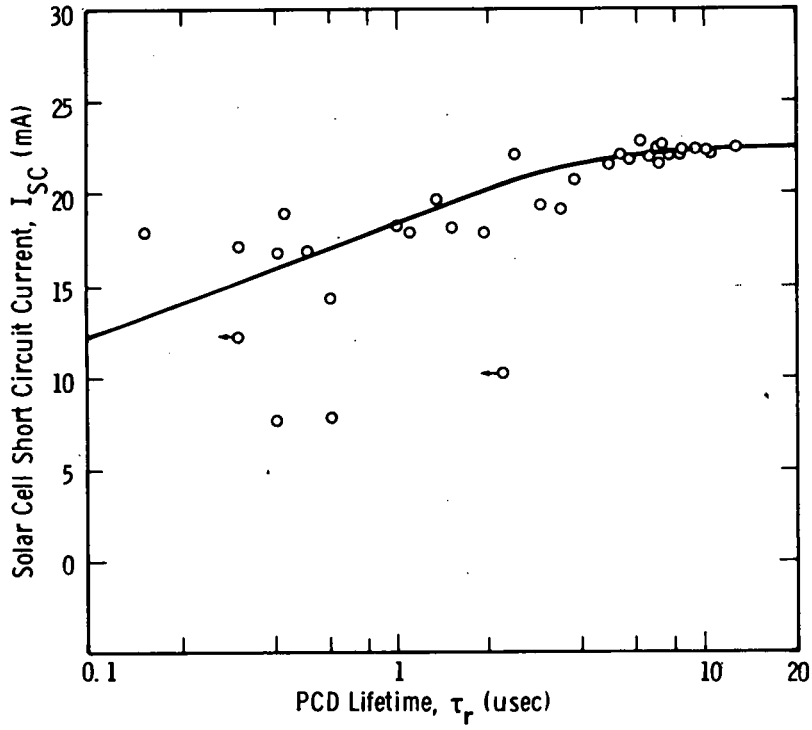

Fig. 4-2. Correlation between bulk recombination lifetime, τ_r, and short circuit output current, I_{SC}, of metal impurity-doped solar cells

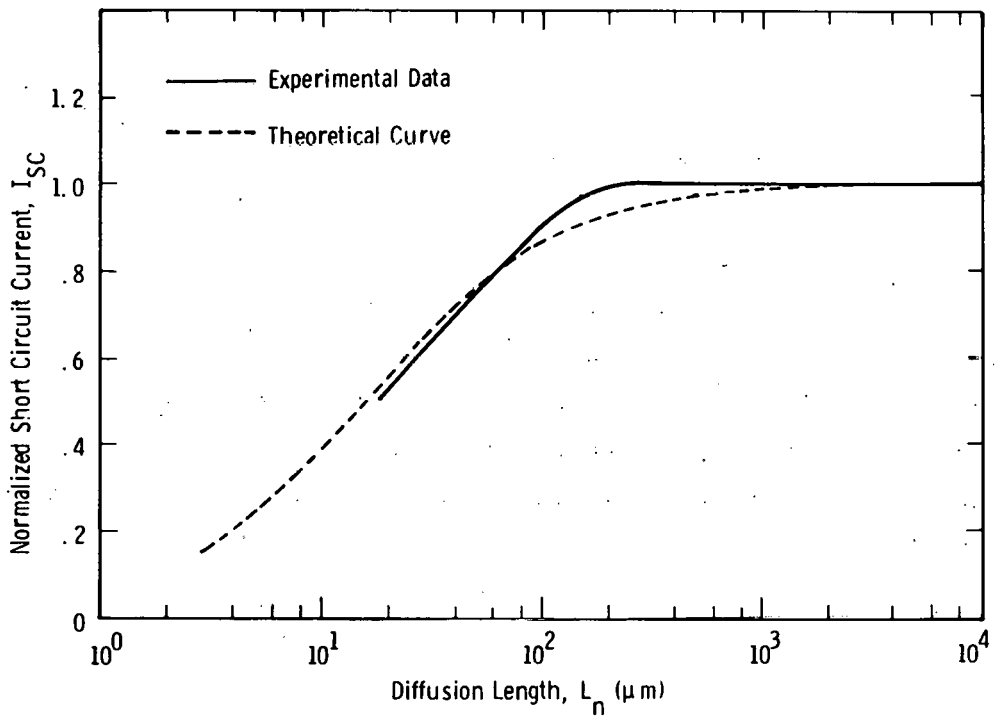

Fig. 4-3. Effect of diffusion length on short circuit current of a silicon solar cell. Theoretical curve was calculated with α = 709 cm^{-1}, d = 0.127 cm, and D_n = 36.5 cm^2/sec

Lifetime measurements formed the basis for a series of investigations of the effects of impurities and processing-steps on solar cell performance. The reductions of solar cell efficiency by impurities were manifested by decreases in short circuit current and were correlated with lifetime data for the cells in Fig. 4-4. An attempt to relate measurements of lifetimes before and after

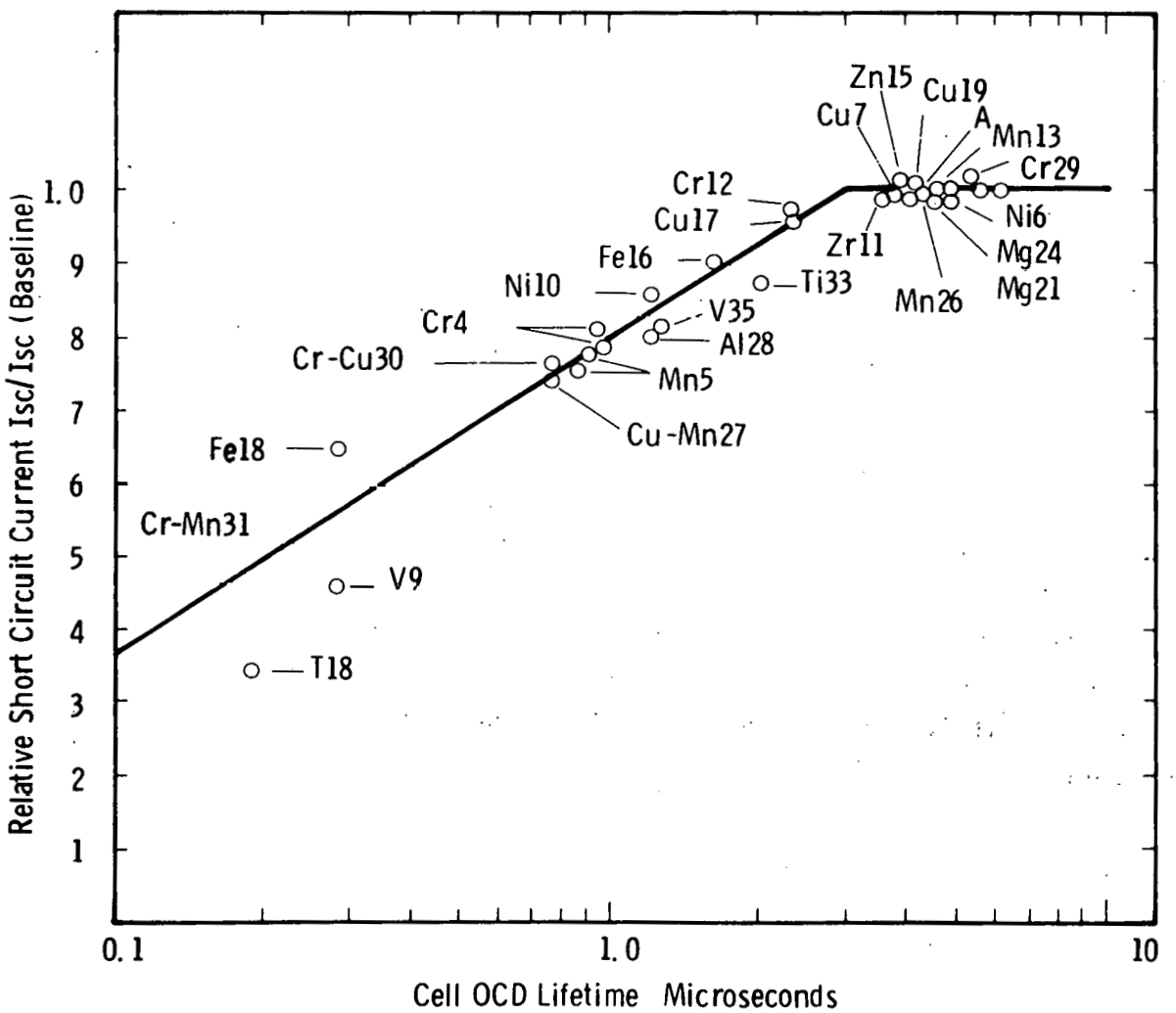

Fig. 4-4. Variation in relative solar cell short circuit current with cell open circuit decay lifetime

processing is shown in Fig. 4-5; the failure to obtain any kind of correlation is apparent. The effects of a set of processing steps on lifetimes are given in Fig. 4-6; there are obvious markedly dissimilar responses to the processing steps for this group, indicating strong influences of the specific impurities. The data presented in Figs. 4-7, 4-8, and 4-9 illustrate different behavior patterns for Mn, Cr, and Ti for lifetimes data as a function of concentration. Each set of data has been used to emphasize that the different responses are dependent on the specific impurities present in the material.

The effects of high temperature P-gettering and damage gettering were examined in some preliminary experiments. The P-gettering was done using $POCl_3$ at 1200°C for 20 minutes; the damage gettering was done by lapping the back surface of the wafer. Wafers doped with Mn, Ti, and V were used. The data are given in Tables 4-5 and 4-6. The following observations were made: (1) the degradation of the baseline material by P-gettering may be due to the propagation of defects into the P-region of the wafer; (2) gettering as a result of damage introduced by the lapping was ineffective; and (3) the responses vary with the impurity. The development of effective gettering procedures for particular impurities will require more extensive investigations.

The characterization of solar cells fabricated from doped ingots is now nearly complete. The data for doubly doped inputs are given in Fig. 4-10 and those for multiply doped ingots in Table 4-7. These data clearly show that the severe degradation of cell characteristics caused by the presence of Ti also occurs in multiply doped ingots. For example, in combination with Zr, which has little effect alone, Ti still drastically reduces the cell performance.

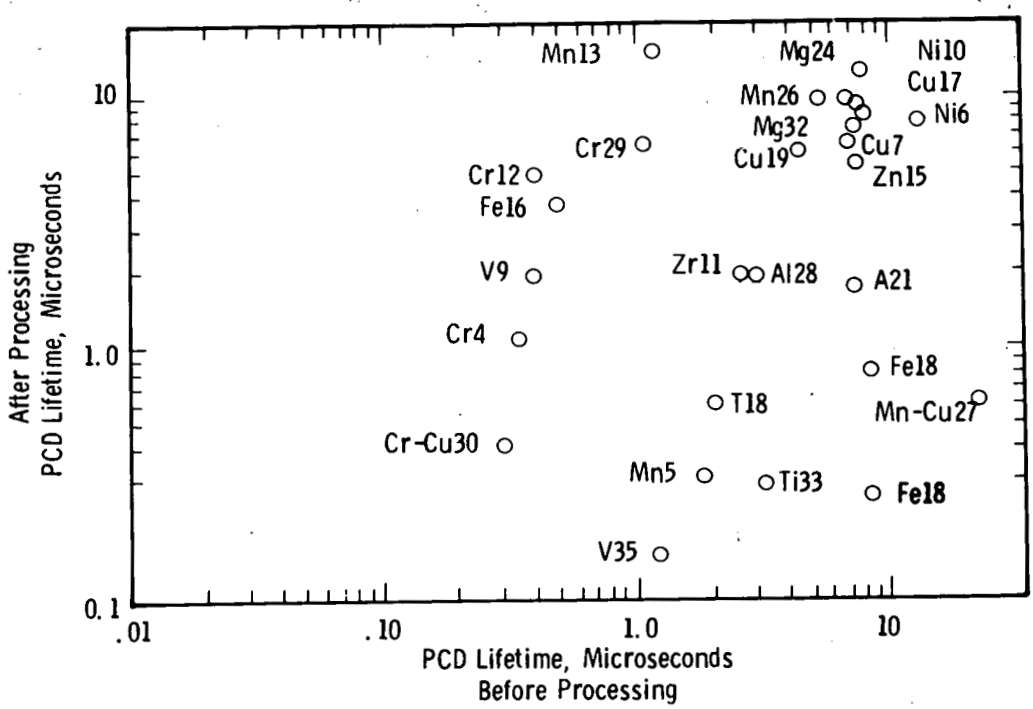

Fig. 4-5. Variation in photoconductive decay lifetime measured on wafers after processing compared to that measured on the as-grown material. No correlation is apparent.

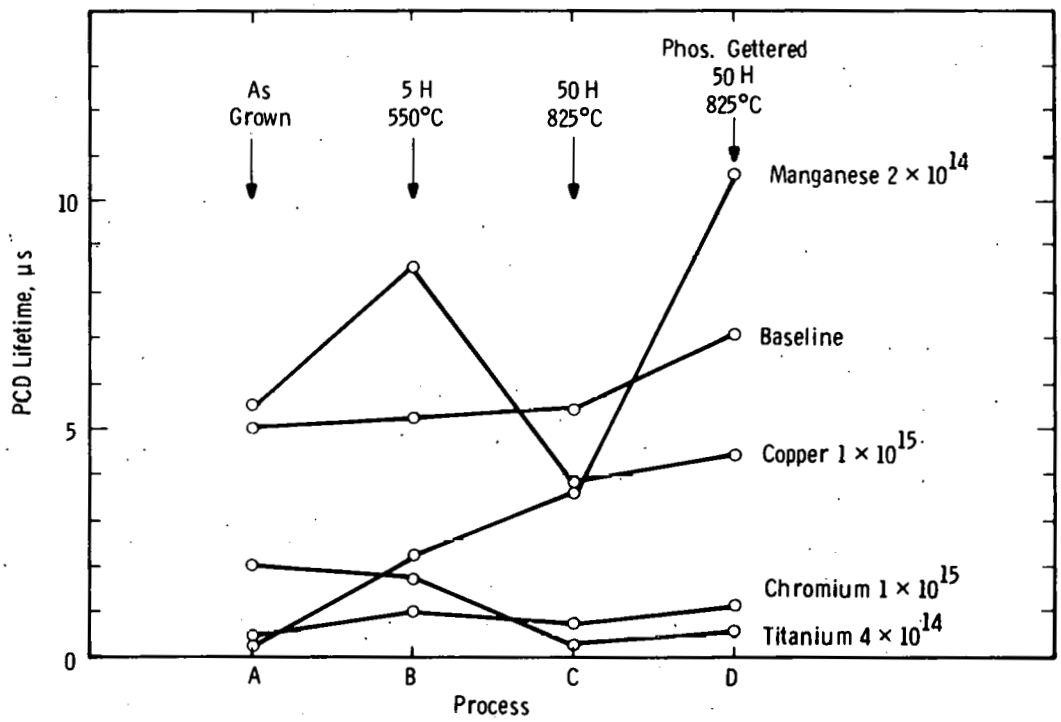

Fig. 4-6. Effect of processing history on photoconductive decay lifetime. Note that impurities may respond in very different ways to the same treatment.

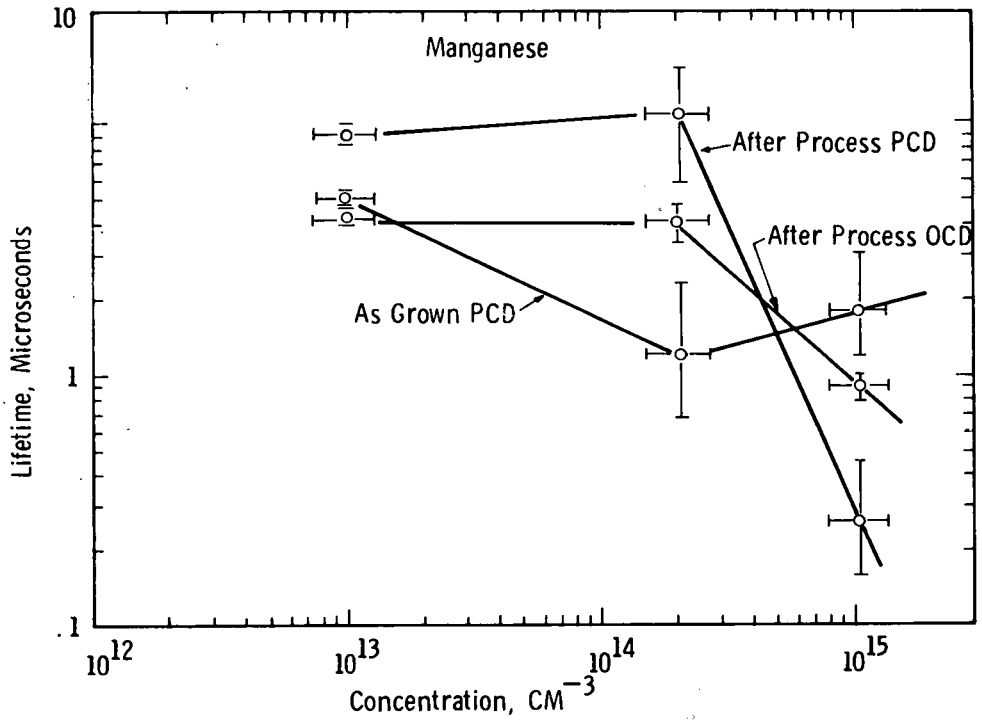

Fig. 4-7. Measured variation in silicon wafer lifetime with manganese concentration (before and after processing)

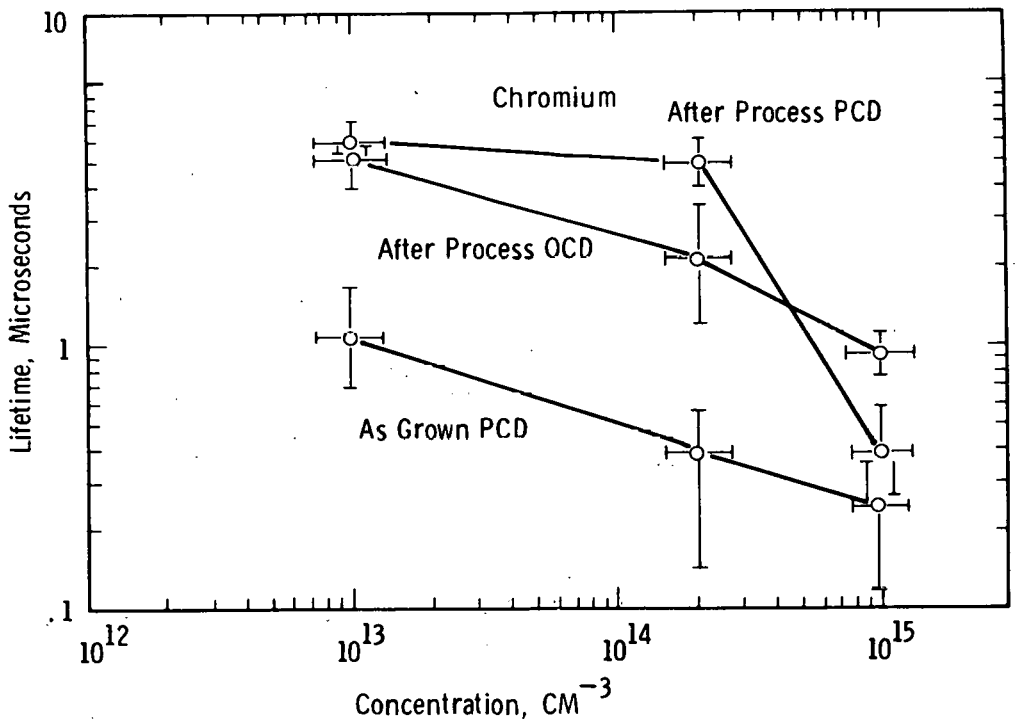

Fig. 4-8. Measured variation in silicon wafer lifetime with chromium concentration (before and after processing)

b. Effects of Impurities and Process-Steps on Silicon Properties and Solar Cell Performance - Monsanto Research Corporation

The experimental program has been completed. The elements of the program were ingot preparation, material characterization and metallographic testing, lifetime measurements before and after diffusion, and the fabrication and measurements of solar cells with P/N and N/P geometry. A final report is being processed.

The following results and conclusions were obtained: (1) as shown by Auger electron spectra analyses, Ti diffused into the Ag and Si at the interface of a Ti/Ag coating on Si and O diffused toward the Ag layer, (2) the use of $Si_3 N_4$ as an antireflective coating increased the efficiencies of cells from 9% to nearly 13%, and (3) nearly identical efficiency values were obtained for cells fabricated from single- and double-sided polished blanks.

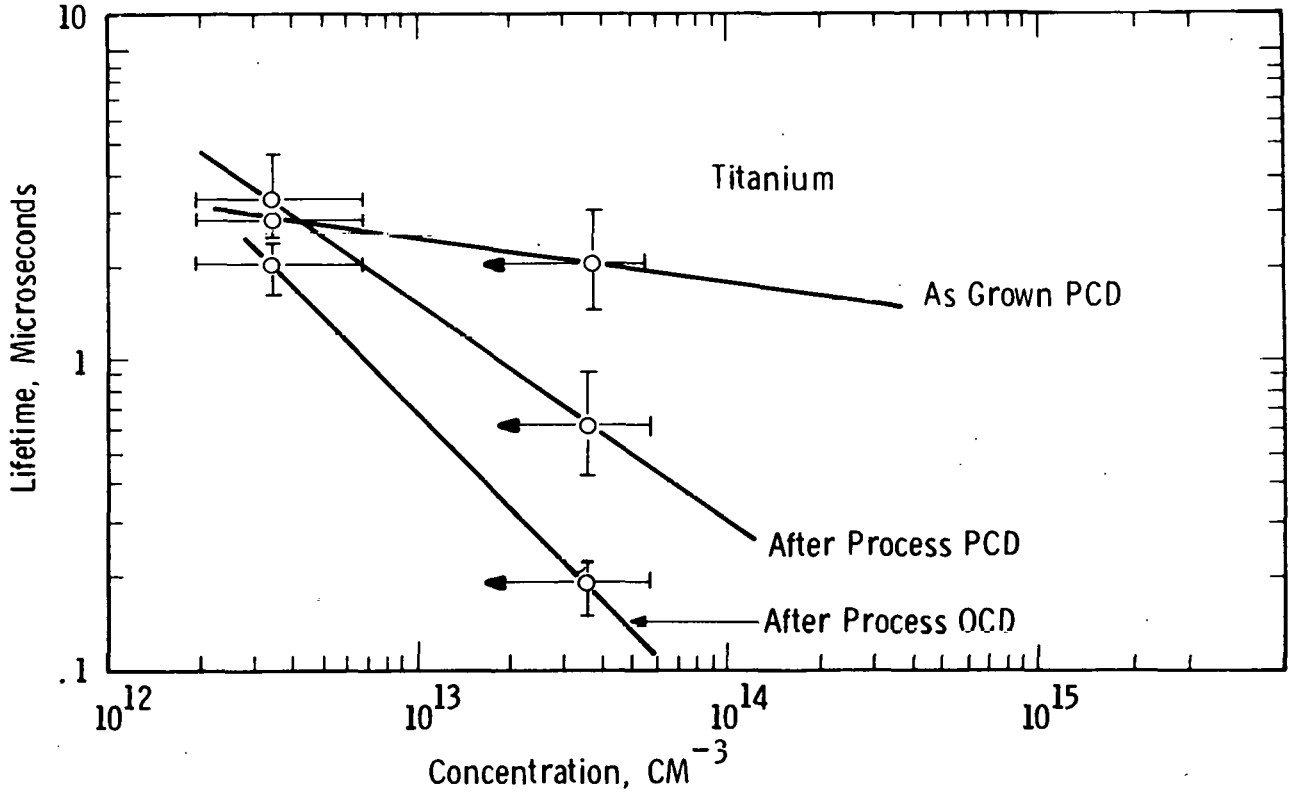

Fig. 4-9. Measured variation in silicon wafer lifetime with titanium concentration (before and after processing)

Table 4-5. Gettering-lapping effects comparison table for Mn-, Ti-, and V-doped

Identification	V_{oc}	I_{sc}	V_p	I_p	I_o	N	FF	Eff	TAU
Normal Baseline	0.536	22.50	0.4471	20.94	2.3×10^{-9}	1.341	0.7764	9.36	4.875
Gettered Baseline	0.526	20.35	0.4370	18.89	4.92×10^{-9}	1.309	0.7711	8.26	2.405
% Change: Gettered Vs. Normal	-1.87	-9.56	-2.26	-9.79	43.5	1.61	-0.68	-11.75	-50.67
Lapped Baseline	0.536	22.5	0.4471	20.94	2.3×10^{-9}	1.341	0.7764	9.36	5.85
% Change: Lapped Vs. Normal	-	-	-	-	-	-	-	-	16.67
Mn-DOPED									
Normal	0.526	18.80	0.4392	17.51	1.67×10^{-9}	1.160	0.7777	7.69	1.30
Gettered	0.465	10.40	0.3781	9.51	1.98×10^{-8}	1.353	0.7437	3.60	0.910
% Change: Gettered Vs. Normal	-11.60	-44.68	-13.91	-45.69	91.56	8.25	-4.37	-53.19	-30.0
Lapped	0.522	18.35	0.4315	16.97	8.63×10^{-9}	1.215	0.7647	7.32	1.43
% Change: Lapped Vs. Normal	-0.76	-2.39	-1.75	-3.08	80.64	7.08	-1.68	-4.81	9.09
Ti-DOPED									
Normal	0.445	8.00	0.3603	7.29	2.28×10^{-8}	1.281	0.7383	2.63	0.455
Gettered	0.480	11.45	0.3939	10.55	9.73×10^{-9}	1.302	0.7554	4.155	0.520
%Change: Gettered Vs. Normal	7.29	30.13	8.59	30.9	-57.32	-2.38	2.26	36.70	12.5
Lapped	0.4450	8	0.3603	7.29	2.28×10^{-8}	1.281	0.7383	2.63	0.390
% Change: Lapped Vs. Normal	-	-	-	-	-	-	-	-	-14.29
V-DOPED									
Normal	0.466	10.70	0.3868	9.93	2.09×10^{-9}	1.246	0.7700	3.84	0.130
Gettered	0.509	15.40	0.4190	14.21	8.20×10^{-9}	1.358	0.7594	5.96	0.975
% Change: Gettered Vs. Normal	8.44	30.5	7.68	30.04	74.5	14.26	-1.37	35.57	86.66
Lapped	4.66	10.50	0.3846	9.70	4.13×10^{-9}	1.341	0.7626	3.73	0.390
% Change: Lapped Vs. Normal	-	-1.86	-0.569	-2.31	49.39	4.53	-0.961	-2.86	66.6

Table 4-6. Effect of gettering on minority carrier lifetime

Sample	Open Circuit Voltage Decay Lifetime, μs		
	Normal Process	$POCl_3$ Gettered	Back Surface Damaged Gettered
Baseline	4.86	2.41	5.85
Mn	1.30	0.91	1.43
Ti	0.46	0.52	0.39
V	0.13	0.98	0.39

Table 4-7. Average solar cell characteristics of multiple-doped ingots

Ingot ID	V_{OC}(V)	I_{sc}(ma)	V_p	I_p	I_o	n	FF	η(%)	τ(μsec)
Zr/Ti	0.4419	7.76	0.3598	7.10	1.56 E-08	1.278	0.745	2.57	0.130
Base	0.5530	22.64	0.4635	21.13	1.98 E-09	1.271	0.782	9.80	5.07
Cr/Ni	0.5164	19.74	0.4297	18.33	3.94 E-09	1.272	0.7716	7.90	1.018
Base	0.552	22.52	0.4644	21.07	1.35 E-09	1.23	0.787	9.79	4.576
Cr/Cu/Ni	0.5107	18.96	0.4145	17.20	1.91 E-05	1.618	0.7384	7.15	0.615
Base	0.555	22.68	0.4684	21.26	7.77 E-10	1.207	0.7907	9.96	4.55

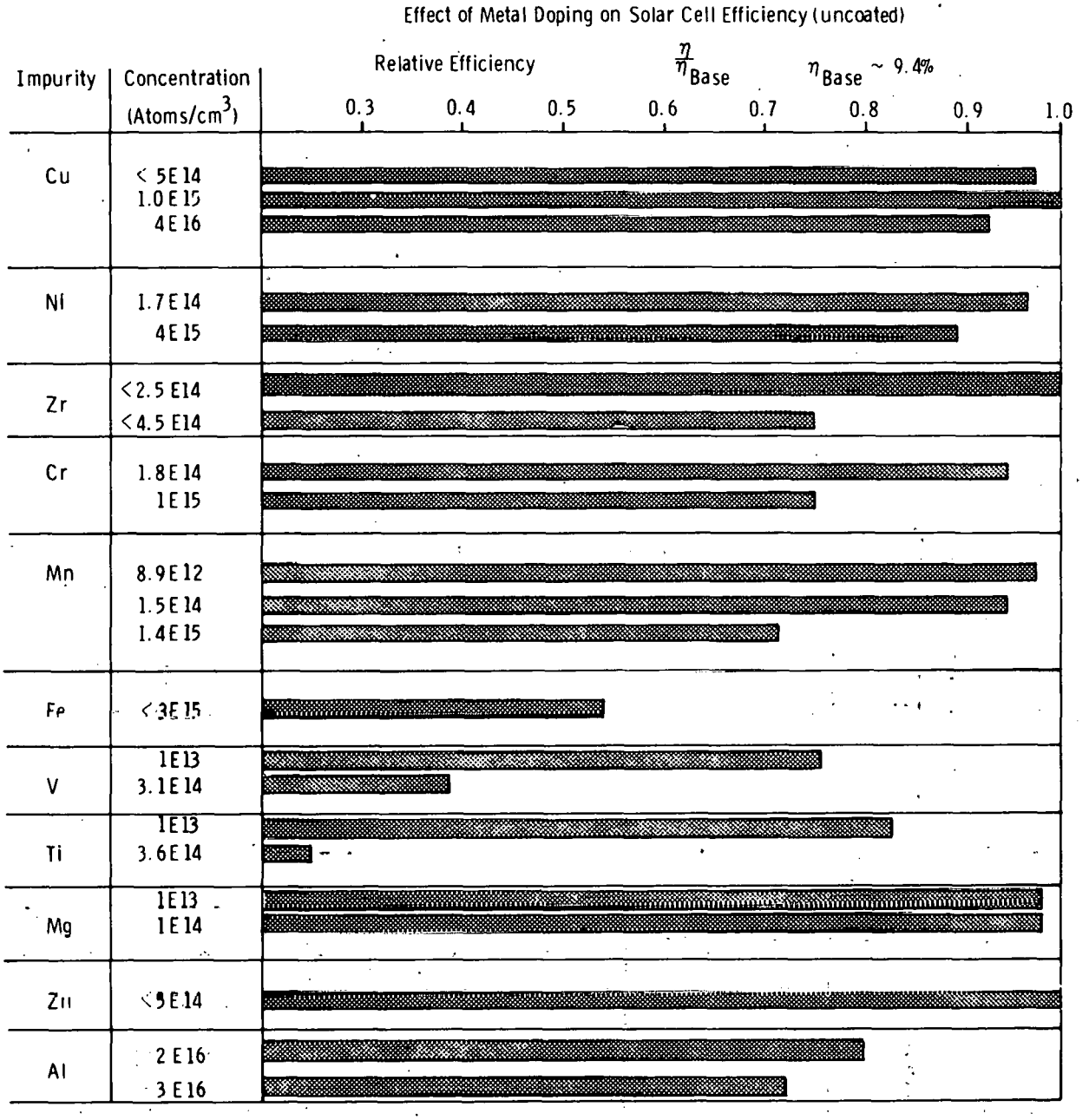

Fig. 4-10. Variation in solar cell performance with metal doping. No antireflective coatings, AM1 quartz-iodine illumination

3. Processes for Producing Solar-Cell-Grade Silicon

The approach used for Part III of Phase I (see Table 4-1) incorporates theoretical studies involving thermodynamics, reaction chemistry, and chemical engineering; chemical reaction investigations consisting of experimental determinations of reaction kinetics, yields, and suitable process conditions; a chemical engineering effort for securing an experimental data base for preliminary process modeling; and energy-use and economic calculations for preliminary process models. In each case the contract requires a demonstration of technical feasibility and a projection of commercial practicality, involving the preliminary analysis of the suitability for a scale-up study. Each process candidate will be evaluated on a separate milestone schedule. Selections for the next phase of scale-up studies will be made at times which are appropriate for individual or collective assessments.

a. Solar-Cell-Grade Si Production by C Reduction of SiO_2 Using an Induction Plasma — Texas Instruments Corporation

The C reduction of low impurity quartz in a plasma heat source is being investigated in this contract. In the first phase several runs were made using a 350-kW dc plasma furnace at Ionarc, Inc. The objectives were to verify the reduction of SiO_2 by C to Si in an Ar plasma, compare the use of a solid rod made of a SiO_2/C mixture and of pellets as feed materials, study a fused silica probe and a water-cooled Cu tube wall as means of collecting the product, and examine the effect of adding Si to the SiO_2/C mixture on the reaction yield. The experimental results were as follows: A small amount of Si was formed in the powder feed runs; the feed rods quickly disintegrated and no product was obtained; and about 3% Si was in the product when a cooled Cu tube was used as the collector. The following problems were identified: The reaction temperature is difficult to predict or control; large volumes of gases complicate the process; SiC and SiO are major contaminants; and the loss of Si in gaseous SiO is not controllable. In view of these results and problems the program plan was modified; chemistry studies using an experimental induction plasma reactor will comprise the sole effort in the remainder of the contract.

In the scoping experiments the use of powder feed was found to be extremely slow, and the use of C as the reductant was ineffective. Experiments were also run with extruded rods of SiO_2 and 5% PVA binder using CH_4 as the reductant. In these runs considerable amounts of C were found in the product. Examination of the effects of feed rate, arc gas flow, and plasma power is continuing.

b. Solar-Cell-Grade Si Production From Na_2/SiF_6 Source Material Using Na Reduction of SiF_4 and the SiF_4/SiF_2 Transport Process — Stanford Research Institute

This contract is for the development of a two-step process for the production of Si. The steps are (1) the reduction of SiF_4 by Na to yield Si and NaF and (2) the subsequent reaction of the Si produced in step 1 with SiF_4 to form SiF_2 followed by the disproportionation of the SiF_2 to yield highly purified Si and SiF_4. The present effort is centered on establishing the optimum conditions for step 1. The work in this quarter was devoted to the design and construction of apparatus which could be operated under controlled conditions.

The main units of the apparatus are a SiF_4 purification unit, SiF_4 storage bulbs, and a detachable reaction kettle assembly. To purify the SiF_4 gas, it is passed over Fe at 800°C to remove air and SO_2 and then fractionally distilled. The method of preparing the Na and introducing it into the apparatus as well as the remainder of the vacuum setup permits operation without contamination.

The results of early experiments have shown that the reduction reaction proceeds readily at 152°C. The temperature increases rapidly to 452°C because of the exothermic nature of the reaction. The temperature and pressure as functions of time for a typical run are given in Fig. 4-11. Since the Na/SiF_4 mole ratio for the reaction is always less than 4, more than the stoichiometric amount of SiF_4 is being consumed. This extra SiF_4 can be accounted for in the formation of Na_2SiF_6 as a by-product. The product also apparently contains some SiO_2, although the major impurity is Na.

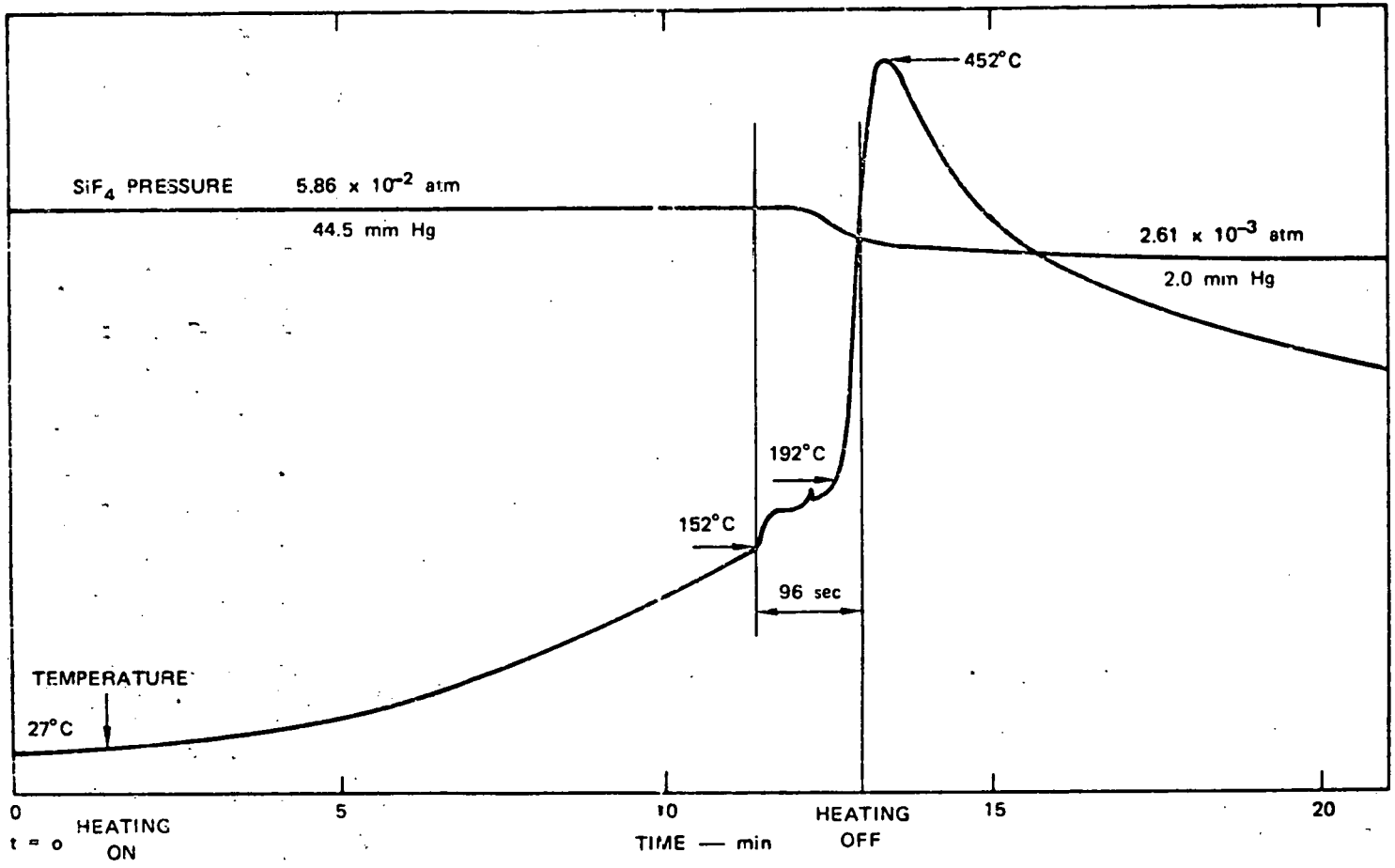

Fig. 4-11. Reaction temperature and pressure vs. time

c. Solar-Cell-Grade Si Production Using Submerged Arc Furnace, Vacuum Evaporation, and Unidirectional Solidification Processes — Dow Corning Corporation

This contract is for the development of a Si production process using, in sequence, a submerged arc furnace, vacuum evaporation and unidirectional solidification. The investigation with the furnace will test these concepts: (1) using quartz and C-reducing materials that are purer than those now used to produce metallurgical-grade Si and (2) incorporating processing and handling procedures that will minimize contamination. The product of the furnace should be considerably purer than metallurgical-grade Si with respect to most of the impurity elements. Its further purification will be examined in studies of the capabilities of the techniques of vacuum evaporation and unidirectional solidification.

Some preliminary conclusions were derived from discussions with the subcontractor, Elkem of Norway, where the experiments will be conducted using a 40-kW development-size furnace. It became apparent that the operating characteristics of a furnace and the composition of its product are dependent upon furnace structure and the nature of the raw materials. Experiments in which one parameter at a time is varied were recommended. The failure of the first run, in which purified forms of quartz and charcoal were used, was attributed to the physical form of the charcoal. The next experiments will use different quartzes and charcoals.

In the vacuum evaporation studies, molten metallurgical-grade Si was kept at 300×10^{-3} Torr for 6 hours. No decreases in impurity-element concentrations were found.

The reduction of impurity-element concentrations in metallurgical-grade Si by solid-liquid segregation using the procedure of unidirectional solidification is being examined. With exception of B and P, the segregation coefficients for very slow growth rates are small enough to provide large separations. The dependence of the degree of segregation on growth rates is to be determined for each impurity element.

Much of the program plan of this contract is based on previous work done by Dow Corning under NSF and ERDA contracts. The final report for these contracts was issued in December 1975.

d. Production of SiH_4 or Si Using a Nonequilibrium Plasma Jet for the Reduction of $SiCl_4$ — AeroChem Research Corporation

The purpose of this program is to investigate the chemical reactions of H atoms with $SiCl_4$ to yield, as end products, SiH_4 or Si. The H atoms are to be produced by passing H_2 molecules through a low temperature glow discharge, which is particularly suitable for the non-equilibrium creation of ions and free radicals. The degree of ionization and dissociation which can be obtained under these conditions would require heating the gas to about 6000°K under thermodynamic equilibrium conditions. This procedure is advantageous in that it permits an efficient energy-use, a very low temperature (which minimizes undesirable side reactions), the activation of the selected reactant H_2 only, the production of extremely reactive species, the minimization of problems of materials of construction, and the capability of selective quenching. The throughputs are large when compared with conventional low temperature discharge systems. The major disadvantage is the need to operate at low pressures, which are 20 to 100 Torr in the discharge region and 5 to 20 Torr in the synthesis region.

The marked advantage of using H atoms in place of H_2 molecules for the reduction of Si compounds was demonstrated by a comparison of equilibrium constants for reactions with three Si-containing compounds. These calculations are given in Table 4-8, where the factors of temperature and product yield are clearly displayed. In further thermodynamic considerations it was shown that the subsequent decomposition of SiH_4 to Si would be thermodynamically favorable if it were initiated by an H atom reaction, such as $SiH_4 + H\cdot = SiH_3\cdot + H_2$. The preparation of SiH_4 or Si by this process was thus shown to be thermodynamically feasible; on the other hand, predictions of the kinetics are inappropriate because reaction rate data is lacking for the steps of the proposed reactions.

Table 4-8. Comparison of equilibrium constants (Kp) with hydrogen molecules and hydrogen atoms as reactants

	log K_p					
	Molecules			Atoms		
	298°K	1000°K	1500°K	298°K	1000°K	1500°K
(1) $SiO_2(s) + 2H_2 \rightarrow Si(s) + 2H_2O$ or 4H	-60.9	-18.1	-10.9	72.3	23.8	14.9
(2) $SiCl_4 + 4H_2 \rightarrow SiH_4 + 4HCl$ or 8H	-52.1	-13.0	-7.73	233	56.4	30.3
(3) $SiHCl_3 + 3H_2 \rightarrow SiH_4 + 3HCl$ or 6H	-36.3	-9.40	-5.79	178	42.6	22.8

The apparatus has been completed. Preliminary experiments are under way. The principal independent parameters are the current and the flow rates of H_2 and $SiCl_4$. The H atom yield is determined by using a chemiluminescent titration technique in which the reactions are: $H + NO_2 = OH + NO$ and $H + NO + (M) = HNO + (M) + h\nu$. The endpoint is observed when NO_2 has reacted with all of the H atoms and the chemiluminescent glow is concurrently sharply reduced from a length of about 95 cm to a few cm. An alternative titration in which the reagent is NOCl is being studied.

e. Solar-Cell-Grade Si Production Using an Arc Heater Plasma Process for the Reduction of $SiCl_4$ with Na, Mg, or H_2 — Westinghouse Electric Corporation

This is an engineering analysis and design effort to demonstrate the feasibility of a system for the high capacity, low cost production of Si using an arc heater. The chemical reactions to be investigated include the reduction of $SiCl_4$ by alkali metals. The program consists of four tasks: (1) thermochemical analyses: (2) plasma reactor design; (3) reactant storage and injection

system design; and (4) product collection and effluent disposal system design. The conclusions derived from the thermochemical analyses will determine the reactant systems to be studied and the designs of the associated equipment.

The chemical equilibria for the Si-H-Cl systems have been described using the equilibrium constant method. Solutions were obtained for several temperatures, pressures, and initial compositions. The theoretical materials and energy requirements for the H_2 reduction of $SiCl_4$ were calculated yielding the minimum requirements of H_2 and energy at 2200°K and 1 atm pressure; the energy need is 57 kW-h/kg Si and the H_2 need is about 37 times the stoichiometric amount. The next step is to utilize these results for the calculation of the economics of H_2 reduction of $SiCl_4$. The material and energy requirements will next be determined for the use of Na, Mg, and Zn as the reductants.

A one-dimensional model was formulated to describe the evaporation of liquid metal droplets injected into an arc-heated gas stream. The description incorporates droplet momentum, heat, and mass transfer equations together with gas mass and energy conservation equations. Negligible thermal diffusion, Dufour effect, gas radiation, and droplet interactions were assumed. The result is a set of five coupled ordinary differential equations. Applying this analysis to the case of Zn droplets injected into arc-heated Ar gas resulted in the following conclusions: (1) particle vaporization is a strong function of gas velocity and duct diameter, i.e., residence time; (2) mass transfer does not affect heat, mass, and momentum transfer coefficients; (3) noncontinuum relations must be used to describe complete droplet evaporations; and (4) the results using practical particle loading densities differ significantly from the single particle treatment.

Operational envelopes were developed for the Na reduction process. These data correlate arc heater performance data and production rates for the Na process.

Equipment and subsystems for the feed and collection system are being analyzed. A subtask for instrumentation and controls has been started. The

first problem will be to determine the control electronics and power system requirements for the operation of the reactant, data collection, and readout information systems.

4. Evaluation of Silicon Production Processes — Lamar University

The objective of this contract is to evaluate the potentials of the processes being developed in the Task 1 program. The economic evaluations will be based upon analyses of process-system properties, chemical engineering characteristics, and costing-economics. The evaluations will be performed for each stage of the Silicon Material Task — technical feasibility, scale-up, experimental plants, and commercial plant — using information which becomes available from the various process development contracts.

Physical Properties

During this report period the effort to determine the physical properties of source materials has been centered on SiF_4 and SiH_4. Experimentally derived values for the critical temperature and pressure for SiF_4 were obtained from the literature; data for the critical constants of volume, compressibility factor, and density are not available. In the case of SiH_4, values of these three critical constants were calculated, since experimental data are lacking. These data are shown in Table 4-9.

SiF_4 Preparation Process

The preparation of SiF_4 is being studied. A part of the initial work was to define the conditions for the precipitation of the Si precursor, Na_2SiF_6, from an aqueous solution of SiH_2F_6 using the sodium salts NaCl, NaF, NaOH, and Na_2CO_3. The preliminary results indicate that the use of NaCl is preferable in that no products other than Na_2SiF_6 were formed and the maximum recovery of the product occurs at a reactant ratio of about 1:1.

Table 4-9. Preliminary data analysis — critical constants and physical properties of SiF_4 and SiH_4

	SiF_4	SiH_4
State (std. cond.)	Gas (colorless)	Gas (colorless)
Molecular weight, M	104.08	32.12
Boiling point, T_b, ^oC	-95.7 (sublimes)	-111.9
Melting point, T_m, ^oC	-90.2 (1318 mm Hg)	-184.7
	-86.8 (1679 mm Hg)	
Critical temp., T_c, ^oC	-14.15	-3.5*
Critical pressure, P_c, atm	36.66	47.8*
Critical volume, V_c, $cm^3/gr\ mol$	- -	130.06**
Critical compressibility factor, Z_c	- -	0.281**
Critical density, ρ_c, gr/cm^3	- -	0.247**

*Questionable value.

**Estimated value.

The thermal decomposition of Na_2SiF_6 is being examined using the parameter of temperature, reaction time, and reaction conditions. The effect of temperature on rate is illustrated in Figs. 4-12 and 4-13. The reaction is essentially complete in 15 minutes at 600°C.

Process Design

During this report period the major effort was devoted to the $Zn/SiCl_4$ process being developed under the Battelle contract. The key items — the process flow diagram, the material balance, the energy balance, property data, and equipment design — have been completed. The process flow diagram, given in Fig. 4-14, includes facilities for the storage of feed raw materials, and disposition of the by-product $SiCl_4$ streams from the purification step. The basic process conditions are presented in Table 4-10. The purification of technical grade $SiCl_4$ by distillation, an assumed 72.4% conversion, as calculated by Battelle, and the recovery of Zn by electrolysis are included.

A program has been started for the computer calculation of equilibrium compositions as functions of state conditions for the processes being developed under the contract to JPL. The results obtained for the H-Cl-Si and Zn-Cl-Si systems have been compared with prior analyses. For the H-Cl-Si system a comparison with the results obtained by Sirtl and Hund is given in Fig. 4-15. A comparison with the Battelle results for the Zn-Cl-Si system is shown in Fig. 4-16. The technique will now be applied to other processes.

Economic Analysis

A survey of methods for the estimation of total product cost was completed during the quarter. The results are shown in Table 4-11; the typical range of values for each subitem is indicated by upper and lower limits. In applying these results to cost estimates of the chemical process alternatives, a generally conservative approach will be taken. For example, the upper limits are being used for estimating the costs associated with maintenance, repair, corrosion, and high temperature operation problems. Most of the effort during the quarter was devoted to analysis of the $Zn/SiCl_4$ process. The following key items have been completed: (1) fixed plant investment

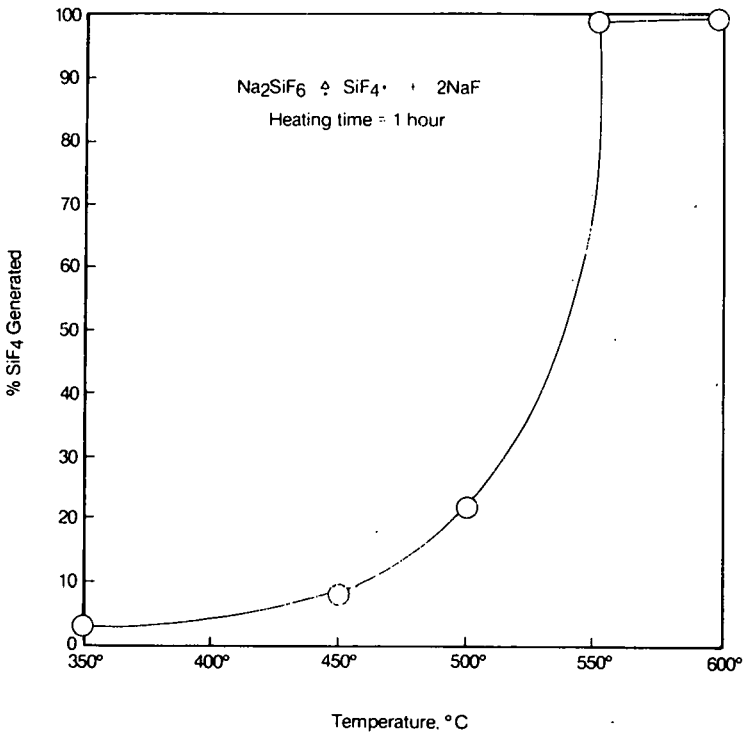

Fig. 4-12. Variation of % SiF_4 generated with temperature

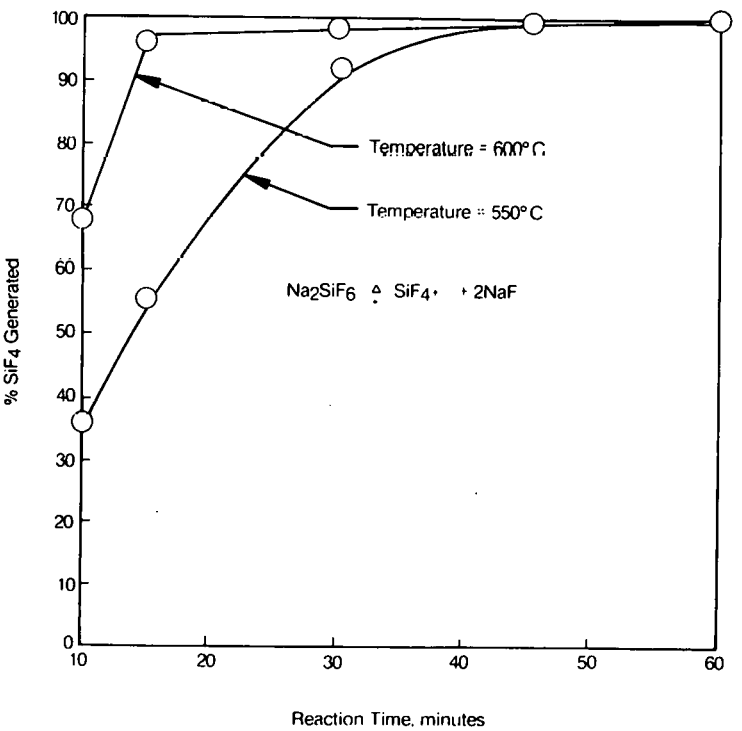

Fig. 4-13. Variation of % SiF_4 generated with reaction time

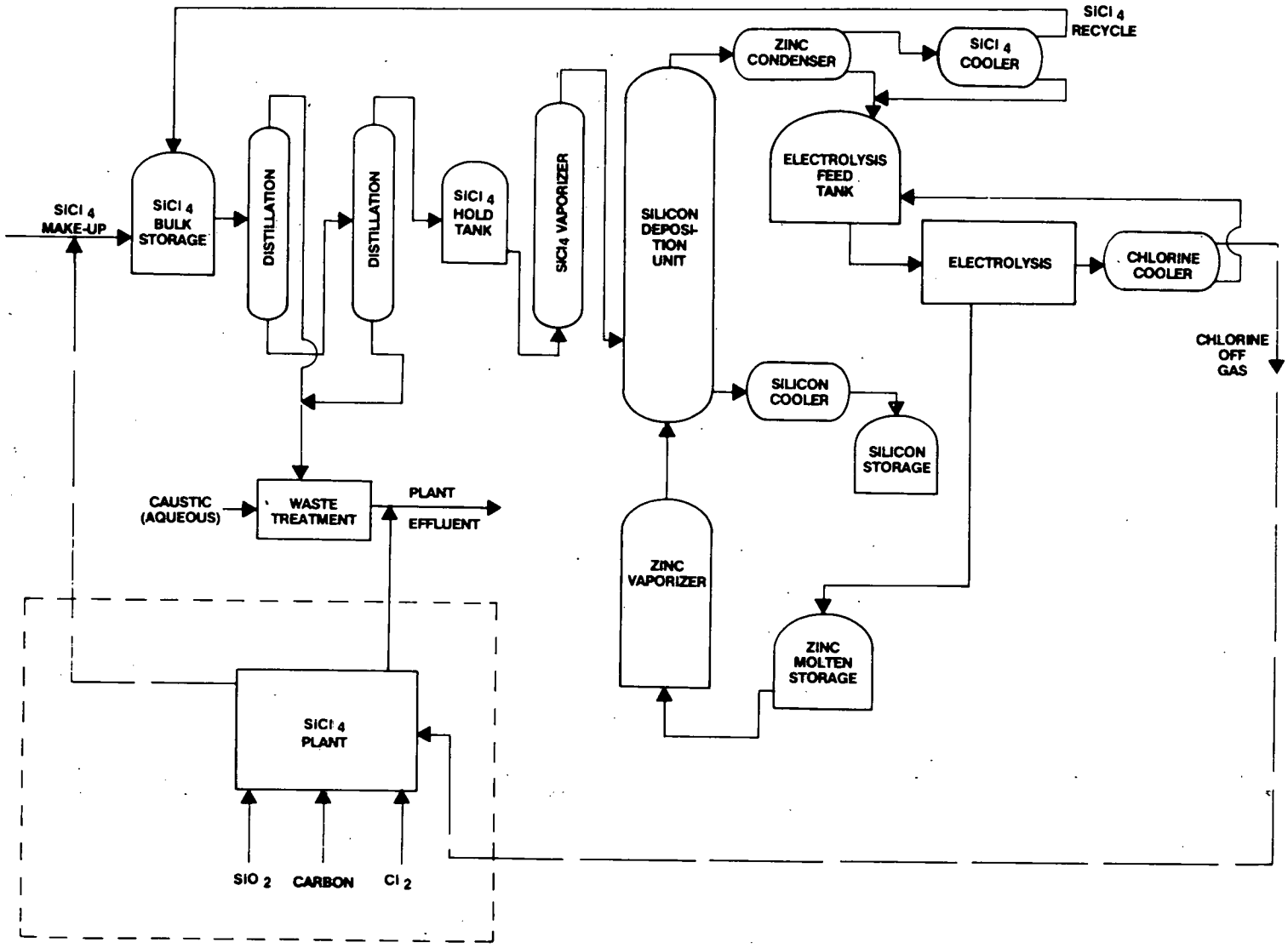

Fig. 4-14. $Zn/SiCl_4$ process flow diagram (Battelle)

Table 4-10. Base case conditions for $Zn/SiCl_4$ process (Battelle)

1. Plant Size
   - Production of 1000 metric tons/year
   - Solar-cell-grade silicon
2. Deposition Reaction
   - Zn reduction of $SiCl_4$
   - 1200°K, 1 atm, 72.4% conversion (Battelle)
3. $SiCl_4$ Purification
   - Technical-grade $SiCl_4$ purification by distillation
   - 10% waste (5% lights, 5% heavies)
   - 90% product (90% heartcut)
4. Electrolytic Recovery
   - Electrolytic recovery of Zn from $ZnCl_2$
   - Cl_2 is by-product
5. Operating Ratio
   - Approx. 80% utilization (79.3%)
   - Approx. 7000 hr/year production
6. Storage Considerations
   - Feed materials (two week supply)
   - Product (two week supply)
   - Process (several days)

and total product cost, (2) base line conditions, (3) raw material costs, (4) utilities cost, (5) purchased equipment cost, (6) production labor cost, (7) estimation of capital investment, and (8) estimation of total product cost have been completed. The estimation of total product cost is given in Table 4-12; the total fixed capital investment for a plant producing 1000 MT/year of Si by the $Zn/SiCl_4$ process is $10,100,000.

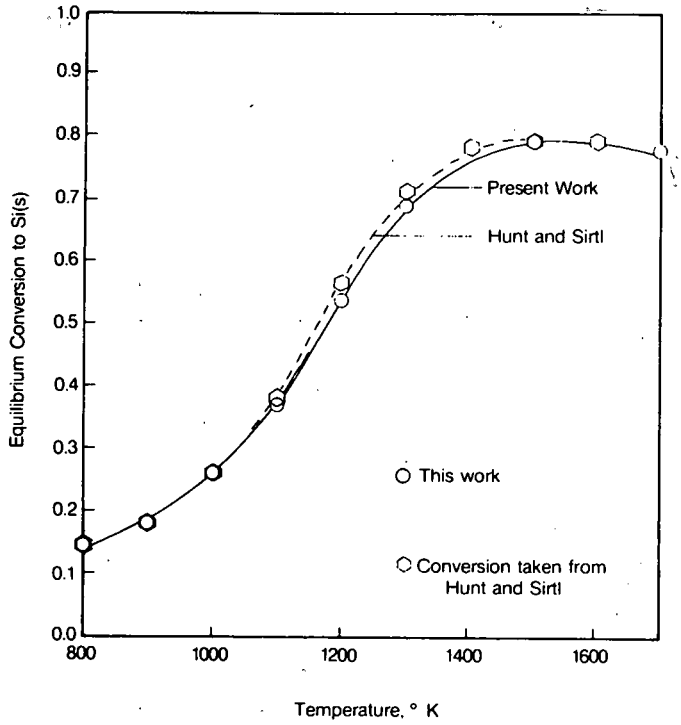

Fig. 4-15. Equilibrium conversion to Si(s) versus temperature

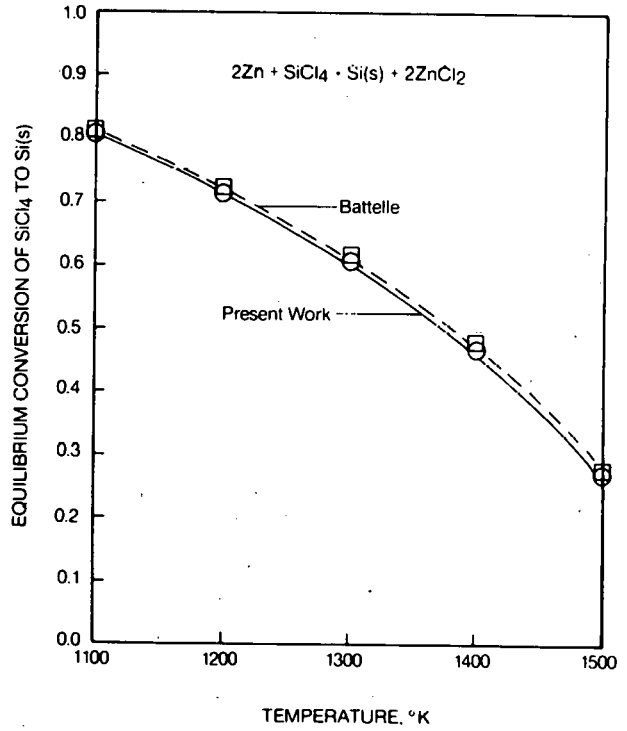

Fig. 4-16. Equilibrium conversion to Si(s) versus temperature for $Zn/SiCl_4$ process (Battelle)

Table 4-11. Economic analysis — survey results for estimation of total product cost

	Typical Range	Selected Nominal Values
1. Direct manufacturing cost (direct charges)		
a. Raw materials*	--	--
b. Direct operating labor*	--	--
c. Utilities*	--	--
d. Supervision and clerical, % of 1b	10-25%	15%
e. Maintenance and repairs, % of fixed capital (50% labor, 50% materials)	2-10%	10%
f. Operating supplies, % of 1e	5-25%	20%
g. Laboratory, charge, % of 1b	3-20%	15%
h. Patents and royalties, % of product cost	0-6%	3%
2. Indirect manufacturing cost (fixed charges)		
a. Depreciation, % of fixed capital	5-10%	10%
b. Local taxes, % of fixed capital	0.5-4%	2%
c. Insurance, % of fixed capital	0.4-2%	1%
d. Interest, % of fixed capital	0.8%	8%
3. Plant overhead, % of labor in 1b + 1d + 1e	40-72%	60%
4. By-product credit*	--	--
4A. Total manufacturing cost, 1 + 2 + 3 + 4		
5. General expenses		
a. Administration, % of manuf. cost	2.3-12%	6%
b. Distribution and sales, % of manuf. cost	2.3-24%	6%
c. Research and development, % of manuf. cost	2.4-6%	3%
6. Total cost of product, 4A + 5		

*From preliminary design.

Table 4-12. Estimation of total product cost for $Zn/SiCl_4$ process (Battelle)

	Selected Nominal Values From Survey*	$/kg
1. Direct manufacturing cost (direct charges)		
a. Raw materials**	--	2.76
b. Direct operating labor**	--	0.52
c. Utilities**	--	0.88
d. Supervision and clerical, % of 1b	15%	0.08
e. Maintenance and repairs, % of fixed capital (50% labor, 50% materials)	10%	1.01
f. Operating supplies, % of 1e	20%	0.20
g. Laboratory change, % of 1b	15%	0.08
h. Patents and royalties, % of product cost	3%	0.29
2. Indirect manufacturing cost (fixed charges)		
a. Depreciation, % of fixed capital	10%	1.01
b. Local taxes, % of fixed capital	2%	0.20
c. Insurance, % of fixed capital	1%	0.10
d. Interest, % of fixed capital	8%	0.81
3. Plant overhead, % of labor in 1b + 1d + 1e	60%	0.66
4. By-product credit**- from prel. design	--	0.37
4A. Total manufacturing cost, 1 + 2 + 3 + 4		8.25
5. General expenses		
a. Administration, % of manuf. cost	6%	0.50
b. Distribution and sales, % of manuf. cost	6%	0.50
c. Research and development, % of manuf. cost	3%	0.25
6. Total cost of product, 4A + 5		$9.49/kg

*From Table 4-11.

**From preliminary design.

5. JPL Task 1 In-House Support

During this quarterly period JPL in-house activities were being implemented to support the contractual efforts: (1) The program for investigations of fluidized bed reactor technology progressed with the assembly of the experimental reactor, the fabrication of a free space pyrolysis reactor, modeling of the fluidized bed process, and studies of methods for heating the reactor for SiH_4 pyrolysis. (2) Microstructural evaluations of the impurity-doped Si materials received from the Monsanto and Westinghouse contracts (Part II of Task 1) continued. The dislocation densities of all of the first generation wafers and some of the second generation as well as a number of multiply-doped wafers from Westinghouse were determined. The finding that these values were generally 10 times larger than those obtained by the contractor is yet to be explained. Additional information for some wafers was obtained using scanning electron microscopy, X-ray topography, and transmission electron microscopy. (3) A laboratory is being prepared for investigations of the effects of impurities on the properties of Si materials. (4) The following studies were prepared by Dr. Oldwig von Roos (under contract at JPL) as engineering memorandums: The Lifetime of Minority Carriers in Solar Cells, Preliminary Study, Analysis of a Degenerate Solar Cell, A Note on the Influence of the DC Electric Field Applied in the PCD Method for Bulk Lifetime Measurements, Theory of a NPP^+ Junction or Back Surface Field Solar Cell, Part I, The Lifetime of Minority Carriers in Solar Cells (Conclusion) A Description of the Control System OSCAR.

TASK 2. LARGE-AREA SILICON SHEETS

The objective of the Large-Area Silicon Sheet (LASS) Task is to develop and demonstrate the feasibility of several alternative processes for producing large areas of silicon sheet material suitable for low-cost, high efficiency solar photovoltaic energy conversion. To meet the objective of the LSSA Project, sufficient research and development must be performed on a number of processes to determine the capability of each for producing large areas of crystallized silicon. The final sheet-growth configurations must be suitable for direct incorporation into an automated solar-array processing scheme.

A. TECHNICAL BACKGROUND

Current solar cell technology is based on the use of silicon wafers obtained by slicing large Czochralski or float-zone ingots (up to 12.5 cm in diameter), using single-blade inner-diameter (ID) diamond saws. This method of obtaining single crystalline silicon wafers is tailored to the needs of large volume semiconductor products (i.e., integrated circuits plus discrete power and control devices other than solar cells). Indeed, the small market offered by present solar cell users does not justify the development of silicon "real estate" production techniques which would result in low-cost electrical energy.

Growth of silicon crystalline material in a geometry which does not require cutting to achieve proper thickness is an obvious way to eliminate costly processing and material waste. Growth techniques such as edge-defined film-fed growth (EFG), web-dendritic growth, chemical vapor deposition (CVD), etc., are possible candidates for the growing of solar cell material. The growing of large ingots with optimum shapes for solar cell needs (e.g., hexagonal cross-sections), requiring very little manpower and machinery would also appear plausible. However, it appears that the cutting of the large ingots into wafers must be done using multiple rather than single blades in order to be cost-effective.

Research and development on ribbon, sheet, and ingot growth plus multiple-blade and multiple-wire cutting, initiated in 1975-76 is in progress.

B. ORGANIZATION AND COORDINATION OF THE TASK 2 EFFORT

At the time the LSSA Project was initiated (January 1975) a number of methods potentially suitable for growing silicon crystals for solar cell manufacture were known. Some of these were under development; others existed only in concept. Development work on the most promising methods is now being funded. After a period of accelerated development, the various methods will be evaluated and the best selected for advanced development. As the growth methods are refined, manufacturing plants will be developed from which the most cost-effective solar cells can be manufactured.

The Task 2 effort is organized into four phases: research and development on sheet growth methods (1975-77); advanced development of selected growth methods (1977-80); development, fabrication, and operation of production growth plants (1983-86).

C. TASK 2 CONTRACTS

The pursuit of optimal techniques for growing silicon crystalline material for solar cell production has led to the awarding of R&D contracts to 11 organizations. The processes being developed by the Phase 2 contractors are shown in Table 4-13. Figure 4-17 shows the schedule for each contract as it was initially negotiated. Follow-on work anticipated for each contract is indicated by the cross-hatched horizontal bars. Research and development work will continue through the end of FY 1977, by which time it is expected that technical feasibility will have been demonstrated. Selection of "preferred" growth methods for further development during FY 1978-80 is planned for late FY 1977 or early FY 1978. By 1980, both technical and economic feasibility should be demonstrated by individual growth methods.

Figure 4-17 also indicates the receipt of silicon "sheet" samples and solar cells from the various growth-process R&D programs. Sheet samples are now being characterized at JPL, with solar cell evaluation to follow.

Table 4-13. Task 2 contractors

Contractor	Technology Area
RIBBON GROWTH PROCESSES	
Mobil-Tyco, Waltham, Massachusetts	Edge-defined, film-fed growth
IBM, Hopewell Junction, New York	Edge-defined, film-fed growth
RCA, Princeton, New Jersey	Inverted Stepanov growth
Univ. of So. Carolina, Columbia, So. Carolina	Web-dendritic growth
Motorola, Phoenix, Arizona	Laser zone ribbon growth
SHEET GROWTH PROCESSES	
Honeywell, Bloomington, Minnesota	Dip-coating of low-cost substrates
Rockwell, Anaheim, California	Chemical vapor deposition on low-cost substrates
General Electric, Schenectady, New York	Chemical vapor deposition on floating silicon substrate
Univ. of Pennsylvania, Philadelphia, Pennsylvania	Hot-forming of silicon sheet
INGOT GROWTH PROCESS	
Crystal Systems, Salem, Massachusetts	Heat-exchanger ingot casting*
INGOT CUTTING	
Crystal Systems, Salem, Massachusetts	Multiple wire sawing*
Varian, Lexington, Massachusetts	Breadknife sawing

*Single contract provides for both ingot casting and multiple wire sawing

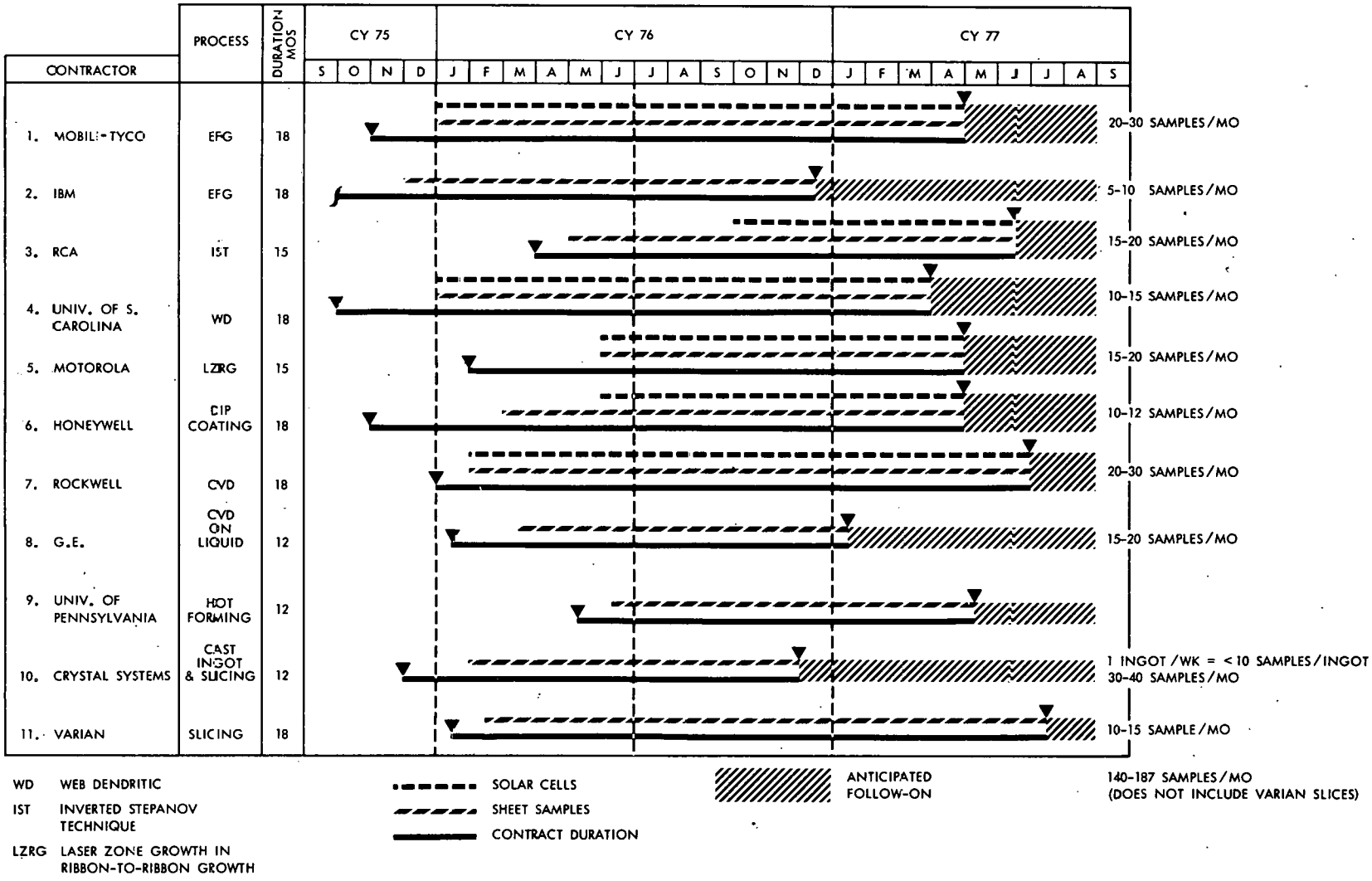

Fig. 4-17. Large Area Silicon Sheet Task schedule

D. TASK 2 TECHNICAL ACTIVITY

1. Silicon Ribbon Growth: EFG Method - Mobil-Tyco Solar Energy Corporation

The edge-defined film-fed growth (EFG) technique is based on feeding molten silicon through a slotted die (as illustrated in Fig. 4-18). In this technique, the shape of the ribbon is determined by the contact of molten silicon with the outer edge of the die. The die is constructed from material which is wetted by molten silicon (e.g., graphite). Efforts under this contract are directed toward extending the capacity of the EFG process to a speed of 7.5 cm/min and a width of 7.5 cm. In addition to the development of EFG machines and the growing of ribbons, the program includes economic analysis; characterization of the ribbon; production and analysis of solar cells; and theoretical analysis of thermal and stress conditions.

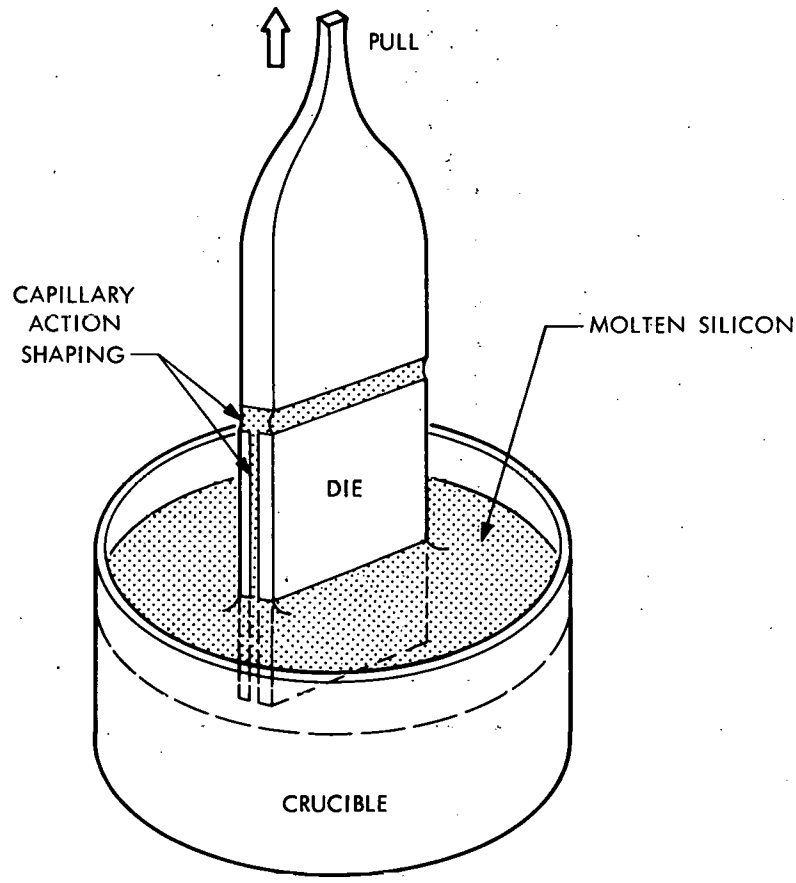

Fig. 4-18. Capillary die growth (EFG and CAST) - Mobil-Tyco and IBM

During the report period, the major effort under this program was directed toward controlling the exit thermal environment surrounding the EFG ribbon. This control is required for two reasons. First, it is necessary to remove heat, near to the crystallization front, in order to maximize the growth rate. This heat removal is being accomplished by means of water-cooled shoes whose thickness, position in space, and configuration are effective in controlling the rate and distribution of heat removal. The heat removal rate may also be influenced by the nature of the inert gas in the growth chamber. It was predicted theoretically, and demonstrated experimentally, that the use of helium, which has high heat-transport properties, will improve the cooling effectiveness. An increase of approximately 50% in growth rates can be predicted theoretically.

Initial difficulties were encountered in using the cooling shoes. Ribbons fractured and buckled as a result of too rapid cooling. A large number of redesigns were required before suitable cooling shoes were obtained. Present indications are that the initial goal of a growth rate of 3 in./min should be achievable.

The second reason for controlling the exit thermal gradient relates to the problem of stress in the ribbon and the requirement for a linear thermal gradient with respect to the direction of ribbon growth. A small heater assembly capable of providing the linear gradient has been placed on both sides of the ribbon and appears to control the stress satisfactorily. Although these two principles (heat removal and a linear exit gradient) are conceptually simple, their implementation, along with the requirement for die-top control heaters, has resulted in an extremely complex mechanical cartridge through which the ribbon passes (Fig. 4-19). The die is physically attached to the lower end of this cartridge. Silicon, at near room-temperature, exits from the top. The complexity of the device and the difficulty of making changes has slowed progress. Nevertheless, considerable progress is being made and a growth rate of 2 in./min for producing low-stress 2-in.-wide ribbon appears readily achievable (Fig. 4-20).

It appears feasible, by extending this approach, to attain the project goal of a 3-in.-wide ribbon produced at a rate of 3 in./min. The width scaling would be a function only of the maintaining of the linear gradient, a straightforward problem. The rate increases will require some changes in the cooling shoe

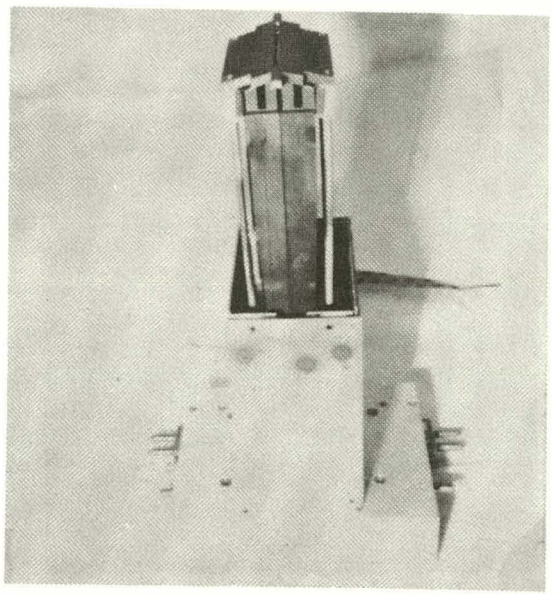

Fig. 4-19. Thermal control cartridge - preliminary version

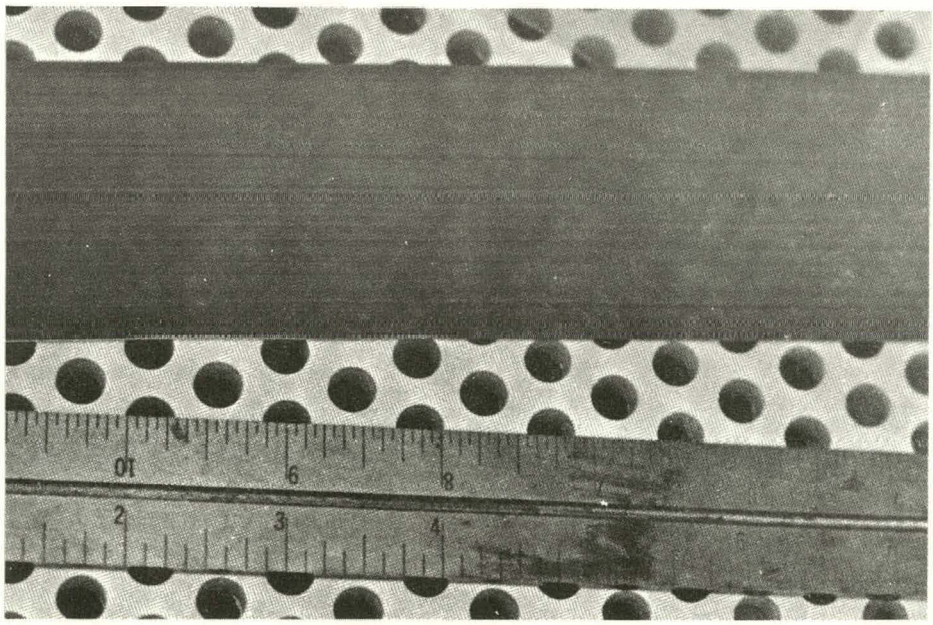

Fig. 4-20. EFG ribbon - 50 mm wide, nominal growth rate of 5 cm/min

operating point. It should be noted that the development of this approach to ribbon growth rate and stress control, using a highly enclosed thermal environment, enhances the potential for achieving multiple ribbon growth from a single machine. Each ribbon effectively operates in its own thermal environment and should not be influenced by its neighbor.

The economic status of EFG ribbon growth is being re-evaluated at this time. No major changes in conclusions are anticipated.

An analysis of the potential for obtaining thin ribbon was conducted based on the sensitivity of ribbon thickness to the various process parameters during growth. The major conclusions indicate that the largest variations in ribbon thickness are related to variations in meniscus height and the second order variations are related to changes in the die-top spacing. Since both of these parameters are influenced by the presence of silicon carbide particles on the die-top, the control of ribbon thickness becomes more difficult when carbide formation is poorly controlled. In any event, the control of ribbon thickness becomes more difficult as thickness decreases. The lack of a thorough understanding of the relationship between ribbon thickness, efficiency, and cost has caused problems in the planning of program activities.

Efforts in the areas of solar cell processing and analysis and material characterization have continued, but at a rather low level. Most of the material coming from the growth machines was fractured by stress — a result of the effort to produce wide ribbon, at a high growth rate. This situation should be remedied shortly as the control of stress improves. Efforts at characterization of the ribbons have emphasized the relationship between EBIC and structure .

Efforts in the near future will be concentrated on completing and optimizing growth studies directed toward the following goals: (1) 2-in.-wide ribbon produced at 2 in./min and (2) 3-in.-wide ribbon produced at 3 in./min. These developments should be either slightly behind schedule or on schedule. As material from the various growth machines becomes available, increased solar cell processing will occur. This is especially true if the ribbon from the wide ribbon machine (capable of growing ribbon 7.5 cm in width) now coming on line provides silicon of the anticipated high quality with respect to impurities.

2. Silicon Ribbon Growth: CAST Method - IBM

The capillary action shaping technique (CAST) is based on the same principle as EFG growth (Fig. 4-21); i.e., it utilizes a die constructed from material which is wetted by molten silicon. Work under this contract is directed toward evaluation of the technical and economic potential of CAST for the preparation of silicon ribbon. The effort concentrates on (1) understanding and extrapolating the effects of growth conditions; (2) characterization of the ribbon, with special emphasis on the correlation of structure and electrical performance; and (3) economic analysis of silicon growth by this and other growth techniques.

The growing of ribbon at speeds of the order of 15 mm/min has been demonstrated. The structure of this ribbon in terms of twins, grain boundaries, and dislocations is quite comparable to that of the narrower ribbons as determined by in-house studies at JPL. In addition, according to studies made by both IBM and JPL, the spreading resistance profiles across the silicon ribbon indicate that fluid flow in the die influences the resistance profile of the ribbon. Figure 4-21 shows a resistance profile across a ribbon having a solid central core construction. This core apparently resulted in a nonuniform distribution of impurities at the solidification front, which produced the observed resistance changes. The effect is easily eliminated by changing the structure of the die.

Characterization efforts have continued to place emphasis on the correlation of lifetime measurements (by means of MOS capacitors) with structure. Results to date support the thesis that grain boundaries and dislocations degrade lifetime, whereas twins do not. Care must be taken to ascertain that twins are free of dislocations, since the occurrence of these features together is both frequent and deleterious.

Other characterization studies have investigated the formation of a surface film on the ribbon; such films tend to occur near the point at which growth is initiated. Analyses of the nature of this film have indicated it to be a silicon-carbide film growing epitaxially on the silicon. It has been observed that the density of the film is highest at low or zero ribbon velocities, suggesting that

a vapor transport mechanism is involved in its formation. At higher velocities, insufficient time at temperature is available for the formation of a significant amount of film.

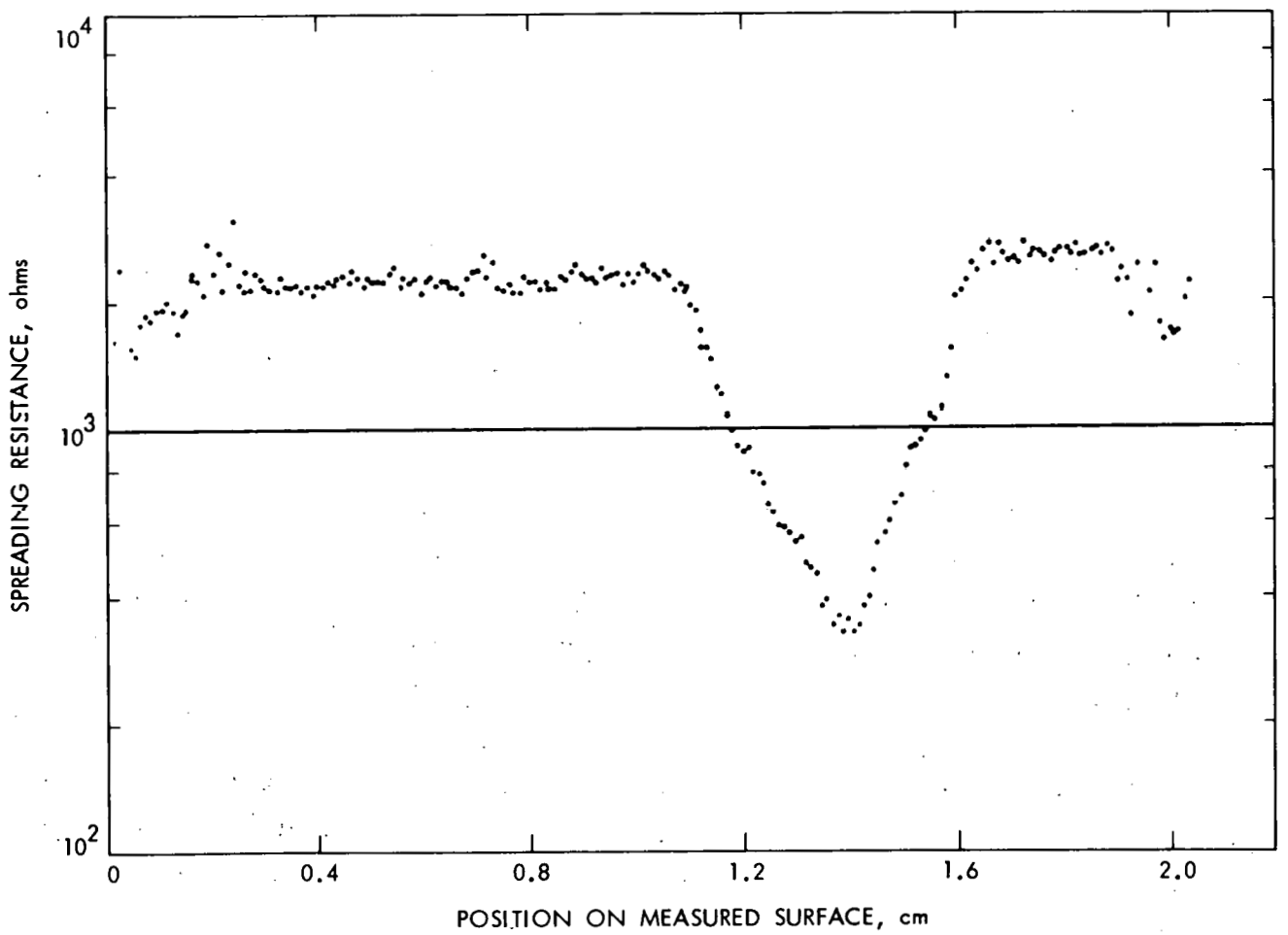

Fig. 4-21. Typical spreading resistance profile across the width of a CAST ribbon

Economic analyses of ribbon growth have suggested that major emphasis be placed on growing wider ribbon, to improve the cost-effectiveness of the CAST growth technique. The economic analyses suggest that the cost potential of single ribbon growth may obviate the need for multiple ribbon growth. This latter conclusion is, however, heavily dependent upon machine capitalization costs.

Economic analyses are also being extended into the area of Czochralski ingot growth and ingot cutting. A computer analysis which includes the various facets of this technology has been performed. Efforts here are continuing.

Plans for the immediate future include developing facilities for growing ribbons 50 mm and, eventually, 100 mm wide. Characterization and economic analyses will continue and completion during the next quarter is expected.

3. Silicon Ribbon Growth: Inverted Stepanov Technique - RCA

In this program emphasis is placed on developing a technique for growing ribbon-shaped silicon using a "non-wetted" die (Fig. 4-22). The use of the "non-wetted" die provides the possibility of minimizing the reaction between the molten silicon and the die material. Reaction between molten silicon and wetted dies is one source of degradation in the crystallographic quality of silicon grown using a wetted die (i.e., the edge-defined film-fed growth method). The introduction of the feed from above and the growth of the single crystal in a downward direction (the inverted Stepanov technique) in part compensates for the hydrodynamic drag in the slot and for the lack of capillary rise. (The capillary rise feeds the material to the die edge in the EFG method.) The inverted geometry also leads to considerable flexibility in the growth configuration when the feed is introduced from a molten zone at the end of a solid silicon rod.

The primary objective of the program is to investigate the basic seeding and growth processes involved in the growth of silicon sheet from "non-wetted" dies. The goal is to establish whether or not significant improvement in the crystallographic properties of the silicon can be realized by the use of "non-wetted" rather than "wetted" shaping dies. Silica and boron nitride shaping dies

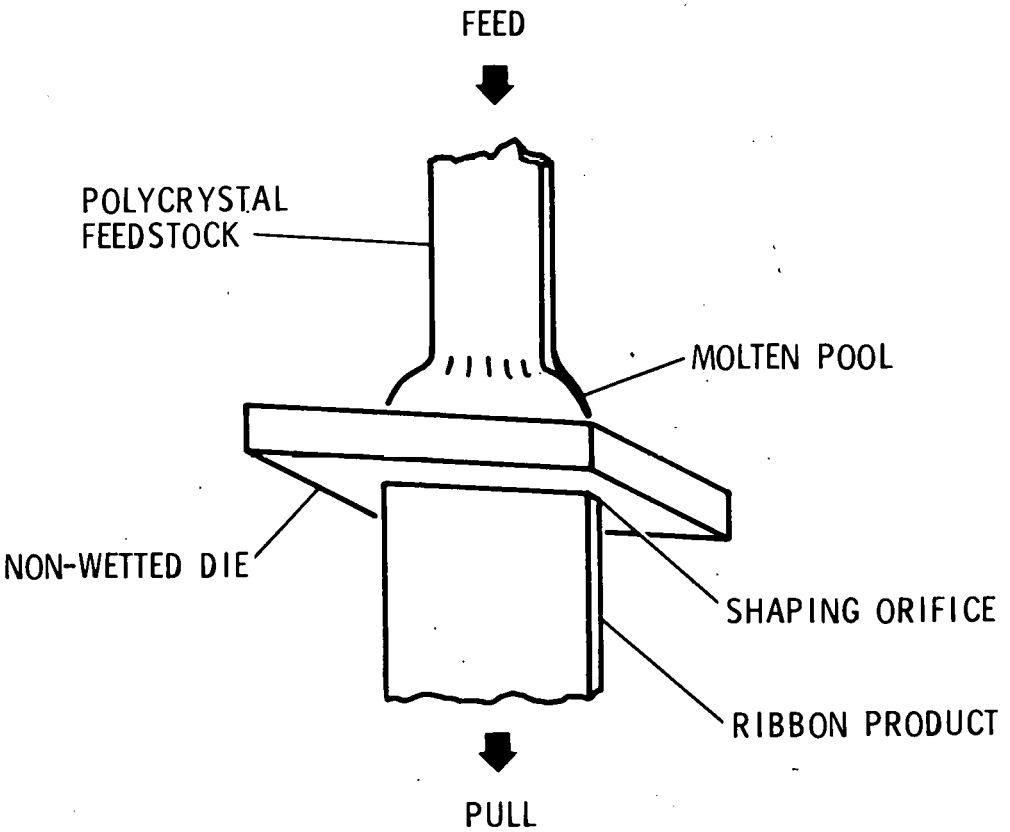

Fig. 4-22. Inverted Stepanov Technique - RCA

will be used. Methods will be sought to compensate for the lack of mechanical strength of silica at the growth temperature. Although boron nitride leads to unacceptable doping of the grown silicon ribbon, it is more rigid than silica and therefore is useful in the identification of fundamental limiting factors in the Stepanov growth method.

As yet, the problems associated with establishing stable growth conditions are unsolved. One of the major factors that leads to growth instabilities is the improper thermal gradients at the solid/liquid interface. The instability results either in freezing the ribbon to the die or in separating it from the melt. To date, adjusting thermal gradients (by using different thermal trimmers) and beveling the inner capillary edge to 45° have not alleviated the problem. During this quarter the actual thermal gradients that exist in the "V"-shaped susceptor-die configuration were measured (Fig. 4-23). The measurements show that

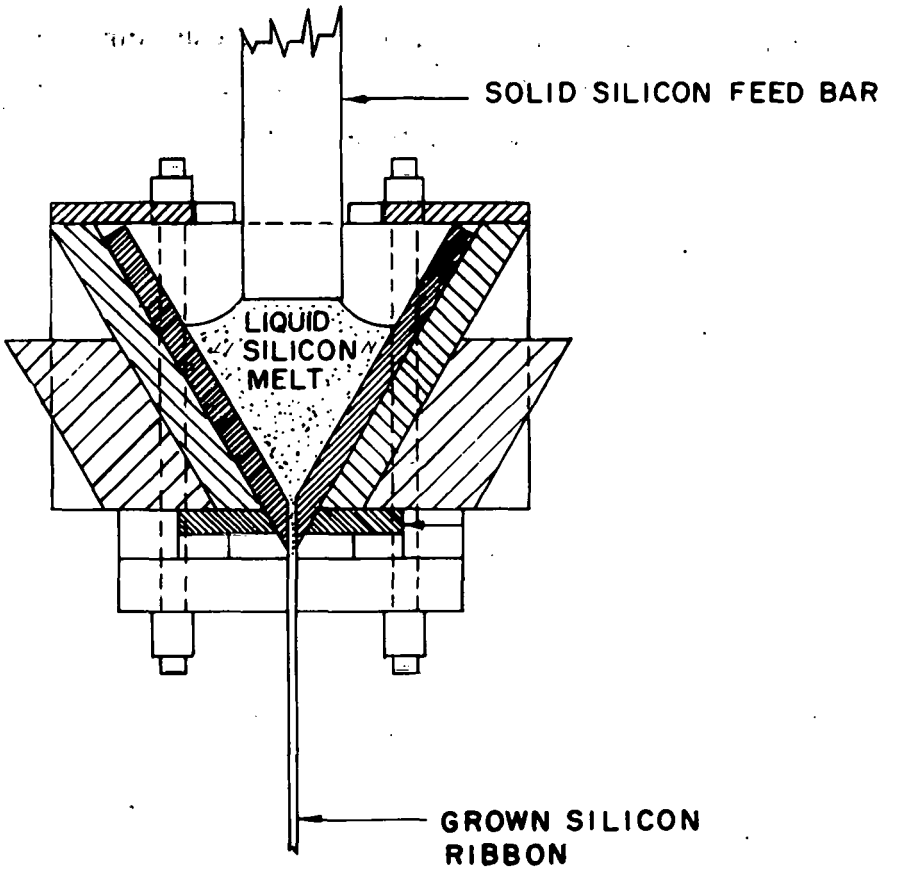

Fig. 4-23. Model 1 IST growth apparatus

the temperature at the middle of the slot is lower than along both sides of it. This is very unsatisfactory and efforts are under way to pump more heat in laterally, toward the slot.

Another factor which results in ribbon growth instabilities is the erratic wetting behavior of the liquid silicon with the fused silica. It has been observed that the silicon melt in the crucible and the die slot is in constant motion in the vertical direction. (This is not true for the boron nitride crucible-die in the same configuration.) Such erratic wetting behavior and mechanical vibration of the liquid silicon in the die slot affect the stability of the meniscus shape. To alleviate this problem, an auxiliary pressure differential was applied to bring the meniscus out of the die slot and to stabilize the growth.

Thermal analysis of IST ribbon growth continued during the report period. The model was used to examine the height of the molten zone as a function of growth velocity for a variety of ambient temperatures, die temperatures, and ribbon thickness. The calculations show that, above a velocity of 2.36 in./min, the zone height rapidly approaches a value of twice the ribbon thickness, suggesting that the geometry of the growing ribbon may change or, if the molten zone is sufficiently unstable, the ribbon may separate at the die top.

In summary, the simulation has led to the following conclusions:

1) The zone height increases with growth velocity, and does so more and more rapidly as a critical growth velocity is approached.
2) The critical growth velocity is, approximately, that velocity which leads to the generation of a latent heat of fusion just equal to the heat conducted away from the die by a stationary ribbon under the same thermal conditions.
3) The highest growth rates are achieved for the coolest ambient temperatures and some increase in growth rate is seen when either the die temperature or the ribbon thickness is decreased.

Milestones related to the growth demonstrations have been delayed by at least 2 months. However, achievement of the overall goals on schedule is still possible.

Plans for the next quarter are specifically directed toward solving the growth instability problems. With proper thermal modifiers and the application of a pressure differential, the problem may be eliminated. One of the first modifiers to be tested is a pyrolytic graphite plate, with regular graphite at the periphery to couple more efficiently to the rf field and, thus, to pump more heat laterally into the pyrolytic graphite plate.

4. Silicon Ribbon Growth: Web-Dendritic Method - University of South Carolina

Web-dendritic growth makes its own guides of silicon, whereas most other ribbon processes must rely on materials other than silicon for the guides

(i.e., dies) (Fig. 4-24). The guides are thin dendrites that grow ahead of the sheet and support the molten silicon between them to form the sheet. The dendrite guides grow in a very precise orientation dictated by their unique growth habit. Thus the orientation of the sheet which grows between them takes on this precise orientation. The twin plane reentrant edge mechanism (TPREM) controls the growth of the edge dendrites, giving them their unique and internally-controlled growth direction allowing them to grow ahead of the sheet and thus acts as guides.

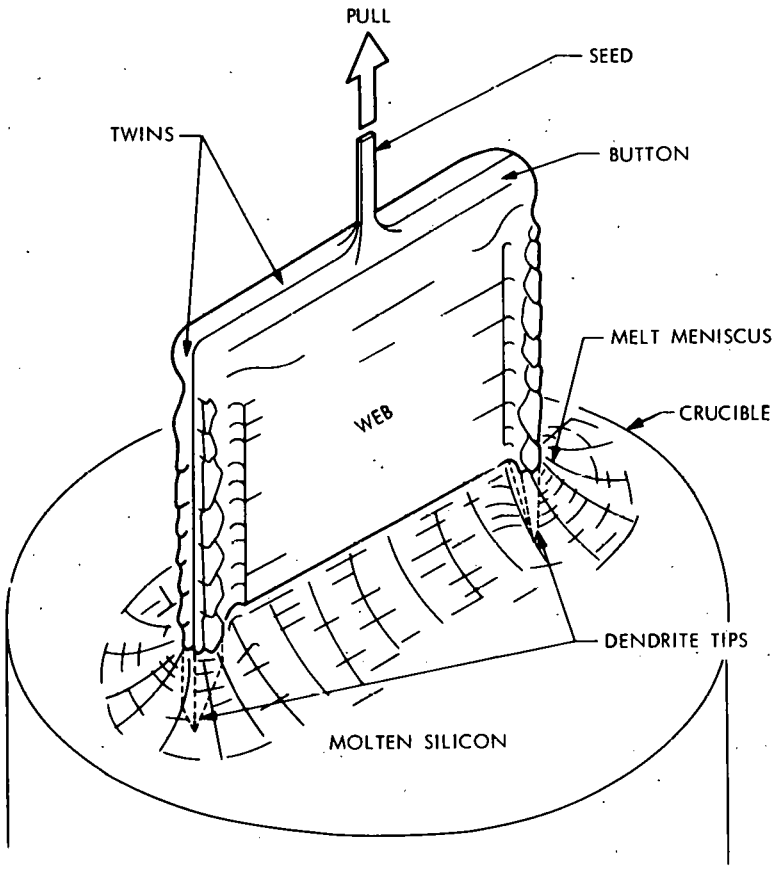

Fig. 4-24. Web-dendritic growth - University of South Carolina

The basic steps, then, in web sheet growth are (1) dip a seed of the proper orientation into a slightly undercooled melt, (2) hold the seed stationary while growth takes place laterally on the surface of the melt, forming what is termed the button, and (3) when the lateral growth has proceeded to the desired width, start the pulling. As the pulling proceeds, two coplanar dendrites grow downward from each end of the button, propagating to a depth of 1-3 mm beneath the surface of the melt. As the button and its dendrites emerge from the melt, silicon is pulled up between them by surface tension, and the resulting sheet solidifies just above the melt surface. The unique orientation and slight undercooling to insure faceted growth give the sheet its almost mirror-flat surface finish. The overall goal of this contract is to develop a better understanding of the web-dendrite process and define in greater detail the basic limitations to the process (especially the maximum growth rate and width).

As yet, the contractor has not been able to sustain web growth after button formation. Considerable work has been completed in the investigation of the effect of changes in the thermal geometry of the furnace. Although shield geometries have been found to optimize button growth and two-dendrite formation, no arrangement of the shields has been found that is suitable for sustaining web growth between the two dendrites. One potential problem that has been identified is the size of the seed initially utilized for button formation. The seed crystals are now etched to a small point. A second problem is the transient initial phase in the starting web formation after button formation (i.e., the growth rate may have been changed too abruptly by temperature changes). A comparison of growth techniques with those employed at Westinghouse revealed a difference in thickness of the top susceptor. The shielding at both the top and the bottom of the susceptor has been modified, but stable web growth has not yet been achieved.

Work has continued on the thermal analysis of the dendritic web growth. A major result of this analysis has been the prediction that, with the present furnace geometry, there exists an upper limit on the pull rate of approximately 4 cm/min. This prediction is based on the assumption that a minimum supercooling temperature of 1407°C must be maintained at the surface of the melt in order to

sustain dendritic-web growth. To increase the pull rate beyond this upper limit of 4 cm/min will require a furnace geometry which allows an increased removal of the latent heat generated at the solid-liquid interface.

The contractor (University of South Carolina) has failed to meet the milestone of producing web growth at the state of the art of 1965. It is believed unlikely they will be able to produce 2-cm-wide web. Without this baseline capability, they will not be able to evaluate changes to increase the width (5 cm as a goal) and to increase the pull (5 cm/hr as a goal).

JPL Characterization of Web-Dendrite Samples

The contractor has sent JPL numerous dendrite samples and a few web samples. The widest sample was approximately 1 cm. This sample was very asymmetric in cross section. Spreading resistance data indicated minimal resistivity changes in the dendrite and web regions. Upon further examination, this sample was found metallographically to contain a third dendrite within the web. However, there was no evidence of the third dendrite based on spreading resistance measurements.

Because of the limited and very narrow samples supplied, it is unlikely JPL will be able to characterize the samples. No characterization work is planned unless the contractor solves this web-growth problem and supplies larger samples.

5. Silicon Ribbon Growth: Laser Zone Growth in a Ribbon-to-Ribbon Process - Motorola

The ribbon-to-ribbon process is basically a float-zone crystal growth method in which the feedstock is a polycrystalline silicon ribbon (Fig. 4-25). The polysilicon ribbon is fed into a preheated region which is additionally heated by a focused laser beam, melted, and crystallized. The liquid silicon is held in place by its own surface tension. The shape of the resulting crystal is defined by the shape of the feedstock and the orientation is determined by that of a seed single-crystal ribbon.

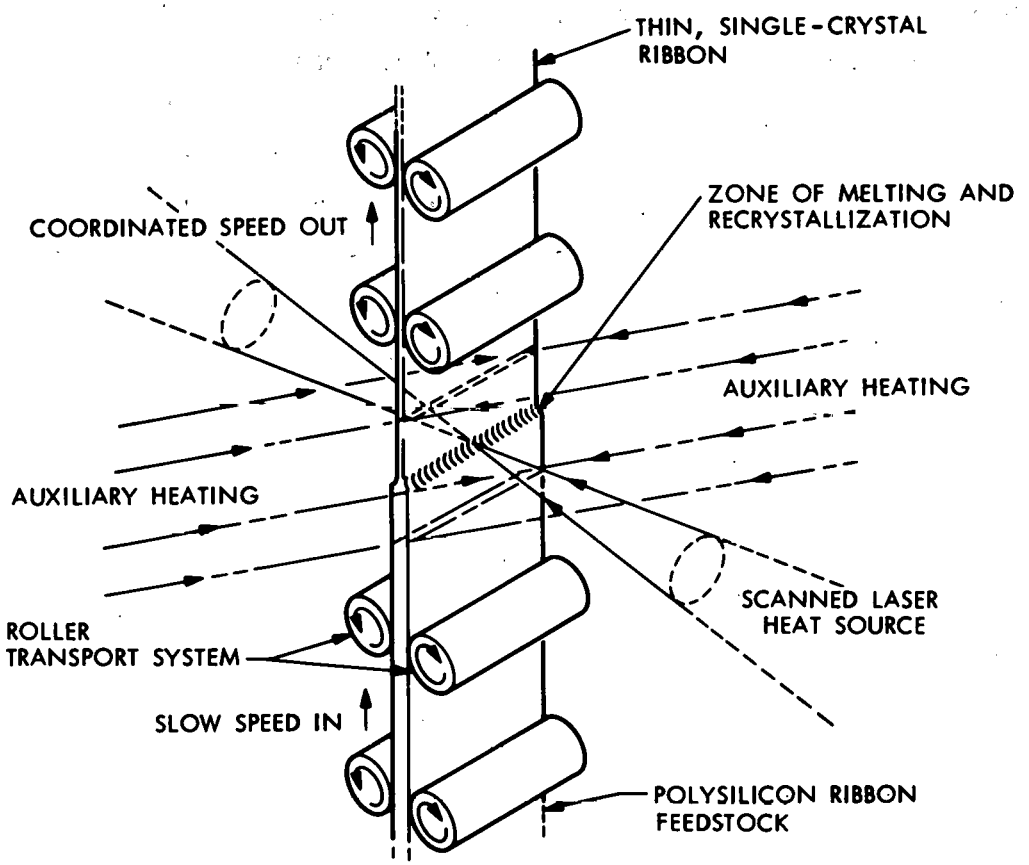

Fig. 4-25. Laser zone crystallization - Motorola

The primary efforts under this contract are to:

- Modify and evaluate the existing ribbon-to-ribbon growth facility to meet the contract goals.
- Operate the facility on a regular basis to study and optimize the growth capabilities of the ribbon-to-ribbon process with particular emphasis on thermal environment, seeding, ribbon velocity, laser input configuration, and throughput.
- Perform characterizations/tests on ribbon samples from each growth run.
- Fabricate and characterize solar cells.

During this report period, major emphasis was placed on achieving higher growth speeds and studying the effect of post-heating on stresses. An order of magnitude increase in growth speeds was achieved (0.25 cm/min to 2.5 cm/min). The width was limited to 1.27 cm. Normally, at such growth rates the ribbons shatter because of thermal stresses. However, such stresses were minimized by post-heating using radiant lamps. As a result, 1.27-cm-wide ribbons were routinely grown at 2.54 cm/min.

An infrared stress-birefringence technique was set up to assess thermal stresses in the ribbons. In the absence of post-heating the stresses are approximately 13.5 kilopounds per square inch. It was found that the post-heating reduced the stress level considerably.

Growth experiments have been initiated to study the effects of a curved melt configuration on grain enhancement and stresses. The curved melt is accomplished by means of simultaneous horizontal and vertical beam deflection and can provide "convex solid" or "concave solid" interfaces. Results so far are encouraging; early experiments have demonstrated single-crystal material from polysilicon ribbon after 2 inches of travel with a curved melt.

Work under this contract is on schedule and no perturbations are expected. Major plans for the next quarter are as follows:

1) Study stress relief by means of gradient-controlled post-heater.
2) Grow wider ribbons.
3) Achieve faster growth.
4) Make diffusion length and solar cell efficiency measurements.

JPL Characterization of Ribbons from the Ribbon-to-Ribbon Process

It was observed in earlier experiments that ribbons produced by the ribbon-to-ribbon (RTR) process exhibited very uniform resistivity distribution. These were ribbons grown from single crystal feedstock. During this report period, Motorola sent JPL a ribbon grown using surface-doped polycrystalline feedstock.

Again, the resistivity was quite uniform both across the width of the ribbon and in the bulk (Figs. 4-26 and 4-27). The variation has some dependence on the grain boundaries (Fig. 4-28).

An interesting observation was made on the dislocation content of these RTR ribbons. The dislocation density is very high, contrary to the results of JPL's earlier analysis. It was accidentally noticed that the "focused-beam-side" (dull side) has a high density of etch pits, which have probably occurred because of thermal etching. Similar pits are not present on "mirror side". (See Fig. 4-29.) Sirtl etching of that side does not readily reveal the pits and hence the earlier observation was misleading. As can be seen from Fig. 4-29, these pits are crystallographic in nature, i.e., rectangular in (100) region and triangular in (111) region. Another observation, which is based on very small number of samples, is that the ribbons grown with polycrystalline feedstock do not show this feature. More work is planned to explore this. Electron-beam induced current observations have not shown anything significant to date.

Lifetime (τ, by MOS capacitance-time), diffusion length (L, by surface photovoltage), and solar cell measurements were made on ribbons "grown" from single-crystal feedstock. MOS capacitance-time and surface photovoltage measurements were made on the same ribbon. The τ by capacitance-time measurements shows wide variation and no correlation either with structure or with the L by surface photovoltage. τ varies from 0.1 μsec randomly whereas L varies from 7 to 40 microns, the higher L being in the unmelted region. Solar cell measurements suffer from the lack of good metallization process and do not exhibit good fill factors. The efficiences of the cells from the regrown material are degraded in comparison to those prepared from the single-crystal feedstock (50-60%).

6. Silicon Sheet Growth: Dip-Coating on Low-Cost Substrates - Honeywell

This program is directed toward the formation of thin silicon films by withdrawing suitably prepared ceramic substrates from a pool of molten silicon (Fig. 4-30). Ceramics were selected because of their superior thermal expansion match with silicon and the greater ease with which this expansion may be

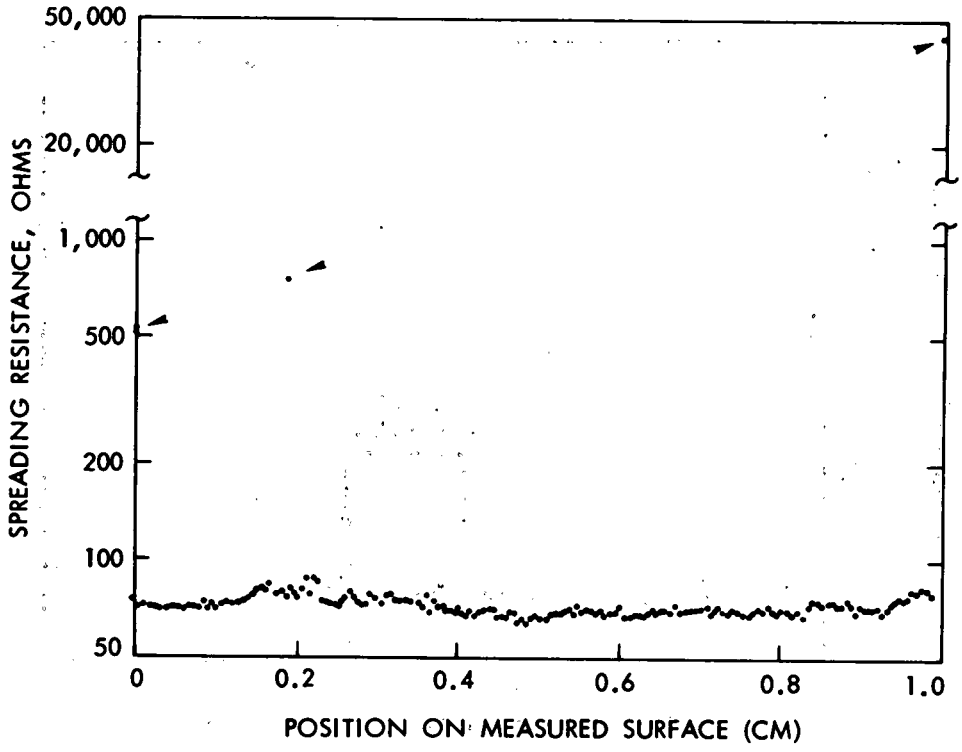

Fig. 4-26. Spreading resistance profile across RTR ribbon (Motorola sample 235), produced from surface-doped polycrystalline feedstock

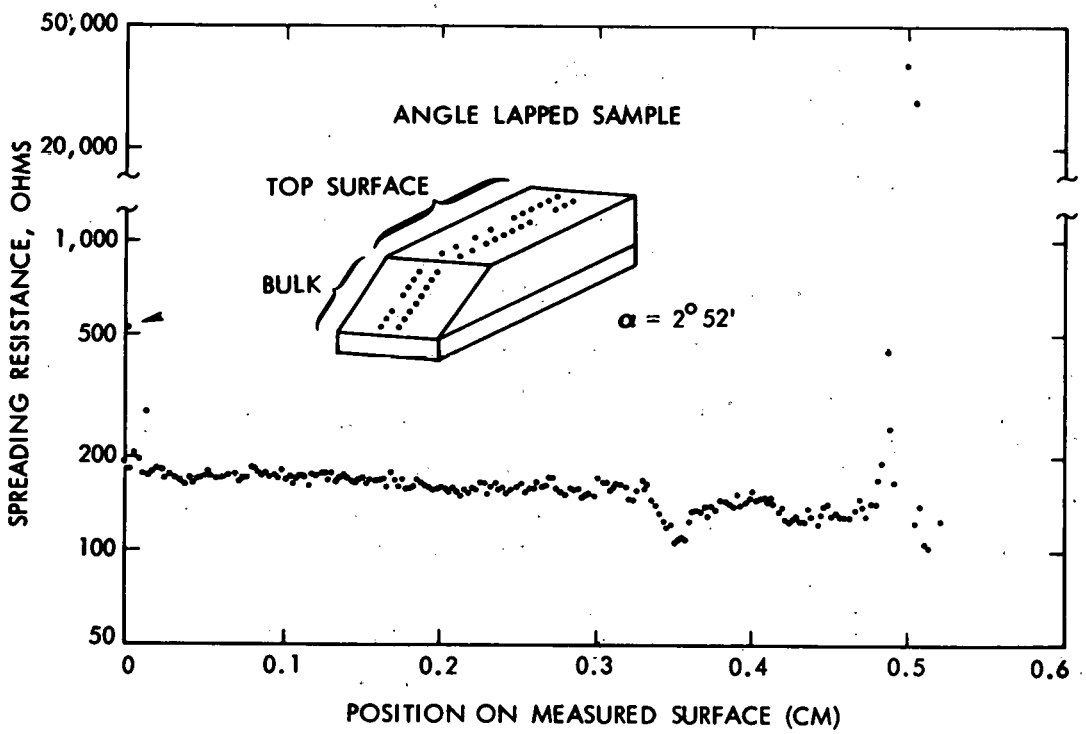

Fig. 4-27. Spreading resistance profile across angle-lapped RTR ribbon (Motorola sample 235-1), produced from surface-doped polycrystalline feedstock

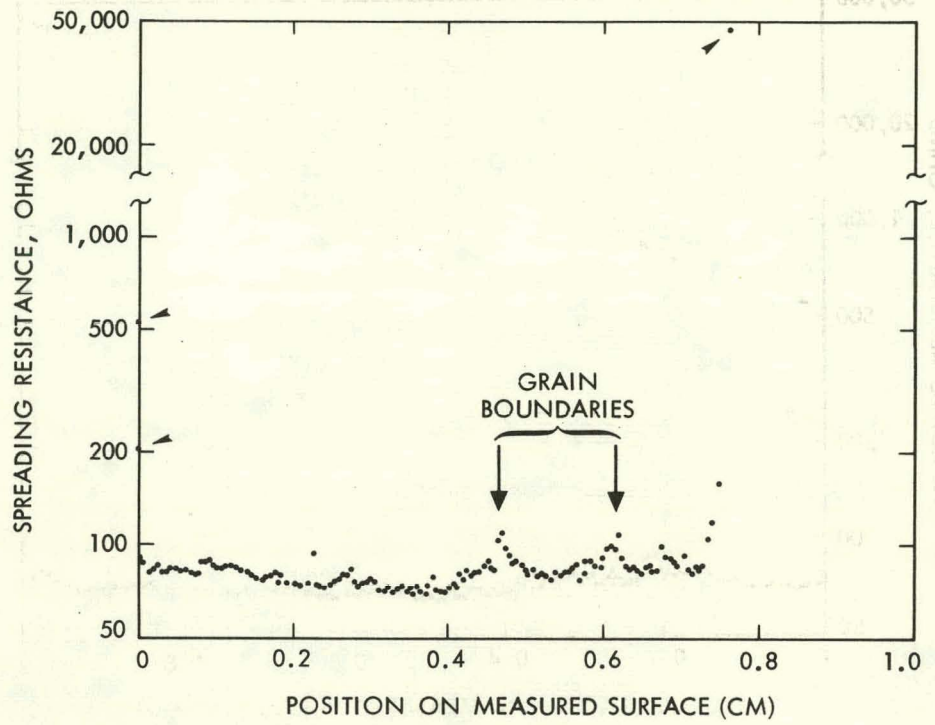

Fig. 4-28. Spreading resistance profile across RTR ribbon (Motorola sample 235), produced from surface-doped polycrystalline feedstock — note effect of grain boundaries

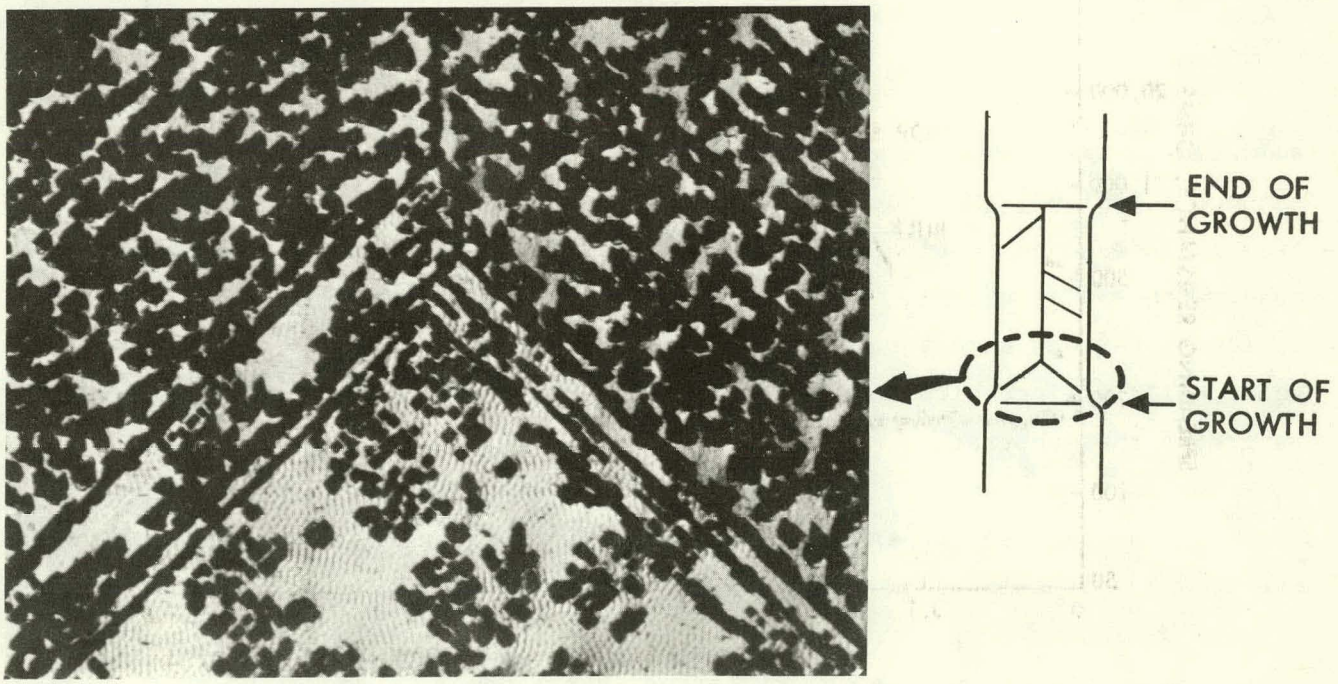

Fig. 4-29. Photograph of "focused-beam-side" of RTR ribbon showing etch pits

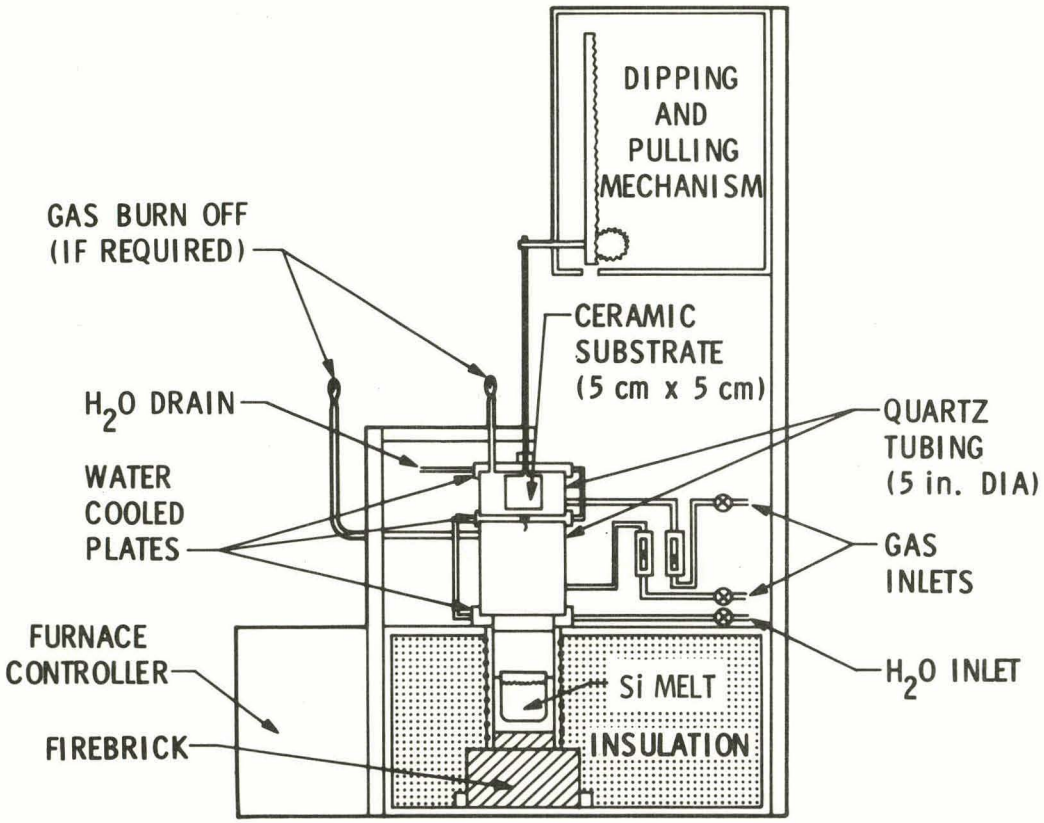

Fig. 4-30. Cross-sectional sketch of basic sheet dip coating growth facility - Honeywell

adjusted. The ceramics are coated with a film of carbon or silicon carbide to enhance adhesion. The concept has been demonstrated previously. The total program includes construction of a dipping facility, selection and evaluation of substrates and associated coatings, production of dip films and their characterization by various structural, chemical, and solar cell performance methods. The solar cells will require some specialized techniques because of the nonconductive nature of the substrate.

During the report period, the test facility was used extensively for preparing films of silicon on ceramic substrates. Emphasis was placed on defining process variables — withdrawal rates, temperatures, and film thicknesses — as well as evaluating a variety of different substrates. In addition, the characterization of the silicon films has continued. This characterization has included structural, chemical, and electrical analysis.

Various substrates have been used to date, including mullite ($2SiO_2 \cdot 3Al_2O_3$), aluminum oxide, zirconium silicate, calcium aluminate, carbon-sintered SiO_2, and pressed fibrous insulation. The mullite substrates have proved to be the most satisfactory and, since this material offers the additional advantage of being low in cost, emphasis has been placed on its use.

Other significant effort during the report period was directed toward evaluating the effect of process variables on the silicon films produced. An initial evaluation indicated that film thickness decreases with increasing melt temperature and withdrawal velocity. It appears that temperatures within a few degrees of the melting point will be desirable in order to achieve films thicker than 10 microns and withdrawal rates of more than 1 mm/sec. However, it was also learned that changes in the thermal environment into which the substrate is withdrawn, had a significant influence on the film thickness obtained. Initial films in the 50-100 micron thickness range had been obtained with a different baffling environment than that used for the evaluation of growth parameters. Results are presently being analyzed to provide requirements for more appropriate baffling. The angle of withdrawal of the substrate from the silicon bath has not yet been evaluated.

These efforts to define process variables, and the minor, but time-consuming, experimental difficulties encountered in the course of this work, have prevented efforts to improve the grain structure of the silicon films produced to date. Such efforts would include optimization of dipping conditions as well as substrate characteristics. These delays may affect achievement of the 5-mm grain size goal.

Efforts are also continuing in characterization of the silicon films produced. Structural characterization indicates elongated grains, approximately 1 mm by 1 cm, with some twinning. Little, if any, grain structure lies in a plain parallel to the substrate surface. Chemical and electrical analyses of the films have been frustrated by the rather unique form of the silicon film produced by this process. Preliminary chemical analyses by X-ray emission spectroscopy by both the contractor and JPL have indicated no gross contamination from the

substrate. Infrared analysis of silicon that has been in contact with the mullite for a period of time has indicated aluminum concentrations of the order of $10^{16}/cm^3$; however, it has not yet been possible to make such analyses on the films in situ.

Electrical analyses to date have continued to yield promising but not definitive results. Initial photodiode results have provided conversion efficiencies of the order of 5% when corrected for series resistance resulting from the thin film. Spreading resistance data, both at JPL and at the contractor's site, have not been informative. No reproducible effects which might be associated with impurities or structure have been observed. Fig. 4-31 shows no apparent change in resistivity as one approaches the silicon-mullite interface.

Plans for the next quarter involve significantly increased emphasis on electrical measurements and solar cell preparation in order to provide more definitive results as to the electrical performance potential of the material being produced. Further efforts are being directed toward improving the definition of processing variables, including the role of dip-angle. In-house measurements at JPL for both electrical and structural characterizations are planned.

7. Silicon Sheet Growth: Chemical Vapor Deposition on Low-Cost Substrates - Rockwell International

The purpose of this contract is to explore the chemical vapor deposition (CVD) method for the growth of silicon sheet on inexpensive substrate materials (Fig. 4-32). Specific technical goals established for the contract include the following:

Silicon sheet:	
Area (per sample)	30 cm^2
Deposition rate	5 μm per minute
Thickness	20 to 100 μm
Crystal structure	100 μm average grain size
Intragrain dislocation density	$<10^4$ per cm^2

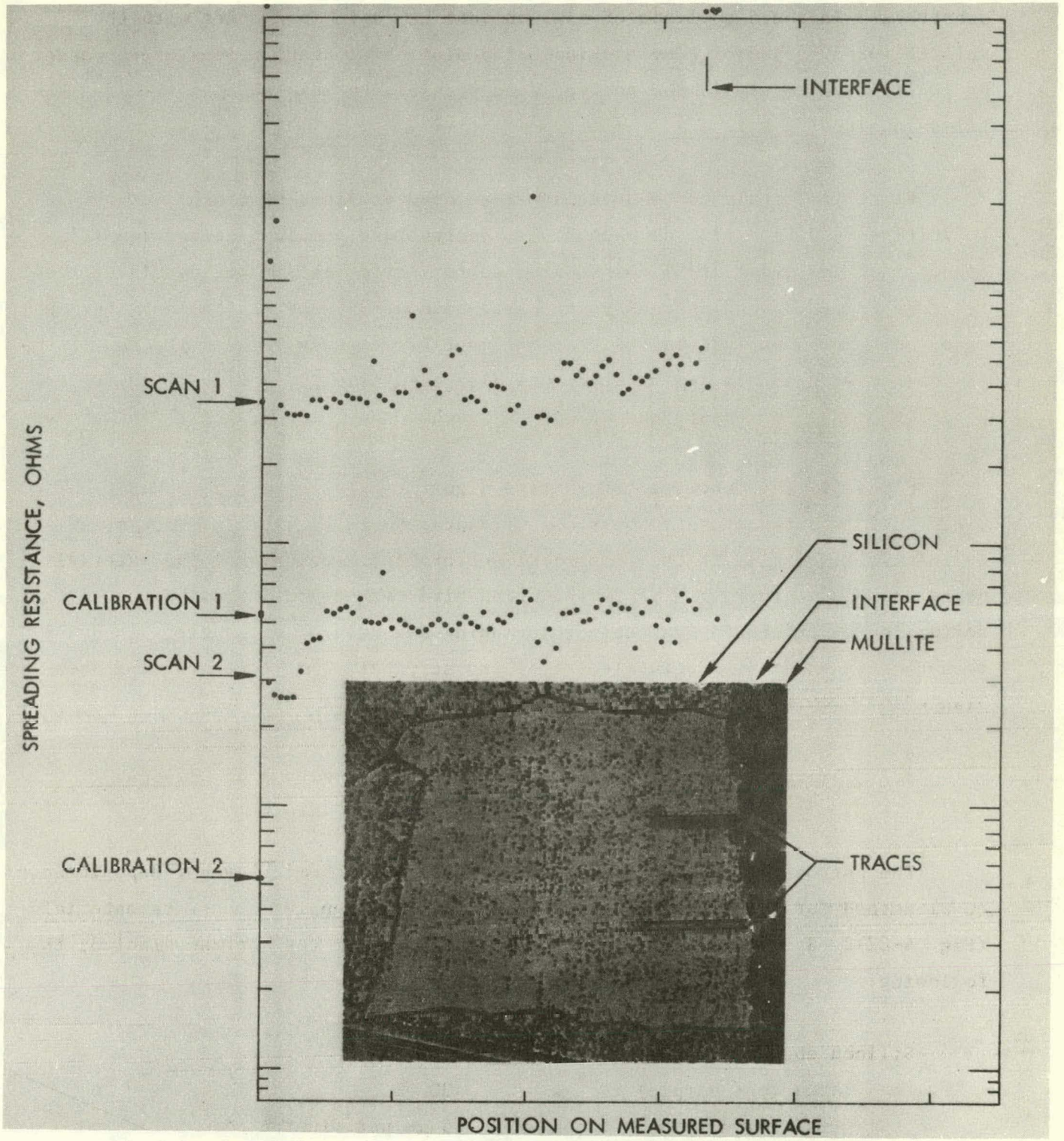

Fig. 4-31. Two spreading resistance scans of region shown in micrograph (Honeywell sample MR-7). Probe separation was 100 μm, with 45 gram load. Specimen surface was angle lapped at 30° and step increment was 0.5 µm. Cal.=0.51 Ω-cm.

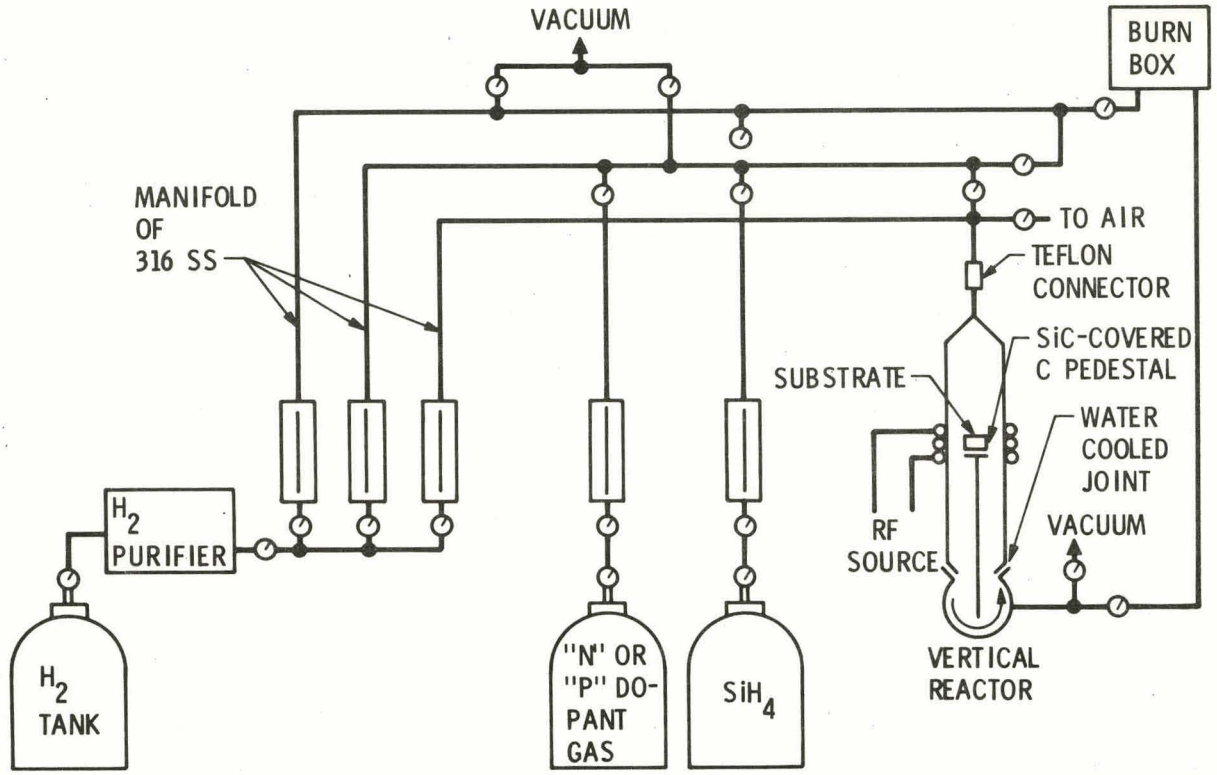

Fig. 4-32. Chemical vapor deposition on low-cost substrates - Rockwell International

The contract program is structured in terms of six main technical tasks, as follows:

- Modification and test of an existing CVD reactor system.
- Identification and/or development of suitable inexpensive substrate materials.
- Experimental investigation of CVD process parameters using various candidate substrate materials.
- Preparation of silicon sheet samples for various special studies, including solar cell fabrication.
- Evaluation of the properties of the silicon sheet material produced by the CVD process.

- Fabrication and evaluation of experimental solar cell structures by Optical Coating Laboratories, Inc., using standard and near-standard processing techniques.

As applied to silicon sheet growth, the method involves pyrolysis, or reduction, of a suitable silicon compound at elevated temperature and approximately atmospheric pressure. A laboratory-type CVD reactor system with a flow-through (open-tube) vertical deposition chamber is used for these investigations. The substrate is mounted on a silicon carbide-coated carbon pedestal heated by an rf coil external to the chamber. The reactor system has been extensively modified by installation of mass flow controllers, automatic process sequence timers, and special bellows-sealed air-operated valves. This system, which has a capacity of 30 cm^2, is used as a research vehicle in an attempt to reach the goals of 100 μm grains deposited 20 to 100 μm thick on inexpensive substrates at rates up to 5 μm per minute.

The properties of the silicon sheet are determined by deposition temperature, reactant concentrations, the nature of the carrier gas, the silicon source compound used, growth rate, doping impurities (added by introduction of appropriate compounds into the carrier gas stream), and the properties of the substrate.

By the end of October, 169 runs, many with multiple samples, had been made in the reactor. Both the substrates and the resulting films were characterized structurally and electrically by a wide variety of techniques, and solar cells were made in some cases.

Since most CVD experience has been with sapphire substrates, polycrystalline alumina (the low-cost substrate most closely resembling sapphire crystallographically) was the first to be extensively investigated. A number of fine-grain substrates were examined by X-ray diffraction (which showed some preferred orientation), scanning electron microscopy (which showed grain sizes of 0.4 to 1.1 μm), and surface profilometry (which indicated peak-to-valley dimensions of 0.1 to about 0.35 μm). The best silicon films grown on these substrates were made at 1025°C in a H_2 carrier gas. They had a strong preferred (100) orientation and surface features, apparently grains, over 5 μm across.

Several high-temperature glasses have been found that will withstand the reaction chamber environment if helium is used as the carrier gas. As Table 4-14 shows, the dimensions of the surface features (probably grains) are greatest at intermediate temperatures, but faceting and degree of preferred orientation are greatest at the lowest temperature.

Boron-doped films, made by adding B_2H_6 to the gas stream, were electrically characterized using both Hall bar and van der Pauw structures. At high boron concentrations, films on polycrystalline alumina are electrically almost the same as those on the sapphire controls, but at moderate doping, majority carrier mobility is much lower and hole concentration is slightly lower on alumina than on sapphire.

Table 4-14. Structural properties of CVD Si films grown by SiH_4 pyrolysis in He on Corning Code 1715 glass

Deposition Temp. (°C)	Average Film Thickness (μm)	Deposition Rate (μm/min)	Ave. Horiz. Dimension of Surface Features (μm)	Preferred Crystal Orientation by X-Ray Analysis*
858	5.9	0.6	0.9	VS {100}; FS {111}; A {110}
914	14	1.4	3.5	FS {100}; FS {111}; P {110}
955	16	1.0	4.0	P {100}; P {111}; FS {110}
1000	20	1.0	3.3	P {100}; P {111}; P {110}

*VS = very strong; FS = fairly strong; P = preferred, but only moderately; A = not detected.

A number of two-step processes have been proposed in which the nucleation and growth are done under different conditions in hopes of achieving larger grain size. The first of these involved depositing a thin full-coverage layer from SiH_4 and then adding HCl to the stream to preferentially etch the smaller grains, but no dramatic improvement was seen.

Twenty-one samples have now been subjected to solar cell processing (for Rockwell by Optical Coating Laboratory, Inc.). These research structures are not expected to have high efficiency — the contacting methods are not designed for that purpose — but they do provide some comparison from one sample to the next. Cells on sapphire controls give slightly lower voltage and considerably lower current than on Czochralski silicon and the cells on polycrystalline alumina give even lower voltages and currents. These were diffused junctions on high-temperature-coefficient substrates, however, and may not give a good estimate of what could result from CVD junctions (which would be used for production) on well-matched glass substrates.

There have been a series of problems with the mass flow controllers in the reactor, which now seem to be solved, but they did slow down the two-step experiments and the electrical characterization. Accordingly, a number of minor milestones in the program were rewritten or rescheduled to allow concentration of effort in the grain-growth area.

In the next quarter, the remaining two-step experiments will be vigorously pursued and emphasis will shift toward glass substrates.

JPL Characterization of CVD Silicon Films on Low-Cost Substrates

An attempt was made to measure diffusion length on CVD films by surface photovoltage, but the surface conditions degraded the signal too much for useful measurements. Better results are hoped for using solar cell structures.

8. Silicon Sheet Growth: Chemical Vapor Deposition on a Floating Silicon Substrate - General Electric

The purpose of this contract is to demonstrate the feasibility of growing silicon sheet on a floating silicon substrate (Fig. 4-33). In the process single crystal silicon is formed by direct epitaxial conversion from gaseous silane. In an appropriate reactor, silane is passed over silicon substrate which is supported on a thin film of molten tin. Single crystal silicon grows to the desired thickness by vapor phase epitaxy. Nucleation of fresh substrate silicon takes place at one end of the reactor where the edge of the growing sheet is in contact with a region of the tin which is supersaturated with silicon. The process lends itself to continuous operation, with the finished sheet being withdrawn from the opposite end of the growth zone. The major portion of the program will focus on nucleation studies and the rapid growth of silicon substrate from supercooled melts. These efforts should lead to a sheet growth demonstration by the end of the first contract year and a design and cost analysis for a prototype sheet growth apparatus by contract close. Explicit studies for the contract include:

- Supercooling in Sn-Si melts.
- Crystal growth from a supercooled Sn-Si melt.
- Silicon uptake by tin from silanes.
- Surface growth.
- Prototype design and cost analysis.

The technical goals for the contract require growth of a single crystal of silicon having an area of 0.5 cm^2 and the determination of the propagation velocity of single crystal silicon growth along a supersaturated hot tin melt surface.

During the report period the seeded growth furnace was completed and operated. Optimum thermal geometry, liquid circulation, gas flows, and withdrawal rates are being determined.

Thin surface growth of silicon has been obtained with growth velocity of 5 to 6 mm/min. This growth has generally taken the form of a layer of interlocking crystals which is thin enough to follow the liquid surface. In one case its

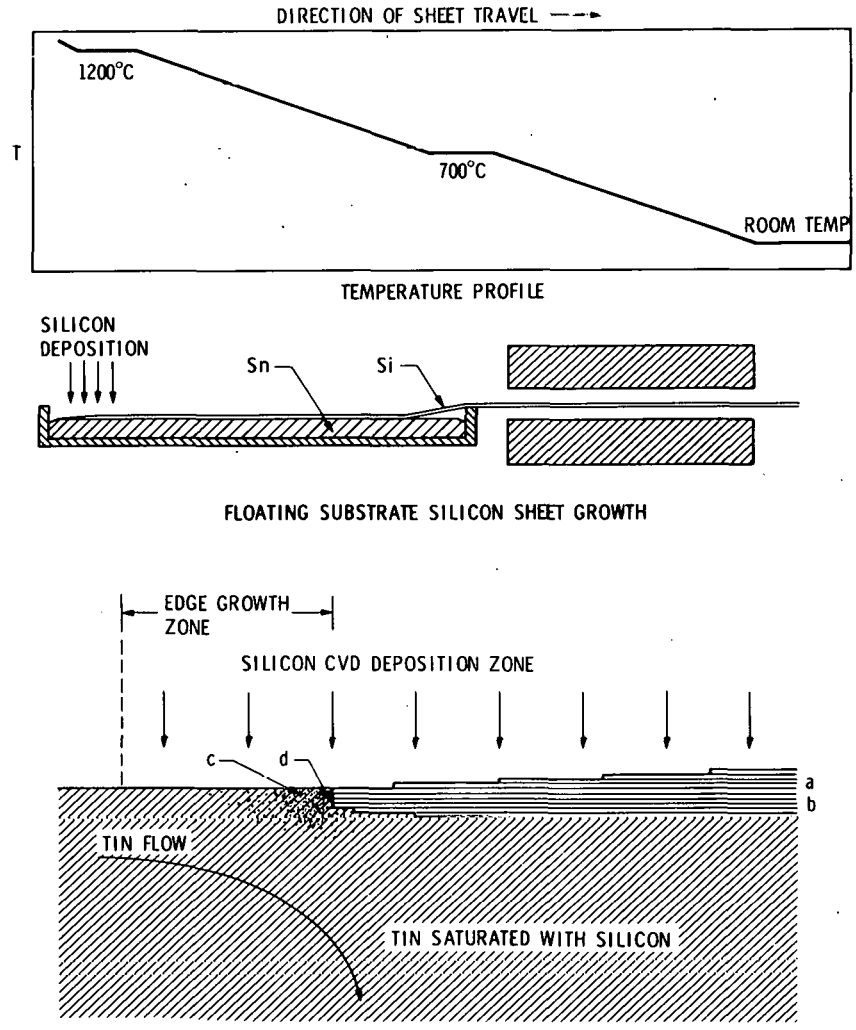

ENLARGED SCHEMATIC VIEW OF GROWING EDGE OF SHEET. (a = FIRST FEW ATOMIC LAYERS OF EPITAXIALLY DEPOSITED SILICON, b = THIN LOWER LAYER FORMED BY GROWTH FROM SILICON SOLUTION, c = SURFACE OF LIQUID TIN SUPERSATURATED WITH SILICON BY DEPOSITION FROM VAPOR PHASE, AND d = LEADING EDGE)

Fig. 4-33. Silicon sheet growth through chemical vapor deposition on floating silicon substrate - General Electric

thickness was determined to be 20 microns. Although this surface growth is not single-crystalline, it was induced to grow from a seed crystal by controlled supercooling and demonstrates the feasibility of controlled, rapid surface growth.

General Electric's efforts are currently focused upon identifying and eliminating those factors which are responsible for the poor crystal quality of the surface growth. The most evident of these is the presence of foreign material on the surface of the melt, which often collects on the end of the seed crystal. This material is produced by a reaction between the Sn-Si alloy and the tray material (which has been either fused quartz or boron nitride in experiments conducted thus far), and by reaction with nitrogen, which has been a principal component of the furnace atmosphere. The seeded growth furnace has been rebuilt using a molybdenum susceptor which supports a box-shaped tray; this tray can be made from a number of refractory materials such as sapphire, beryllia, or tungsten. It is anticipated that this new design will eliminate the foreign material on the melt surface and lead to improved crystal structure.

A series of experiments was performed to determine whether the reactor gas streams were contamination sources. Nitrogen was found to react with silicon slices at 1100°C and coat their surfaces with a film 30-150 Å thick. Silicon slices heated in hydrogen at temperatures between 1000°C and 1200°C maintained a very clean "film-free" surface. On the basis of these results, future experiments in the seeded growth furnace will be conducted using atmospheres that are free of nitrogen.

9. Silicon Sheet Growth: Hot-Forming of Silicon - University of Pennsylvania

This contract is designed to determine the feasibility of hot-forming silicon in a cost-effective manner. The procedure to be followed is high-strain-rate ($\dot{\epsilon}>1$), high-compression deformation of silicon. From this information, one can construct the hot-forming diagram for silicon and make some extrapolations of the economics of the process. The program also includes evaluations of metallurgical properties such as hot-forming texture, recrystallization texture and grain size, and of electrical properties.

Compression testing within the maximum strain rate capabilities (8×10^{-2} sec^{-1} at 1100-1380°C) of the Instron Machine was completed during the report period. Higher strain rate tests (1 to 10 sec^{-1}) are being initiated on the MTS machine. For several data points, preliminary agreement between the results on the Instron machine and MTS machine has been obtained. Texture measurements show that each successive deformation results in a $\{110\}$ orientation along the compression axis and a $\{111\}$ orientation along the reference (needle crystal) axis. Each subsequent successive annealing results in a $\{100\}$ orientation along the compression axis and a $\{110\}$ orientation along the reference axis. The deformation texture work is almost complete; a few tests remain to be run on cast polycrystalline samples.

The recrystallization work is on schedule. Data points for several time-and-temperature curves as a function of percentage of recrystallization have been obtained. These include annealing periods up to 40 minutes, temperatures at 1380°C, and true strains to about 0.6. Crystallite sizes to approximately 0.3 mm have been observed in these tests.

During the next quarter, data on high strain rates (1 to 10 sec^{-1}) should be obtained. From these data, one should be able to predict whether high rolling speeds and minimal annealing cycles are possible for hot-forming silicon.

JPL Effort

Several doped ingot samples were prepared by JPL and sent to the University of Pennsylvania for deformation testing. These samples included (1) millimeter-sized grains, (2) large twin grains, and (3) single crystal grains. From these samples, the University of Pennsylvania investigators can unambiguously determine the effect of prior structure on deformation texture. In addition, these samples were p-type 1 ohm-cm material which will enable the evaluation of some electrical properties. Further work will be performed when JPL receives back the deformed doped samples.

10. Ingot Growth: Heat Exchanger Method - Crystal Systems

The Schmid-Vicchnicki technique (heat-exchanger method) has been developed to grow large single-crystal sapphire (Fig. 4-34). Heat is removed from the crystal by means of a high-temperature heat exchanger. The heat removal is controlled by the flow of helium gas (the cooling medium) through the heat exchanger. This eliminates the need for motion of the crystal, crucible, or heat zone. In essence this method involves directional solidification from the melt where the temperature gradient in the solid might be controlled by the heat exchanger and the gradient in the liquid controlled by the furnace temperature.

The overall goal of this program is to determine if the heat-exchanger ingot casting method can grow large silicon crystals (6 inches in diameter by 4 inches in height) in a form suitable for the eventual fabrication of solar cells. This goal is to be accomplished by the transfer of sapphire growth technology (50-pound ingots have already been grown), and theoretical considerations of seeding, crystallization kinetics, fluid dynamics, and heat flow for silicon.

During this report period, Crystal Systems improved the crystallinity (larger grains) of the ingots. The two major changes that led to these improvements were raising the heat exchanger 1 inch higher in the heat zone and improved temperature sensing.

By raising the heat exchanger in the hot zone, the heat exchanger temperature was increased and the melt superheat decreased. The temperature profile across the diameter of the heat zone was flatter from this modification. The growth interface is still observed to break down approximately 1/4 inch below the last portion to solidify (top). The interface is present in polycrystalline samples as well as single crystal samples. Iron from the graphite furnace has been identified as the major contaminant by the contractor.

A radiation pyrometer focused on the bottom of the cup appears to give temperature control to within $\pm 3°C$ instead of the previous $\pm 6°C$. The larger grained ingots also are evidence of improved control.

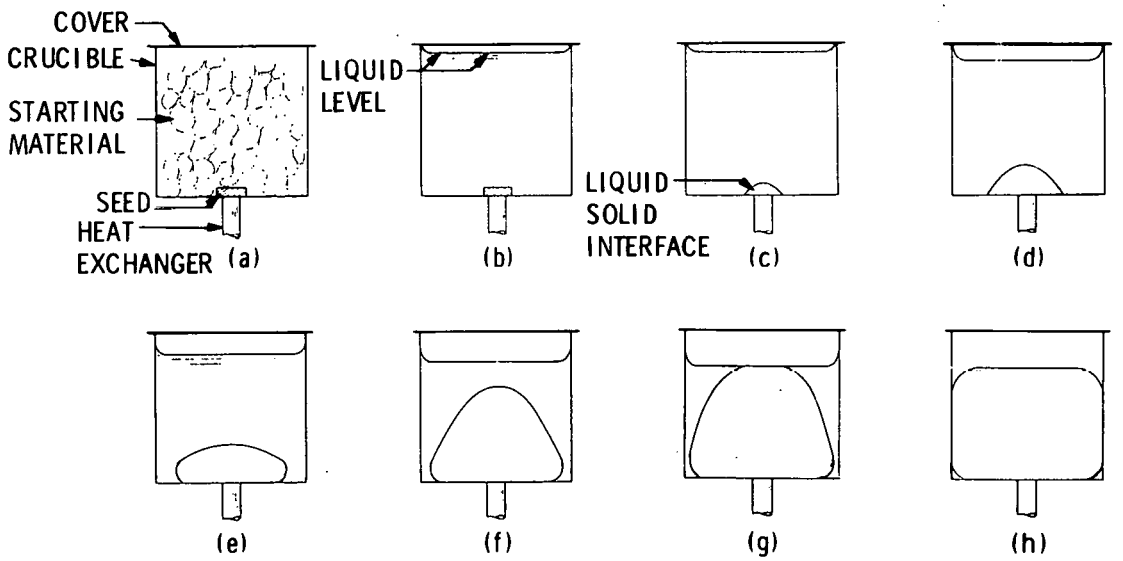

Growth of a crystal by the heat exchanger method:
(a) Crucible, cover, starting material, and seed prior to melting.
(b) Starting material melted.
(c) Seed partially melted to insure good nucleation.
(d) Growth of crystal commences.
(e) Growth of crystal covers crucible bottom.
(f) Liquid-solid interface expands in nearly ellipsoidal fashion.
(g) Liquid-solid interface breaks liquid surface.
(h) Crystal growth completed.

Fig. 4-34. Crystal growth using the heat exchanger method - Crystal Systems

All of the ingots have cracked when cooled below 700°C. Fracturing occurs on $\{111\}$ planes with secondary fracturing on $\{110\}$ planes. Fracturing has been identified as a major problem to be solved in demonstrating the technical feasibility of the heat exchanger method.

11. Ingot Cutting: Multiple Wire Sawing - Crystal Systems

Today most silicon is sliced into wafers with an inside diameter saw, one wafer at a time being cut from the crystal. This is a big cost factor in producing solar cells. The lesser-used multiblade slicer can be utilized to slice

silicon. The multiblade slicer has not been developed for the semiconductor industry since this method produces bow and taper unacceptable for integrated-circuit applications.

The overall goal of the slicing program is to optimize multiblade (wire) silicon slicing, investigating the following parameters in particular:

- Rate of material removal and kerf removal.
- Slice thickness, wire blade dimensions, cutting forces, wire/blade tension, and other machine variables.
- Wires versus blades as a cutting tool.
- Variation of rocking motion.
- Introduction of abrasive during slicing operation.
- Effect of surface condition of tool, including consideration of hardness and method of plating.
- Effect of diamond abrasive particle size and type.
- Effect of cutting fluid composition.

The slicing operation employs a rocking motion and utilizes 50 8-mil wires. These are 6-mil steel wires surrounded by a 1-mil copper sheath, which is impregnated with diamond as an abrasive. The shape of the abrasives and their interaction with the copper and steel is an unknown variable and will be investigated. The individual wires within a multiple wire package are equitensioned by the use of a single jig in the form of a weaving machine.

The variables for slicing have been specifically identified. The independent variables are feed force, speed, rocking angle, and phase angle; the dependent variables are cutting rate, deflection, degradation of diamond, and cut profile of y versus x.

During the report period, cutting rates of from 1 to 4 mil/min were achieved for feed forces from 0.05 to 0.25 lb/wire. As expected, the cutting rate was heavily dependent on the concentration of diamond particles in the wire. When diamond-impregnated wire having low and nonuniform diamond concentrations was

used, low cutting rates and wire damage resulted. Some of the wires were copper-plated and charged with 45 μm diamonds. Certain of these exhibited cutting rates greater than 4 mil/min.

The degradation in cutting ability appears to be due primarily to the diamonds being pulled out and secondarily to diamond wear.

JPL Effort

Approximately 14 ingot samples were received, sectioned, polished, and examined metallographically by JPL. Several ingots contained a number of particles at what appeared to be the initial seed-melt interface. From their color and generally hexagonal morphology, these particles appeared to be silicon carbide.

Micro-hardness measurements of the particles and silicon matrix were made using Knoop hardness indenter at 25 and 50 gram loads. DPH values of 6400 were obtained for the particles and 1600 for the silicon. Both of these values appear high by a factor of approximately 2, although the substantially higher hardness of the particles is still suggestive of silicon carbide.

In addition, a sample was placed in the scanning electron microscope, using the wavelength dispersive analysis unit capable of recording data for carbon. Analyses for carbon in the particles indicated approximately 10-15% carbon based on standardization against carbon inks. This value is low (SiC contains 50% carbon), but matrix effects and geometry errors because of the thickness of the specimen again suggest silicon carbide.

Since these analyses do not completely agree with those of the contractor, further studies including ion mass spectroscopy, X-ray emission spectroscopy, and possibly Auger analysis will be pursued. The contractor's analysis identified iron as the major impurity. JPL will also look for particles at the breakdown of the interface about 1/4 inch below the last portion to solidify.

The JPL in-house work confirmed that larger grains were produced after the furnace geometry was changed by the contractor. Preliminary surface photovoltage measurements in a single crystal section revealed a diffusion length of 31 microns.

The scanning electron microscope was utilized at JPL to examine the distribution of diamonds embedded in the 8-mil wire used for slicing. It was found that (1) the diamonds were irregularly imbedded and (2) the diamonds were not wearing out. Wherever the wire was smooth, either the number of diamonds had been insufficient to start with or the diamonds had pulled out. These results identified proper diamond embedding in the wire as a problem in this program. As a consequence, Crystal Systems has employed a subcontractor to do scanning electron microscope work.

12. Ingot Cutting: Breadknife Sawing - Varian Corporation

The purpose of this contract is to develop a multiple-blade sawing process that will significantly reduce the cost of cutting wafers from ingots or blocks of single crystal silicon for solar cell fabrication and has the potential to be scaled up for eventual large production environments (Fig. 4-35). The major portion of the program consists of a systematic experimental investigation of:

- Variation in cutting loads.
- Speed of slicing head.
- Blade dimensions.
- Abrasive, size, and concentrations.
- Blade material properties and costs.
- Lubricants.
- Specimen mountings.

The investigations will be conducted on a Varian 686 wafering machine which will be modified for experimental studies. It will be supplemented by a parallel

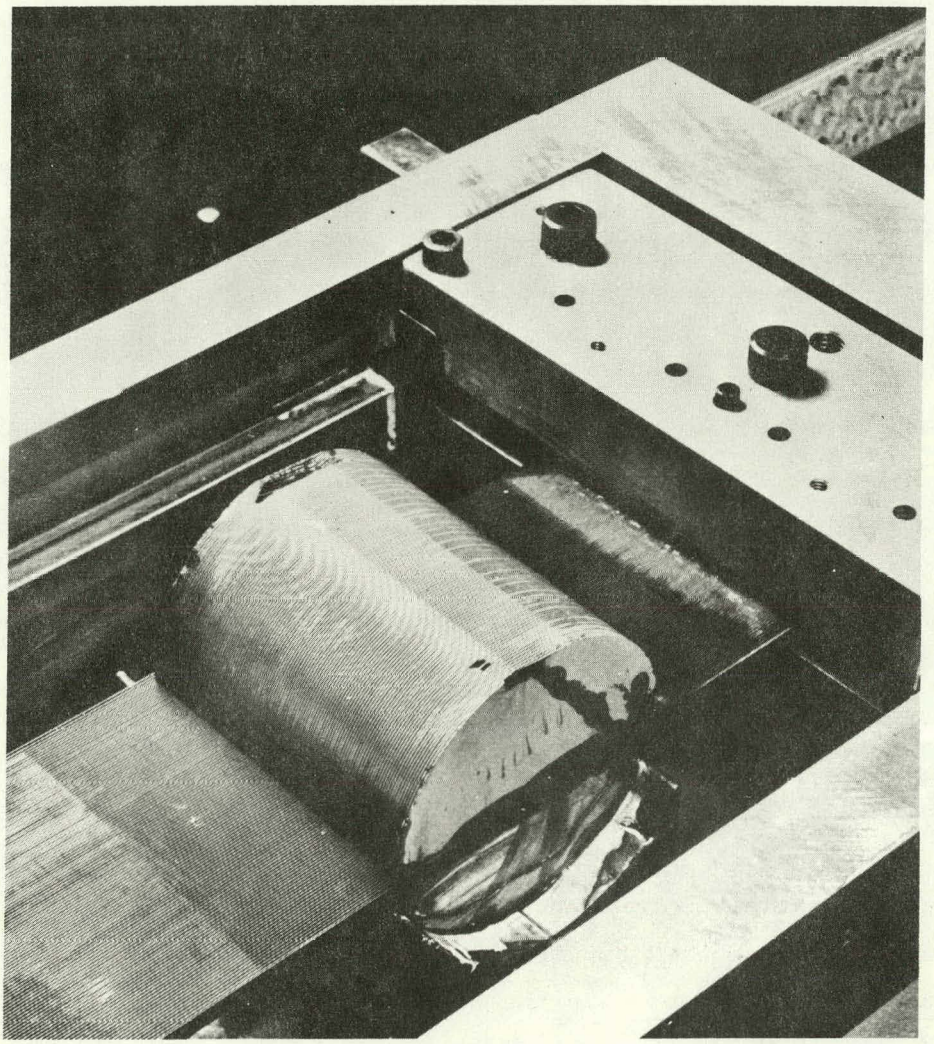

Fig. 4-35. Three-inch-diameter silicon ingot in multiblade wafer saw - Varian

theoretical effort to parametrize system performance as affected by modified abrasive wear and to establish practical limits to wafer accuracy and thickness, blade instability, abrasive blunting, etc. The major technical goals for the program are:

- Wafer thickness: 5 mils
- Slicing rate: 10 miles per minute
- Kerf loss: 5 mils
- Number of parallel slices: 100
- Stock size: 4 inches

It has been determined that a cutting time of 17 to 20 hours is required to cut a 10-cm-diameter ingot, using 0.020 cm blades, a 115 gm/blade loading, and a 600-grit abrasive. Side losses are about 0.005 cm, resulting in a total kerf loss of about 0.025 cm. The maximum number of blades currently possible is 230. This limit is imposed by the total tension capacity of the blade head. This head and blade configuration, at current costs of materials, results in an add-on cost for wafering of about $\$25\text{-}30/m^2$. Finer abrasives, such as 800 grit, result in less side loss and reduced kerf, but the cutting rate is also reduced substantially because of problems associated with the delivery of abrasive to the cutting area. Variations in slurry viscosity and application technique may avoid these difficulties.

Blade wander and slice accuracy have been shown to be related to slurry viscosity, as well as to the average cutting force. Additional work in this area may provide substantial improvements in slice accuracy. Slurry and/or abrasive life has not been considered explicitly, but preliminary indications are that the accumulation of silicon debris in the oil causes slice taper.

Blade wear is related to kerf volume removed. For the improved slurry techniques now in use, the ratios of blade loss to kerf removed are in the range of 0.04 to 0.05. Cutting experiments with thin blades (0.01 cm) have not been successful. The major problems are blade breakage and excessive wander.

Characterization of abrasive-induced damage was pursued during the report period. The initial efforts used step etch techniques to reveal damage profiles in the wafered samples. Damage depths of about 15-20 μm were indicated. The uncertainty of planar etch interactions with the as-sawn silicon surface left the conclusions in doubt. An angle lap experiment using chemical-mechanical polishing with fine abrasive (≤ 0.03 μm) indicated that the damage was principally due

to microscopic cracks and extended to a depth of about 15 μm. X-ray topography and scanning electron microscopy examinations confirmed these results. Further experiments are under way to confirm the first findings and to investigate how the damage is related to abrasive particle size, blade loading, and sliding speed. The nature of the damage revealed to date is consistent with the multiblade slurry sawing process.

13. JPL Crystal Growth Program

JPL is conducting experiments to determine the effect of impurities on the shape and stability of the growth interface during fast Czochralski growth (12 to 20 cm/hr). The effect of the impurities on the resulting solar cells will be evaluated. (Copper, nickel, and tungsten have been ordered, for use in introducing controlled levels of impurities.)

It is necessary to grow dislocation-free crystals to serve as a baseline for impurity studies. During this report period four Czochralski crystals were grown at JPL in an attempt to optimize growth rate and growth conditions. (The Czochralski furnace charge was 3,000 - 3,500 grams of silicon per cyrstal.) Improper helium flow was found to be creating a problem in the growing of dislocation-free crystals. A related problem arose from impurities in the helium (1% N_2, 1/2% O_2), which resulted in polycrystalline growth because of SiO_x formation in the melt and oxidation on the crystal surface. The origins of the dislocations were traced metallographically.

Attempts will be made to purify metallurgical silicon by the Czochralski process to evaluate the recent Dow Corning (Task 1) results which indicate that single crystal purification can occur. This is not the same result as that which appeared in the Dow Corning-University of Pennsylvania report. Fifty kilograms of metallurgical silicon has been ordered from Union Carbide.

A demonstration by AGA of their Thermovision, an instrument capable of providing a live thermal display, was given on the JPL Czochralski puller during silicon crystal growth. These demonstrations reinforced the observation that

there is much reflection from the heater and that temperature sensing is a very complex phenomenon. AGA claimed a sensitivity of $\pm$0.5°C, but owing to reflections, the resolution was probably $\pm$5°C. Even with the optimum lensing system, the resolution was such that further investigation was not worthwhile. As a result of these observations and the general situation in the utilization of manpower, it was decided not to investigate the temperature profile in ribbon growth as originally proposed. This effort would have required dedicated research and is too sophisticated for the present status of this work.

14. JPL Refractory Materials Program

The objective of this program is to make a preliminary evaluation of the compatibility of selected high temperature refractory materials with molten silicon. The program involves the measurement of wetting angles of sessile drops of molten silicon on selected refractories. Approximately 50 sessile drop experiments will be conducted to provide a basic core of data, and to permit conclusions to be drawn concerning the influence of physical and chemical variables of the refractories.

The basic experiments being conducted involve measuring the contact angle of drops of molten silicon on solid substrates at a temperature just above the melting temperature of silicon. A photographic system is utilized to permit actual measurements to be made from a series of photographs depicting preselected time and temperature conditions. These photographs serve as permanent records and records for comparison where some modifications are made, such as a changed atmosphere, in otherwise identical test conditions.

Post-test analysis involves the measurement of the amounts and mode of penetration of molten silicon into the solid substrates, as well as chemical changes in the silicon and substrate during the tests.

Silicon for the test samples is obtained by core-drilling 1/4-inch-diameter rods from single crystal silicon disk blanks. These rods are cut to a length of 1/4 inch, cleaned, weighed, and then melted on polished and cleaned surfaces of selected refractories. Melting is accomplished in a modified Hoffman crystal

growing furnace, which has been equipped with a viewing port and window to permit photographic access to the molten silicon drop on the refractory surface (Figs. 4-36 and 4-37).

A 35mm Nikon F-2 camera equipped with an f/2.8 lens and motor drive permits photographs to be taken at selected and variable time intervals through the incorporation of an intervalometer. Thus, the camera drive and furnace temperature recording instrumentation permit the accurate identification of time, temperature, and wetting angle sequentially through each experiment.

Laboratory tests to date have shown that a uniform and controllable temperature can be achieved. A crucible positioning and rotating mechanism incorporated in the Hoffman furnace permits accurate alignment of refractory test specimens of differing thicknesses within the field of view of the camera.

In the laboratory tests, all silicon and refractory test parts are heated to 1430°C $\pm$ 10°C in a flowing helium atmosphere and allowed to stabilize for 10 minutes. Photographs are taken at 30 second intervals for 10 to 15 minutes. Subsequently, visual measurements of the wetting angles are made directly from enlarged prints of selected frames, using a protractor. The class and type of refractory materials received for testing are summarized in Table 4-15.

Table 4-15. Test refractory materials

Hot Pressed	
Silicon carbide	Boron nitride
Silicon nitride	Black glass (C-SiO_2)
Pyrolytic or Chemical Vapor Deposited	
Silicon carbide	Hafnium oxide
Boron nitride	Graphite and carbon
Hafnium carbide	
Reaction Sintered	
Silicon nitride	Mullite
Self Bonded	
Silicon oxynitride	

Fig. 4-36. Hoffman furnace set-up showing furnace control panel, optical pyrometer, 35mm camera, tripod, and intervalometer

Fig. 4-37. Inner view of Hoffman furnace and sessile drop sample on central graphite stage. Also shown is externally aligned Nikon F2 35mm camera with bellows extension and 135mm f/2.8 lens.

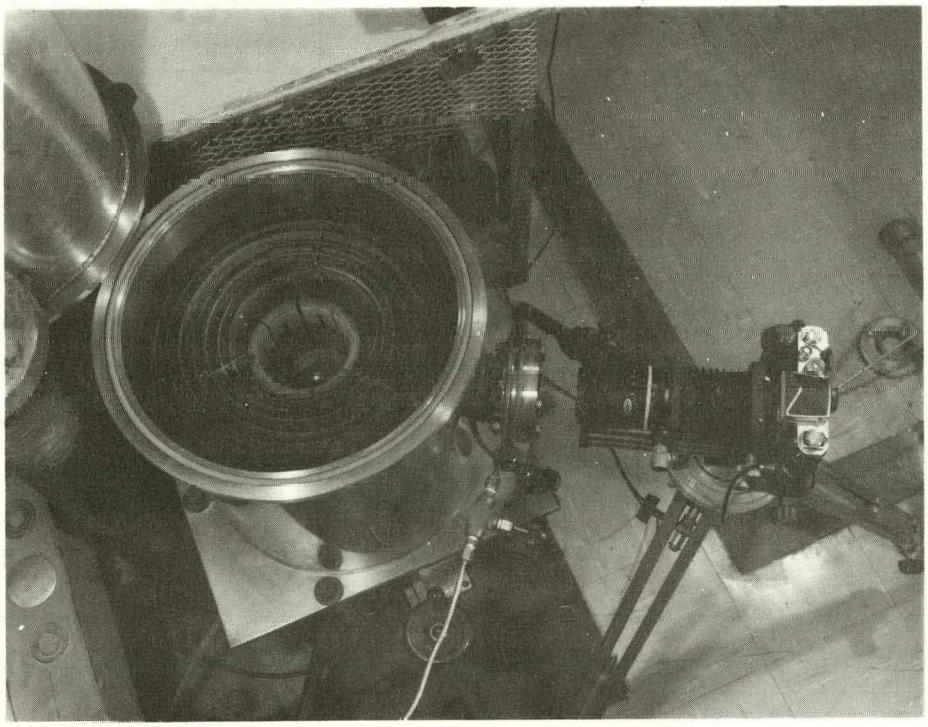

To date, sessile drop angle and density measurements have been made on silicon carbide, silicon nitride, mullite, and boron nitride, manufactured by hot pressing, sintering, and chemical vapor deposition. An initial attempt to measure wetting angles on black glass (C-SiO_2) substrates proved unsuccessful owing to unexpected warpage of the substrate at temperatures near 1300°C. Steps are being taken to determine the cause(s) of this reaction.

Table 4-16 summarizes initial wetting angle and density measurements. Since this table was compiled, several other substrates of mullite and hot-pressed boron nitride have been tested. The latest mullites tested and measured gave results consistent with the wetting angle measurements on the initial mullite substrates; the boron nitride substrates tested thus far have shown nonwetting characteristics, i.e., wetting angles $\theta > 90°$. Figures 4-38 and 4-39 show, respectively, a silicon sessile drop solidified on a silicon nitride substrate and two sessile drop profiles photographed at temperature (i.e., 1430°C $\pm$ 10°C).

Table 4-16. Refractory materials evaluation - LSSA Task 2

Sample No.	Material	Fabrication	Density (gm/cm^3)	Measured Wetting Angle
SD-1	SiC	Hot pressed	3.28	40° ±3°
SD-2	SiC	Hot pressed	3.28	38° +3°
SD-3	SiC	----	3.10	No angle*
SD-4	SiC	----	3.10	No angle*
SD-5	SiC	----	3.10	No angle*
SD-7	SiC	Vapor deposited		40° ±2°
SD-10	Si_3N_4	----	3.18	50° ±3°
SD-11	Si_3N_4	----	3.18	52° +3°
SD-13	Si_3N_4	Hot pressed	3.37	
SD-37	Mullite	Sintered	2.50	86° ±3°

*Silicon absorbed completely by substrate material.

Ceramagraphic samples have been sectioned and mounted for silicon carbide, silicon nitride, mullite and black glass (C-SiO_2) substrates both in the as-received condition and post-test sessile drop profile. Chemical reactions have been documented for mullite (Figs. 4-40, 4-41, and 4-42) and silicon nitride.

In the coming quarter, all sessile drop melt tests and subsequent wetting angle measurements will be completed. This means approximately 25-30 more refractory substrates will be tested and measured. Also in the coming quarter a significant quantity of sessile drop samples will be sectioned, mounted, polished, and etched to reveal the presence, if any, of chemical reactions between the molten silicon and refractory. Refractory material polishing is a slow, time-consuming process and requires experimentation since some of the tested materials exhibit unique grinding and polishing properties.

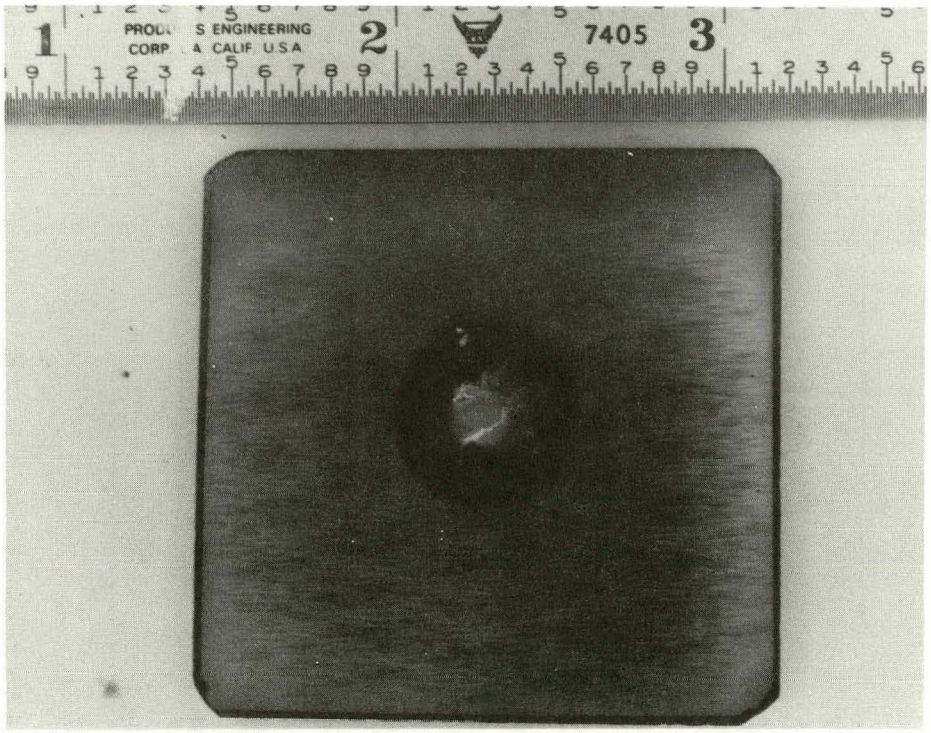

Fig. 4-38. Photomacrograph of silicon sessile drop (solidified) on a refractory material substrate (Si_3N_4)

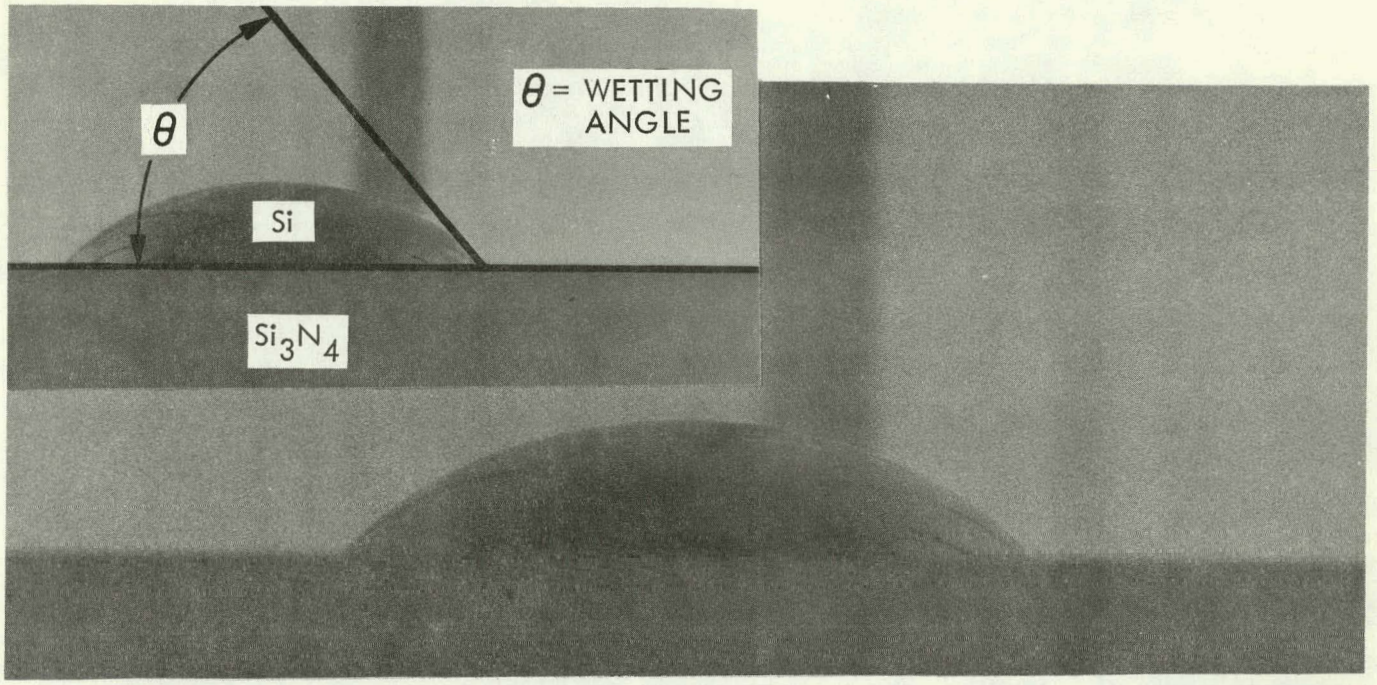

(a) Refractory substrate: Si_3N_4

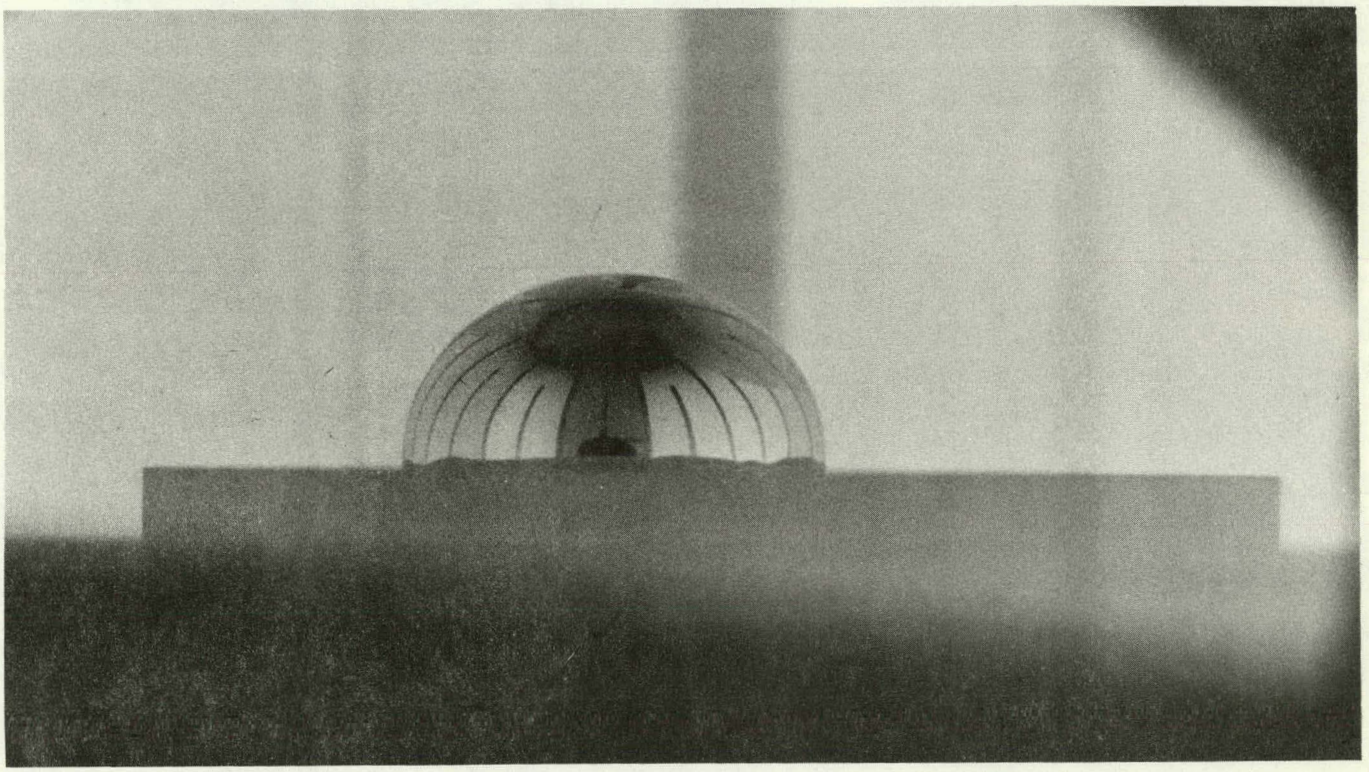

(b) Refractory substrate: mullite

Fig. 4-39. Photomacrographs of silicon sessile drop profiles at temperature (i.e., 1430°C ± 10°C) and the refractory substrates beneath them

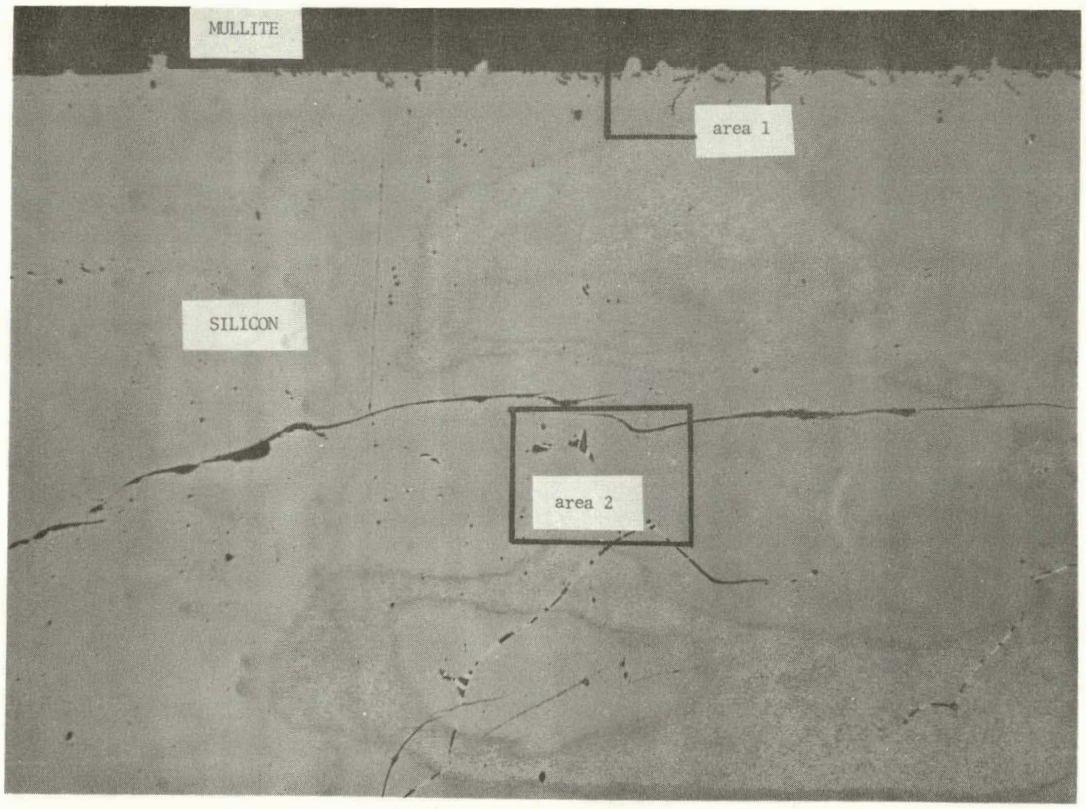

Fig. 4-40. Mullite/silicon interface (magnification - approximately 150X). Mullite substrate at top (M), silicon below (Si).

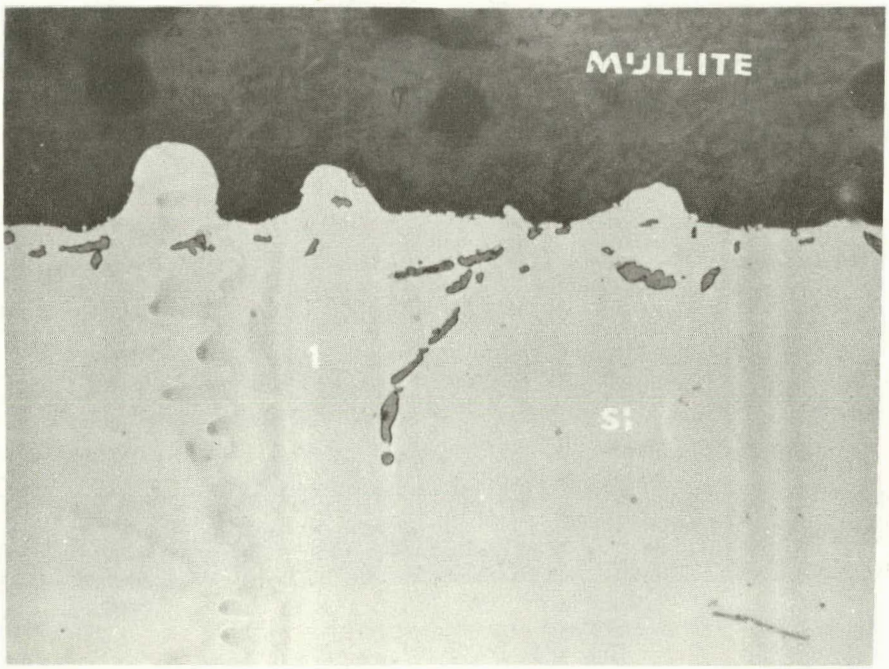

Fig. 4-41. Enlarged photomicrograph (1000X) of mullite/silicon interface, area 1

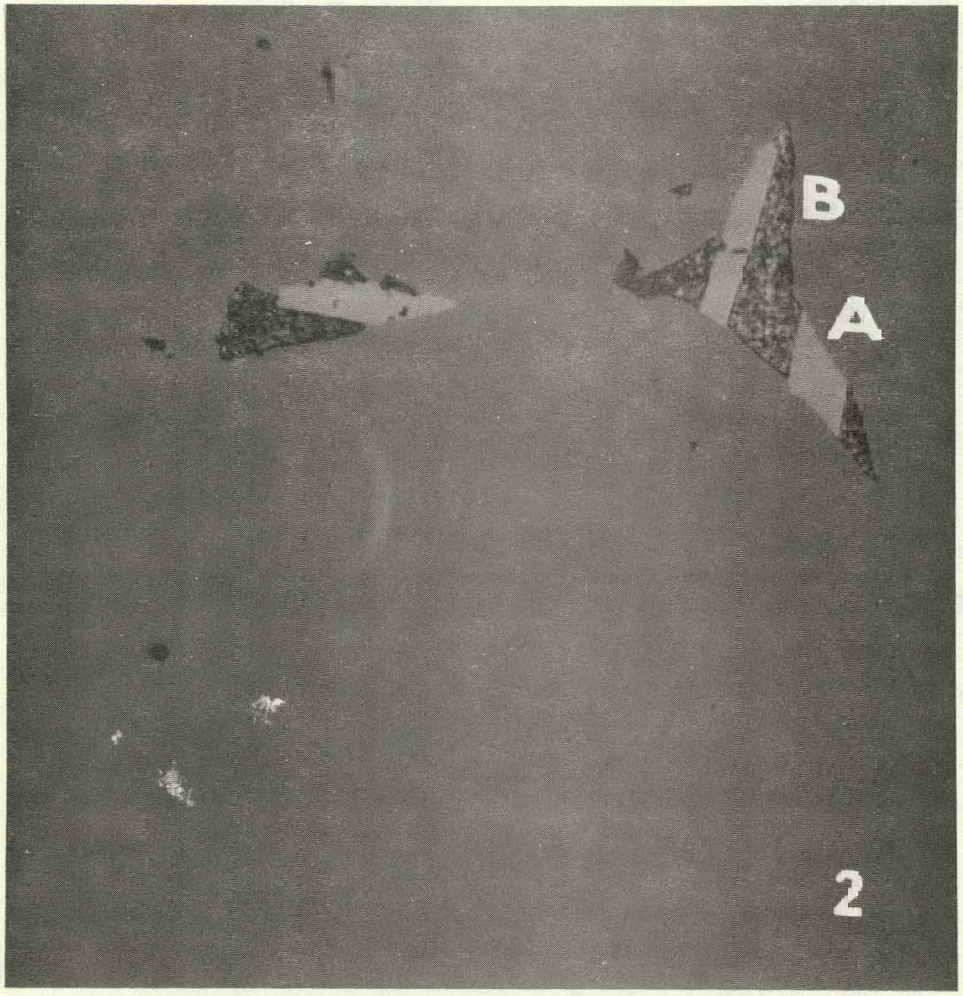

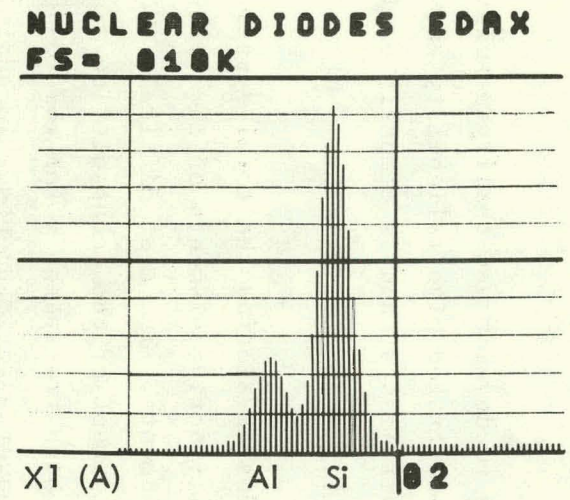

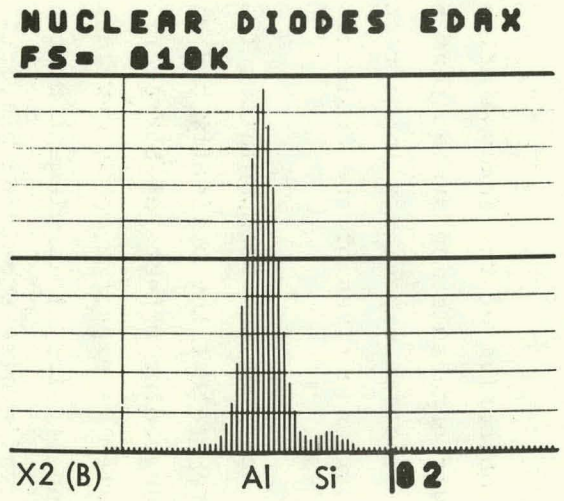

Fig. 4-42. EDAX readings on precipitates formed in silicon, area 2, melted on mullite. Magnification of photomicrograph - 1000X

TASK 3. ENCAPSULATION

The objective of the Encapsulation Task is to develop and qualify a solar array module encapsulation system that has a demonstrated high reliability and a 20-year lifetime expectancy in terrestrial environments, and is compatible with the low-cost objectives of the Project.

The scope of the Encapsulation Task includes developing the total system required to protect the optically and electrically active elements of the array from the degrading effects of terrestrial environments. The most difficult technical problem is expected to be developing the element of the encapsulation system for the sunlit side; this element must maintain high transparency for the 20-year lifetime, while also providing protection from adverse environments. In addition, significant technical problems are anticipated at interfaces between the parts of the encapsulation system, between the encapsulation system and the active array elements, and at points where the encapsulation system is penetrated for external electrical connections. Selection of the element for the rear side (i.e., the side opposite to the sunlit side) of the encapsulation system will be based primarily on cost, functional requirements, and compatibility with the other parts of the encapsulation system and with the solar cells.

Depending on the final solar array design implementation, the encapsulation system may also serve other functions, e.g., structural, electrical, etc. - in addition to providing the essential protection.

At present, options are being kept open as to what form the transparent element of the encapsulation system will take - glass or polymer sheet, polymer film, sprayable polymer, castable polymer, etc. The transparent element may contain more than one material and may be integral with the photovoltaic device, or be bonded to it, or installed as a window or lens remote from the device.

A. TECHNICAL BACKGROUND

Photovoltaic devices (solar cells) and the associated electrical conductors which together constitute solar arrays must be protected from exposure to the

environment. Exposure would cause severe degradation of electrical performance as a result of corrosion, contamination, and mechanical damage.

In the past, test experience by government organizations and industry has confirmed that spacecraft solar arrays are poorly designed to survive the earth environment. Arrays designed for terrestrial use have shown mixed results. These results, and analyses performed as part of this task, suggest that long-life, low-cost encapsulation is possible under terrestrial conditions; however, at present, successful protection from degradation by the environment is associated with encapsulation materials and processing costs which are excessive for large-scale, low-cost use. Thus, an acceptable encapsulation system — one that possesses the required qualities and is compatible with low-cost, high-volume solar array processing — has yet to be developed.

B. ORGANIZATION AND COORDINATION OF THE TASK 3 EFFORT

The approach to be used in achieving the overall objective of Task 3 will include an appropriate combination of contractor and JPL in-house efforts. The contractor efforts will be carried out in two phases. Within each phase some parallel investigations will be conducted to assure timely accomplishment of objectives.

During Phase I the contractor and the JPL in-house effort will consist primarily of a systematic assessment and documentation of the following items:

- Potential candidate encapsulant materials based on past experience with the encapsulation of silicon and other semiconductor devices and on available information on the properties and stability of other potential encapsulant materials and processes.
- The environment which the encapsulation system must withstand.
- The properties, environmental stability, and potential improvement of potential encapsulant materials and processes.
- Test and analytical methods required to evaluate performance and predict and/or verify lifetime of encapsulant materials and encapsulation systems.

The results of this effort will then be used to specifically define additional research, development, and evaluation required during the subsequent phase.

Throughout the task atypical or unique approaches to solving the encapsulation system problem will be sought and evaluated. For example, Phase I will include an evaluation of the feasibility of utilizing electrostatically-bonded integral glass covers as part of the encapsulation system.

In Phase II, contractor and JPL in-house efforts will be conducted to identify and/or develop one or more potentially suitable encapsulation systems and then verify the expected lifetime and reliability of these systems. Depending on the results of Phase I, the contractor effort in this phase will include an appropriate combination of some of the following items:

- Evaluate, develop, and/or modify test and analytical methods and then validate these methods.
- Perform materials and interaction testing, using these methods to evaluate candidates and demonstrate the reliability of encapsulation systems.
- Modify materials and processes used in encapsulation systems to improve automation and cost potential.
- Modify potential encapsulation system materials to optimize mechanical, thermal and aging properties.
- Implement research and development on new encapsulant materials.

C. TASK 3 CONTRACTS

Task 3 contracts are shown in Table 4-17. In addition, Professor Charles Rogers, Department of Macromolecular Science, Case Western Reserve University serves as a consultant to this task. Dr. Rogers is a specialist in polymer characteristics and aging as well as the field of diffusion through polymers. He serves as a technical specialist and also provides assistance in defining the overall scope and direction of the task activities. At a later date, he may implement selected supporting experimental investigations in the laboratories at Case.

Table 4-17. Task 3 contractors

Contractor	Technology Area
Battelle Memorial Institute Columbus, Ohio	• Identification of candidate encapsulant materials based on a review of (a) worldwide experience with encapsulant systems for silicon solar cells and related devices and (b) the properties of other available materials. • Definition of environmental conditions for qualifying encapsulant materials. • Evaluation of encapsulant material properties and test methods. • Analysis of accelerated/abbreviated encapsulant test methods.
Rockwell International Anaheim, California	Experimental evaluation of accelerated/abbreviated encapsulant test methods.
Simulation Physics Burlington, Massachusetts	Electrostatically-bonded glass covers.
DeBell and Richardson Enfield, Connecticut	Polymer properties and aging.

D. TASK 3 TECHNICAL ACTIVITY

The sequence of Task 3 technical activities is shown in Fig. 4-43.

1. Identification of Candidate Encapsulant Materials: Worldwide Experience and Available Materials - Battelle

Work on this study was completed during the April-June quarter. During the present report period, the entire effort consisted of work on the final report. Several iterations were prepared by Battelle and reviewed by JPL. The final draft was approved, and the report is to be issued in late October.

During the course of the study over 1000 documents were reviewed, out of approximately 6000 identified in various literature searches. These documents relate primarily to worldwide experience in encapsulation in various kinds of devices and the terrestrial use of transparent materials. Specific references on appropriate materials and their properties were also included. No one or group of outstanding candidate encapsulant materials was identified from this effort. The lack of definition of module design implementation requirements precluded specific identification of leading candidates. The information gathered will provide the basis for candidate selection as module design requirements are defined.

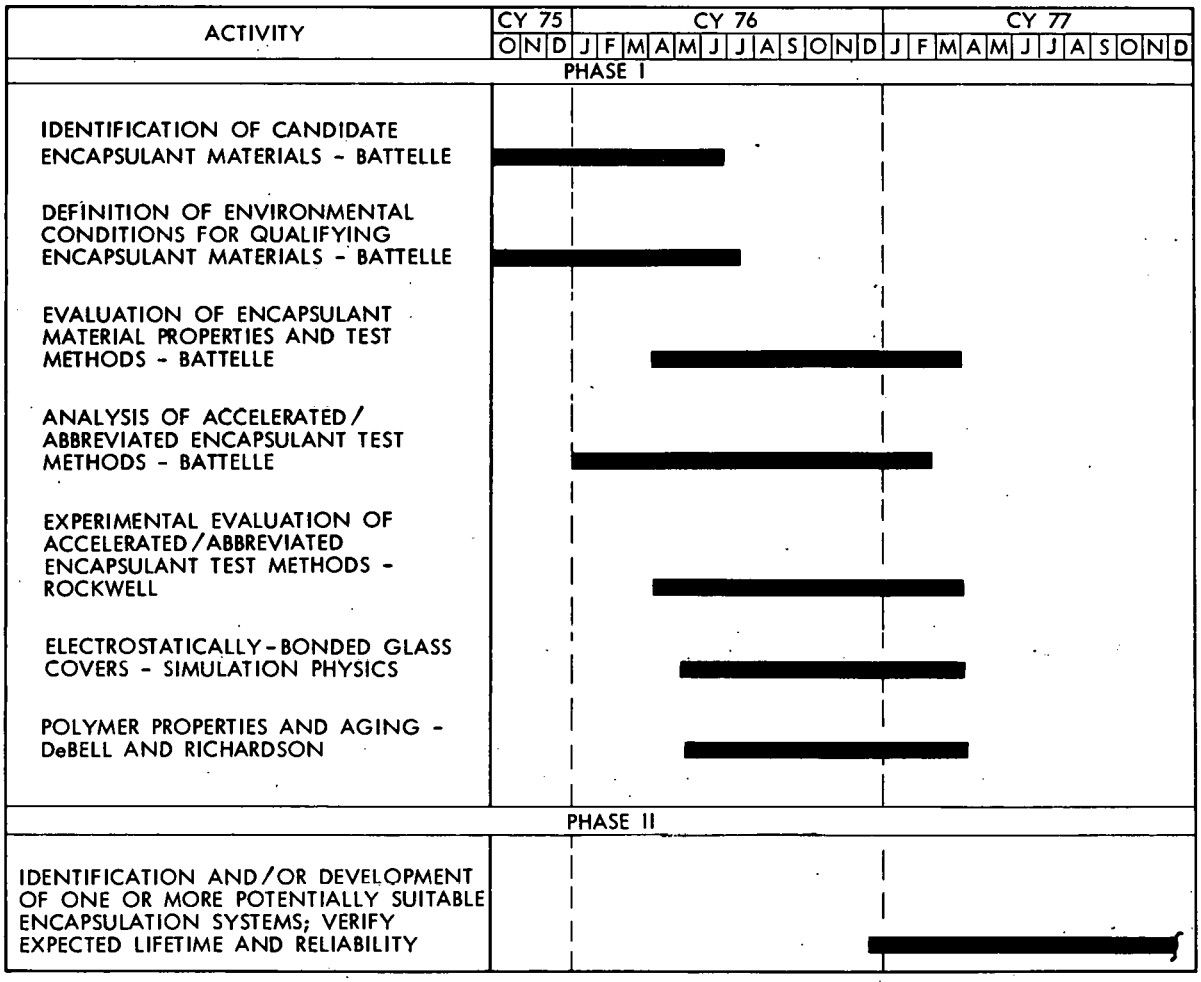

Fig. 4-43. Encapsulation Task schedule

2. Definition of Environmental Conditions for Qualifying Encapsulant Materials - Battelle

Work on this study was completed during the April-June quarter. During the present report period, the entire effort consisted of work on the final report. Several iterations were prepared by Battelle and reviewed by JPL. The final draft was approved, and the report is to be issued in late November.

This study was concerned with developing an understanding of the environments which the module must withstand. Real-time field testing to the 20-year lifetime is obviously impossible; testing in a wide variety of locations is impractical; and materials selection to unrealistic environmental requirements would prove excessively costly. The validity of extrapolating available aging data, laboratory test data, or field test data to 20 years in a particular environment depends on the relationship of the test environment to that of the longer period.

The decision as to whether to seek a single encapsulant suitable for all possible locations or several climate-unique designs depends on many factors including production, economics, etc. In either case, a knowledge of the various environments is essential to such a decision.

3. Evaluation of Encapsulant Materials Properties and Test Methods - Battelle

A preliminary investigation of test methods for determining the properties of materials was completed during this report period. Although it was concluded that standard ASTM and Federal Test Methods are satisfactory for routine testing of materials, it was also concluded that routine and simplistic approaches to materials testing will not give the answers required to meet Project goals. The development of test methods must be an ongoing activity and must be coordinated with other elements of the Encapsulation Task and other tasks, particularly Task 4 and the Large Scale Production Task. It has been determined in the study of accelerated /abbreviated encapsulant test methods (paragraph 4, below), for

example, that the test methods reported in the literature for use with accelerated and natural aging tests of materials are grossly inadequate. It is apparent at this time that the investigation of test methods will be a continuing Encapsulation Task effort and will not be completed by the present study effort.

The effort to determine the properties of candidate encapsulation materials has undergone a change in emphasis because of the systems types of failures observed in testing the modules of the 46 kilowatt procurement and also because of the information on worldwide experience with field modules obtained in the Battelle literature search (paragraph 1, above).* This is a change in emphasis, not a redirection. The materials tested and the types of tests will be based on materials interactions, compatibilities, and synergistic effects. In addition, a portion of the effort on this study will be in support of the accelerated/abbreviated encapsulant test methods study. Materials testing is required to supply a base of materials degradation data to help in developing a methodology for designing statistical and experimental techniques for life prediction.

4. Analysis of Accelerated/Abbreviated Encapsulant Test Methods - Battelle

A literature search has revealed no data suitable for use in the validation of life prediction studies. This finding has been a serious blow to the development of a suitable methodology for designing statistical and experimental techniques. The inadequacies of the data include a lack of sufficient replication, insufficient precision and accuracy of measurements, and a lack of established relationships between degradation modes and measurement methods/techniques.

---

*Carmichael, D.C., et al., Review of World Experience and Properties of Materials for Encapsulation of Terrestrial Photovoltaic Arrays, Report No. ERDA/JPL-954328-76/4, Battelle Columbus Laboratories.

Lack of precision and accuracy of measurements has called attention to the lack of knowledge about and need for diagnostics.* More information is required in the areas of precision of instrumentation, measurement procedures, reproducibility of data from instrument to instrument of the same make and model, the effects of the measurement procedures on the test specimens, destructive versus nondestructive testing, and the capability of making in situ measurements. This information is required for all types of instrumentation used for measuring physical, chemical, mechanical, and electrical properties. Of special importance is the detection of minute property changes during natural or accelerated aging so that accurate life prediction estimates can be made.

One of the results of this study will be to establish methods for discriminating between mathematical models for life prediction. A simple study was run recently at Battelle to test discrimination methods found in the literature. Artificial data were generated from the "true" equation. $P = 850 - 40t$, where P is the property level at time, t, in years. For $t = 20$ years, P has the true value $P = 50$. Two years of artificial data were generated, each item of which included an assumed error. Twenty equations including the "true" equation were fitted to these data. It was demonstrated that known discrimination methods would select the "true" model as the "best" equation in approximately 2 years of test data. It is obvious that this comparatively simple exercise is not sufficient to solve the complex problem of predicting a 20-year life from 2 years of data. However, it demonstrates feasibility and points the way toward further development of the life prediction methodology.

---

*Diagnostics in this context is the practice of using instrumentation to measure characteristics related to or indicating the changes in the properties of materials undergoing natural or laboratory weathering or aging tests.

5. Experimental Evaluation of Accelerated/Abbreviated Encapsulant Test Methods - Rockwell International

The objective of this contract is to develop statistical models and test methodology to allow the prediction of solar cell encapsulant performance during a 20-year outdoor exposure.

A review of the literature has suggested that outdoor weathering tends to follow the Weibull model in which an encapsulant property, e.g., light transmission, varies as an exponential function of time raised to some power greater than 1. When time is not raised to a power, the equation is reduced to a simple exponential type, and this is the model usually fitted by fixed-condition degradation in laboratory tests.

For evaluating encapsulants, a Universal Test Specimen has been designed and specimens fabricated. This comprises solar cells and field effect transistors (more sensitive than the cells in responding to water and ionic contamination) on a ceramic board with gold circuitry. Three encapsulant systems are being tested. Two of these include plastic films (Lexan, Tedlar), samples of which are also being weathered separately.

To obtain internally-consistent indoor (accelerated) and outdoor data for statistical modeling, two simultaneous exposure programs have been initiated: outdoor exposure in Phoenix and Miami, accelerated outdoor exposure in Phoenix, and accelerated exposure in a xenon-lamp chamber of Rockwell's design. The outdoor exposures began on September 1 and 12, 1976. The weathering chamber has been completed and the xenon lamp characterized. The solar simulation is good. Specimens will be installed in October and accelerated exposure will begin early in November.

The statistical analysis of degradation rates, outdoor versus accelerated, will permit the consolidation of hypotheses and the development of a generally-applicable predictive model for outdoor exposure of encapsulants in terms of inherent weatherability. This is controlled by three factors: insolation,

temperature, and humidity. The effect of complex conditions, such as rapid temperature changes, will have to be superimposed on the baseline estimate.

6. Electrostatically-Bonded Integral Glass Covers - Simulation Physics

The purpose of this program is to develop the use of electrostatic bonding (ESB) for integral glass encapsulation of solar cell arrays. Experimental work involves approaches to hermetically sealing the active components of the array between two glass sheets. The objective is to establish all procedural techniques necessary to prepare and test functioning demonstration modules of a few cells each.

By July 1976, which was the third month of this 14 month effort, preliminary technical assessments required under the program had been completed, types of glass which might be compatible with the method had been identified, and facility design and experimental work had been initiated. In addition, a preliminary electrostatic bonder apparatus had been constructed and the first successful integral attachment of 2-inch-diameter silicon solar cells to sheets of Corning 7740 and 7070 glasses had been performed.

During the past 3 months, investigations have been performed to establish procedures for preparing individual cells, in order to be able to begin the development of module configurations. Technical requirements for the main electrostatic bonder to be assembled for the program have been determined using the interim unit. Several glasses selected as candidates for use with ESB integral encapsulation have been experimentally evaluated and it has been decided that Corning 7070 borosilicate glass is the best commercially available material for overall compatibility with module and process needs.

Using temperatures of 450 to 600°C, it has been found possible to plastically deform 7070 glass satisfactorily around all the irregularities of a terrestrial cell surface. The glass surface quality is not critical and good results can be achieved with as-rolled and as-pressed sheet.

To facilitate the fabrication of completely enclosed modules, it will be necessary to use two sheets of glass which will be sealed together, at least around their edges. Electrostatic bonding will not bond glass to glass. Successful glass-glass attachment has been accomplished with a silicon film bond interface on one glass surface. Other interfaces are being examined for bonding and for electrical feedthrough purposes.

Work during the next quarter will emphasize multiple cell assembly techniques. Tests will be started to evaluate the quality and stability of integral components.

7. Polymer Properties and Aging - DeBell and Richardson

The goal of this program is to develop and test materials and encapsulation or coating processes that will be suitable for protecting solar cells during a service life of at least 20 years in a terrestrial environment. The materials selected for this program have been chosen for three general properties: clarity, toughness, and weatherability. The testing program incorporates the evaluation of initial properties and subsequent retesting after exposure to accelerated aging conditions. The aging environments consist of combinations of heat, humidity, and ultraviolet light, with sample testing at three time intervals.

The testing program consists of three basic approaches:

1) Mechanical - Tensile strength, modulus, brittleness, impact strength.
2) Optical - Total integrated transmittance, haze, absorption versus wavelength, infrared attenuation.
3) Miscellaneous - Water vapor permeability, insulation resistance, fungus resistance, abrasion resistance.

Experiments during this report period have shown that variations in ultimate tensile elongation appear to be the most sensitive indicator of degradation in polymers. Although no resins have survived the accelerated aging conditions totally unchanged, the fluoropolymers are the most resistant. Evaluations of total integrated transmittance versus aging condition also serve as a useful

screening tool and many materials may be eliminated on the basis of increasing opacity.

8. Review and Analysis of Task 3 Progress - Professor Charles Rogers, Consultant

A report, Review and Analysis of Task 3 Progress, has been received from Dr. Rogers and is now in review.

9. JPL In-House Task 3 Activity

Fracture Mechanics of Interfaces

Work has been initiated by Dr. W. Knauss (Caltech) to evaluate delamination using a fundamental fracture mechanics approach.

Test Module Development

The purpose of the test module development program is to identify and analyze various material relationships such as synergisms, compatibilities, and causes of "systems" failures. This program will be correlated and integrated with other efforts, under Task 3 and the Large Scale Production Task, and programs at Rockwell, DeBell & Richardson, and Battelle. A study of the failure modes observed in arrays and modules was made. A schematic representation of these failure modes is shown in Fig. 4-44. Test specimen design at this point is preliminary as shown in Fig. 4-45. It consists of three 3-inch-diameter silicon cells using various encapsulants. A preliminary selection of test materials has been made; processing/manufacturing relationships which require definition and implementation have been identified; and anticipated exposure/testing modes which also require definition are being identified. A preliminary qualification testing procedure is shown schematically in Fig. 4-46. As indicated above, the program is in its preliminary definition stages. Considerable work remains to be done to complete specimen design, complete processing/manufacturing documentation, and to definitize the exposure/testing methodology.

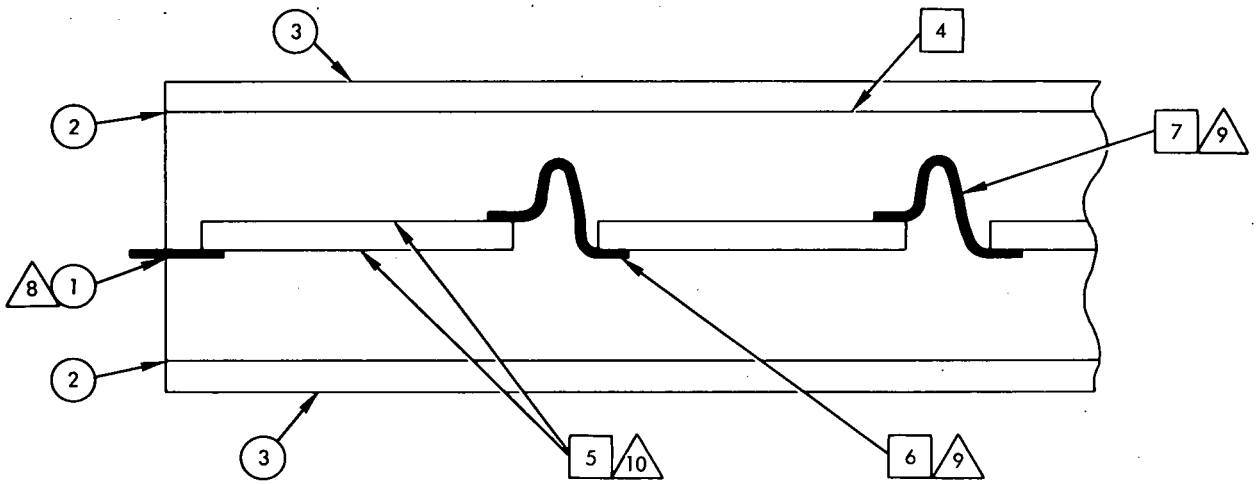

1. THROUGH LEAD EXIT
2. AT INTERFACE
3. THROUGH COVER
4. DELAMINATION AT COVER
5. DELAMINATION AT CELL
6. SOLDER CONNECTION
7. LEAD FLEXURE
8. CORROSION OF LEAD END & SOLDERED CONNECTION
9. CORROSION OF INTERCONNECT & SOLDERED CONNECTION
10. CORROSION OF CELL METALLIZATION & SOLDER

○ MOISTURE
□ MECHANICAL
△ CORROSION

Fig. 4-44. Failure modes in arrays

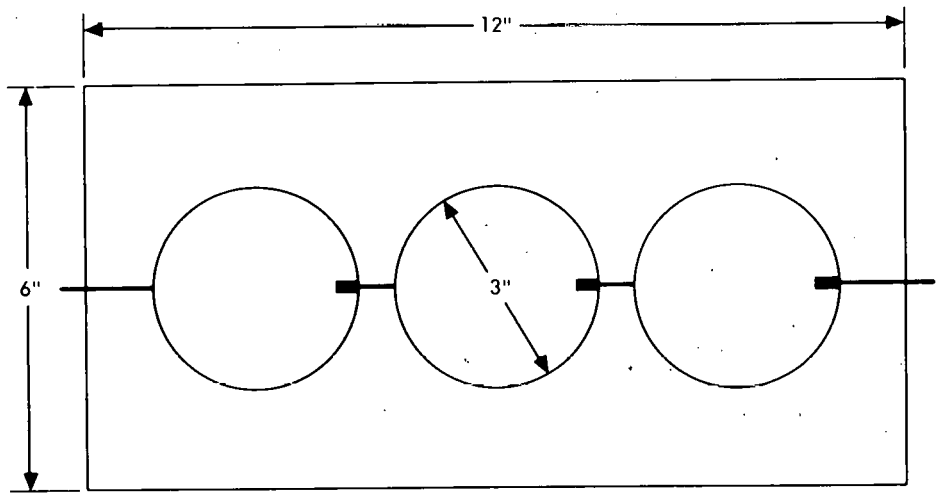

1. TOP AND BOTTOM ENCAPSULANT TO BE THE SAME.
2. MIDDLE ENCAPSULANT AND ADHESIVE TO BE THE SAME.
3. SN 63 SOLDER MILDLY ACTIVE FLUX (CLEANING).
4. SOLDER COATED CU MESH INTERCONNECTS.
5. AG OUTPUT WIRES (PLATED WITH CU), VINYL-INSULATED.

Fig. 4-45. Test specimen design

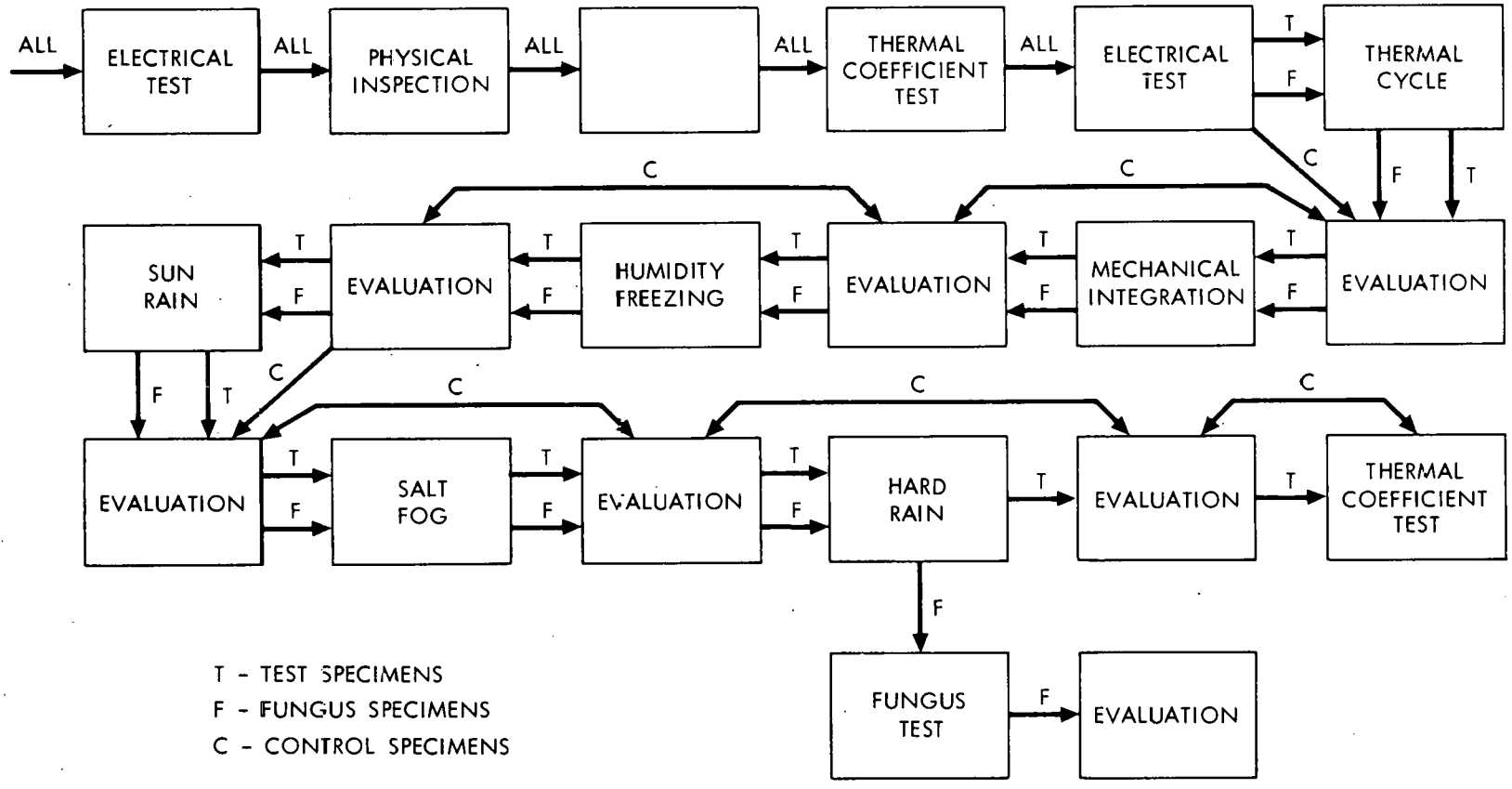

Fig. 4-46. Qualification testing procedure (preliminary)

Failure Analyses for Modules of the 46 Kilowatt Procurement

The engineering/operations tasks were supported by carrying out analyses of the failures that occurred during the testing of modules from the 46 kilowatt procurement. Failure analysis techniques included chemical and mechanical testing; scanning electron microscope examination; and analysis by energy dispersive X-ray (EDAX).

Support of the 130 Kilowatt Procurement

Activities in support of the 130 kilowatt procurement are being planned. They will be similar to those carried out for the 46 kilowatt procurement, including failure analyses and general materials support.

Accelerated Weathering Tests on Several Transparent RTV Silicone Rubbers

Early in 1976, difficulty was experienced by the fabricators of modules for the 46 kilowatt procurement in obtaining transparent RTV silicone rubbers. These procurement difficulties were encountered because of manufacturing problems experienced by the two major producers of silicone rubbers. These problems were (1) lack of manufacturing capability brought about by a reduction in manufacturing on-line facilities during the preceding recession, lack of inventory, and increased demand because of the return to economic prosperity and (2) a temporary difficulty experienced by one of the producers in producing quality transparent material. Because of these procurement difficulties, the Encapsulation Task was flooded with inquiries as to the interchangeability and weatherability of various transparent RTV silicone rubbers under consideration for use as pottants and adhesives in modules of the 46 kilowatt procurement. Since very little specific data was available on the effect of weathering on the transparency and mechanical properties of these materials, it was decided to conduct accelerated weathering exposure tests on them.

Material availability is no longer a problem and has not been for 6 months. However, accelerated weathering and testing of the following transparent RTV silicone rubber pottants have proceeded and been completed:

Material	Manufacturer
Sylgard 182	Dow Corning Corp.
Sylgard 184	Dow Corning Corp.
RTV 602	General Electric Co.
RTV 615	General Electric Co.
RTV 655	General Electric Co.
RTV 670	General Electric Co.

Sylgard 184 and RTV 615 are currently used as pottants in silicon solar cell modules. RTV 602 has been used as a cover glass adhesive in space solar cell modules. RTV 670 is a new methyl/phenyl type still under development. Sylgard 182 has been discontinued.

The results show that none of the materials were significantly internally degraded after exposure to 1000 hours of accelerated weathering in an Atlas Twin Arc weatherometer per ASTM D 1499 with intermittent water spray. There was, however, a significant surface degradation. These results will be presented and discussed in a forthcoming report.

Evaluation and Analysis of Module Delamination

A program has been initiated to investigate delamination (adhesive failures) in modules. Delamination includes bond failures of pottants to solar cells, interconnects, module frames, and lead wires. This investigation includes an effort to find a quick, reasonably accurate, and economical means of finding small voids in the adhesive used to bond cells to a substrate. This is needed in order to evaluate the effect of voids in causing (initiating) delamination.

TASK 4. SOLAR ARRAY AUTOMATED ASSEMBLY

The overall objective of Task 4 is to develop the technology necessary to achieve high-volume, low-cost production of silicon solar array modules. The goal of this task is to develop the capability to fabricate solar array modules of 10% or better conversion efficiency at a selling price of $0.50/watt or less, at a rate of 500 megawatts per year, with a 20-year operating life. Many of the decisions that must be made during the Task 4 effort cannot be made independently and will result from trade-offs with other decisions that are made both within this task and in conjunction with other tasks of the Project.

A. TECHNICAL BACKGROUND

The manufacture of solar cells and arrays is presently accomplished under the judgment and direct control of individual operators. Because of the limited quantities of solar cells and arrays produced, costs are high. Automated solar cell production, as proposed, will lead to significant reductions in manufacturing cost. In addition, automation will result in uniformity of cell processing with a reduction of waste due to rejected product.

B. ORGANIZATION AND COORDINATION OF THE TASK 4 EFFORT

Task 4 is divided into five phases, occurring over a 10-year period of time (Fig. 4-47). The phases are:

I. Technology assessment.
II. Process development.
III. Facility and equipment design.
IV. Experimental plant construction.
V. Conversion to mass production plant (by 1986).

Phase I was initiated in February 1976 and has been under way for 9 months. Phase I has these specific objectives:

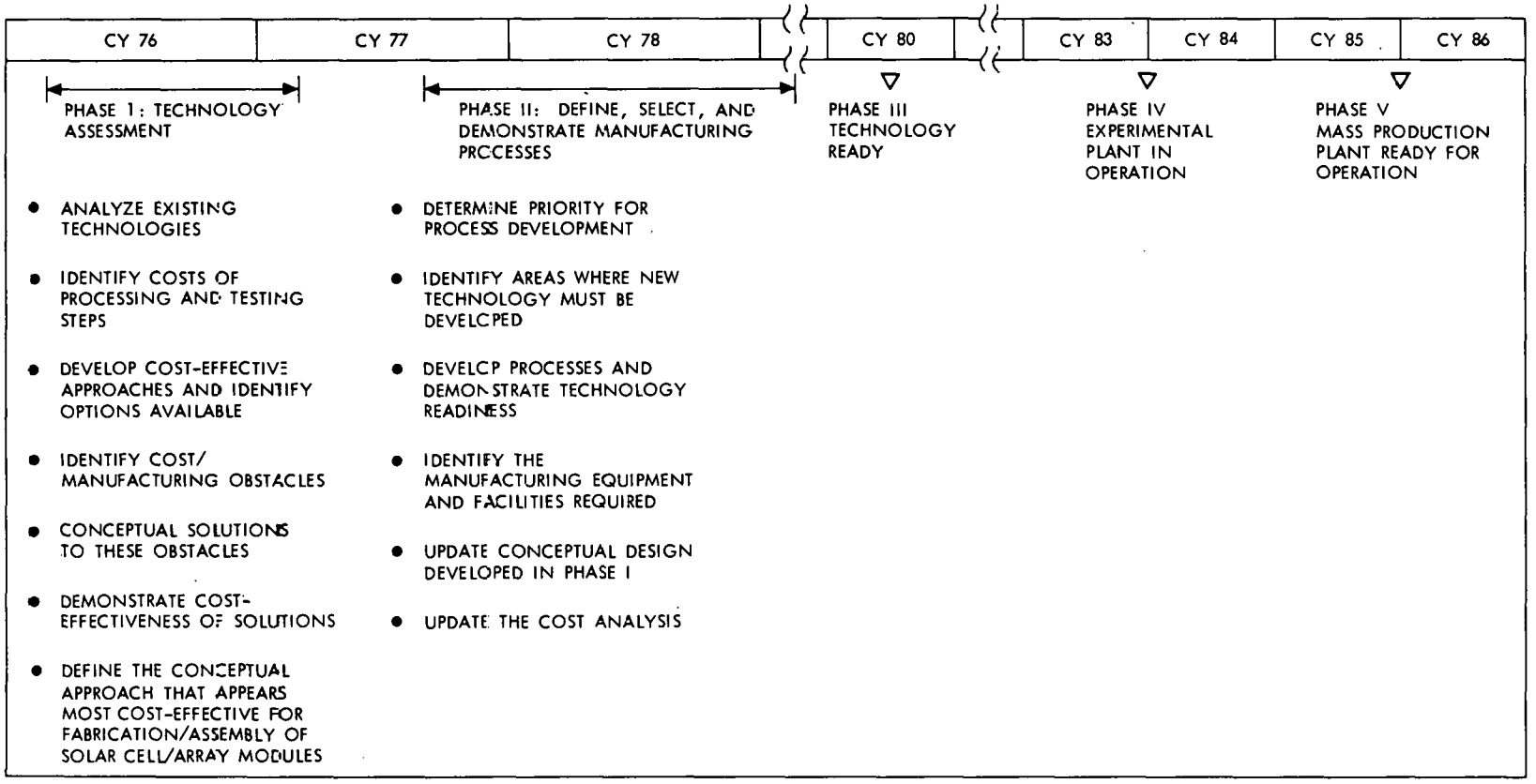

Fig. 4-47. Solar Array Automated Assembly Task schedule

- To identify the requirements for economical manufacturing processes and facilities.
- To assess the technology currently used in the manufacture and assembly processes that could be applied to solar arrays.
- To determine the level of technology readiness to achieve high-volume, low-cost production.
- To propose processes for development.

It is anticipated that the Request for Proposal package for Phase II will be distributed to industry early in 1977.

C. TASK 4 CONTRACTS

During the report period, work continued under Phase I contracts awarded to three contractors (Motorola, RCA, and Texas Instruments) to perform parallel efforts (Table 4-18). The three-contractor parallel-effort philosophy was selected to obtain the broadest possible view of recommendations and conclusions upon which to base the contractual efforts of Phase II (Fig. 4-47). During Phase I, these contractors are defining the requirements for an automated solar cell manufacturing sequence by evaluating processes now used by the semiconductor industry and the ways in which these processes can be modified/selected for high-volume, low-cost production of solar cell modules. Cost analyses are being conducted to provide economic guidelines to maintain an overall view of LSSA Project objectives.

Work also continued under contracts for two support efforts (Table 4-18) that emphasize development in specific areas of concern and thereby contribute to achievement of the Task 4 objectives. In September 1976, Simulation Physics completed a study of the feasibility of a unique process for forming solar cell P/N junctions at room temperature. In March 1976, Texas Instruments started work on the optimization of proven semiconductor techniques to produce silicon wafers in the most cost-effective manner.

Table 4-18. Task 4 contractors

Contractor	Type Contract	Technology Area
Motorola Phoenix, Arizona	Phase I	Manufacturing processes assessment
RCA Princeton, New Jersey	Phase I	Manufacturing processes assessment
Texas Instruments Dallas, Texas	Phase I	Manufacturing processes assessment
Simulation Physics Burlington, Massachusetts	Support	Electron-beam solar cell fabrication
Texas Instruments Dallas, Texas	Support	Large area Czochralski silicon ingot growth and wafering improvements

D. TASK 4 TECHNICAL ACTIVITY

1. Manufacturing Processes Assessment - Motorola, RCA, and Texas Instruments

Motorola

Studies on design improvement, process adaptation, process sequencing optimization, analysis of processing costs, solar cell fabrication, encapsulation design, and encapsulation progressed during this quarter in accordance with the contract program plan; no significant problems were identified.

A matrix of processing steps has been evaluated and individual processes have been placed in four categories of projected usefulness. Of the 49 processes evaluated, 15 have been dropped from further consideration, 6 need technological advances before further evaluation, 9 must be studied further to determine usefulness, and 19 are deemed likely to be included in a future manufacturing process. Four of the processes earmarked for further study are

gettering processes. (A literature survey on gettering has been performed and a bibliography on the subject has been prepared.) Detailed cost analysis of individual processes has been initiated as well as a study of future factory requirements.

Motorola has chosen a process sequence for initial fabrication of solar cells. The process includes texture etching, ion implantation, silicon nitride (antireflection coating), and plated contacts.

Reliability considerations for solar cell modules dictate a moisture-resistant cell metallization and a redundant, parallel-oriented interconnection scheme. A protective coating for steel makes it competitive with stainless steel with respect to corrosion. A stress test to study moisture ingression into modules has been developed and is currently being investigated for effectiveness.

RCA Laboratories

RCA's technology assessment phase of Task 4 has been completed. A summary of existing technologies applicable to solar array module manufacturing is given in RCA's quarterly report No. 3 (September 1976). Some highlights are given in the following paragraphs.

After reviewing the various forms of starting silicon material, RCA has concluded that wafers from Czochralski-pulled ingots are the only form of silicon that will be available for automated array processing during the next several years.

RCA has developed and tested a new procedure for optimized performance of both the front and back contact metallizations. The chief technical uncertainty in contact metallization is found to be the metal-silicon contract resistivity, ρ_c. A general criterion can be stated that ρ_c must be $\lesssim 10^{-2}$ ohm-cm^2. If this condition is met, a number of cost-effective options for both front and back contacts appear to offer satisfactory performance.

RCA has completed a survey of current solar cell contact and interconnect metallization technologies. The survey utilized criteria to determine technical applicability to silicon solar cells, large scale manufacturing feasibility (10^6 to 10^8 cells per year), production cost, and device reliability. Analyses of selected contact and metallization processes were then conducted using computerized cost analysis techniques. Based upon all analyses conducted by RCA, screen-printed silver contacts appear to be the most cost-effective.

RCA's quarterly report No. 3 describes and recommends one complete solar array module manufacturing sequence. Supporting technical and cost analysis documentation are included. The sequence — using gas diffusion junction formation technology, screen-printed silver contacts, spin-on antireflective coating, gap welding for interconnects, and a glass plate/conformal coating/metal foil moisture barrier panel — produces panels at a manufacturing cost of $0.9/W. The basic material costs have been brought to the $0.30 to $0.40/W range for 11% efficient cells, 9% efficient panels. Since the cost analysis documentation has been included in RCA's report, the interested reader can determine the exact origin of the costs for each of the process steps in the recommended sequence. Such a collection of cost analysis documents can be produced on demand when any sequence is selected from the list of evaluated processes included in the report. RCA's comparison of final solar panel costs provided the basis for selecting the particular manufacturing sequence recommended in the quarterly report.

A more speculative study, upgrading and refining existing technologies, is under way at RCA. In this area, technologies such as vapor epitaxy and ion implantation (which at present do not provide cost-effective processing alternatives) are being reevaluated using new conceptual equipment designs. According to RCA, the importance of high conversion efficiency is difficult to overstate in striving for low panel costs.

Texas Instruments

During the report period, Texas Instrument's efforts were concentrated on demonstrating process elements that appear to offer the lowest cost approaches, and on identifying the most effective approaches to higher cell efficiency. The techniques utilized for the implementation of these efforts were device modeling and device characterization.

Device modeling was used to assess the impact of changes in single parts of the cell model on the cell output. Modeling was achieved by using computer simulation of a "best fit" model for a 7.6 cm hexagonal cell. Families of current-voltage (I-V) characteristic curves were generated by fixing the model parameters and varying one parameter at a time. I-V curves generated by varying only the series resistance established the fact that series resistance at any level is a source of power loss in a solar cell. An improved solar cell design must therefore minimize series resistance in order to minimize power loss. I-V curves generated by varying only the excess component of current (I_s') established the fact that increases in I_s' (typically caused by improperly passivated junctions) are attended by a severe degradation in solar cell output current and power. Accordingly, the model shows the importance of good diode characteristics to solar cell performance. Cell design, cell fabrication, and module fabrication processes must all be optimized to provide stable diode characteristics over the life of a solar cell module. Further modeling is recommended by Texas Instruments and will continue into the next quarter.

Device characterization was used to verify the cell model and to evaluate several process elements. Device characterization (in darkness and light) was implemented to develop a better understanding of the factors that limit the conversion efficiency of an operating solar cell. Sample cells were evaluated to test the acceptability of different fabrication and mounting techniques such as cell junction edge effects and solder mounting of cells on printed circuit boards.

The design of an improved efficiency solar cell was also initiated by Texas Instruments during this quarter. An optimized solar cell design was formulated by utilizing a set of design equations in combination with the data from device modeling and device characterization. The cell design is primarily a metallization pattern generated to improve output power by increasing both the conversion efficiency and fill factor of the cell. Design assumptions were based on an assessment of the state-of-the-art in solar cell fabrication, silicon sheet technology, and module packing density. The goal of this design is to reduce series resistance, provide a cell that can be bonded to a substrate with a minimum of contacts, and utilize currently available high-quality silicon shee

material. The design is optimized to minimize the sum of the resistive losses and the transmissive loss due to metal coverage. A metallization mask pattern, based on the design efforts of this quarter and the next, should be available in the next quarter.

2. Electron-Beam Processing of Solar Cells - Simulation Physics

At Simulation Physics, a one-year program to develop a new concept for silicon solar cell production was completed during this report period. The purpose of the program was to demonstrate feasibility of silicon solar cell fabrication featuring significant reductions in the cost, material waste, and energy consumption normally associated with the production of silicon solar cells. The feasibility of producing high performance cells at high speed by a simplified vacuum processing sequence at room temperature has been demonstrated.

This new approach to solar cell processing is based on using pulsed energy techniques in conjunction with ion implantation. Some advantages of ion implantation in cell production are the ability to affect only the material surface being processed, the ability to introduce junction dopant at room temperature, and the possibility of achieving very high processing rates and throughputs.

For this program, pulsed energy techniques were used by Simulation Physics to subject specific surface regions to momentary elevated temperature transients. Energy deposition was achieved by large-area pulsed beams of relatively low energy, 15 to 40 keV, electrons. The electrons deposit their energy close to the surface involved and the pulse is so short, less than a microsecond, that little heat can be lost from the region during the pulse. Consequently, only a small mass of material is heated and very high temperatures can be achieved in the process region through the use of a very small amount of energy. Within microseconds, the temperature transient decays and the material as a whole is left at room temperature. Satisfactory conditions for the annealing of implant damage and sintering of electrical contacts have been achieved. Conventional procedures requiring long periods at high temperatures are replaced by single, momentary-pulse operations performed on room temperature substrates.

Ion implantation is known to offer excellent control of the dopant impurity profile, providing uniformity and reproducibility. It therefore has special potential for solar cell production. Ion implantation is a vacuum process and is usually performed at room temperature. It introduces pure isotope dopant directly into the impact surface; it does not result in the formation of surface oxides or foreign residues which must subsequently be removed as in other cell doping processes. Simulation Physics contends that these features make ion implantation ideally compatible with a simple automatable processing sequence having a high throughput potential.

For demonstration purposes, cells exhibiting up to 10% AMO efficiency have been prepared by room temperature vacuum operations requiring a total time of less than 2 minutes. In a production facility, even higher processing speeds would be possible, but probably would not be necessary.

It has been shown under this contract that solar cells can be produced without the generation of any waste materials, i.e., without the use of any gases, solvents, or acid etching solutions. The only consumables necessary, other than silicon, are the source of junction dopant for the ion implanter, the cell contact and antireflective-coating components, and input energy for the facilities. The total energy consumption associated with the processing method is small. Payback requirements are expected to be as low as a few hours of the output of the cells produced.

3. Large-Area Czochralski Silicon Ingot Growth and Wafering Improvements - Texas Instruments

The purpose of work under this contract is to optimize current proven semiconductor techniques so as to produce silicon wafers in the most cost-effective manner. Accordingly, technical activity has primarily centered on establishing acceptable silicon crystal pulling and slicing rates.

Crystal Pulling

A computer model to predict Czochralski growth rates was developed by Texas Instruments during the first quarter (April - June 1976) of this contract.

The model has been utilized extensively to investigate the effects of various puller parameters on pull rates. Emphasis during this report period has been on 12-cm-diameter crystals grown from a 12-kg crucible. This modeling work has produced the rather surprising result that pull rate is fairly insensitive to parameters such as ambient temperature and environment, crucible dimensions, or auxiliary cooling schemes such as cooling coils around the growing crystal.

Texas Instruments reports that the greatest enhancement in pull rate can be achieved by minimizing the thermal influence of the crucible sides on the crystal. This can be accomplished in two ways: (1) maintaining the melt level as close to the crucible lip as possible by continual melt replenishment (semi-continuous growth) and (2) decreasing the crucible side heat emittance with a reflective heat shield. The first approach can increase the maximum pull rate from 15 cm/h average for a single charge pull to around 17.9 cm/h for semicontinuous growth. The crucible heat shield could effect a 10-20% increase in pull rate. In any event, it appears that a nominal 18-cm/h pull rate is the maximum achievable for 12-cm-diameter crystals.

The use of a cold coil around a growing crystal to cool it rapidly, thereby increasing the pull rate, was shown experimentally to have neglibible impact. This experiment did, however, offer experimental verification of the computer model which predicted a pull rate of 21.6 cm/h versus an observed maximum pull rate of 22 cm/h for a 7.6-cm-diameter crystal pulled from a 6-kg crucible.

Experimental work with 12-cm crystals has been delayed pending delivery of needed parts to retrofit an 8-kg puller to 12 kg.

The results of pull rate determinations made thus far under this contract can be summarized as follows:

1) Puller ambient temperature has a negligible influence on pull rate provided it is held below 600°K.
2) Convective heat transfer has only a minor effect on pull rate, being less than 1 cm/h.

3) The maximum pull rate varies as $(1/r)^{1/2}$ as predicted by simplified models, where r = crystal radius.
4) Cooling coils have a negligible effect on pull rates and are not worth further consideration.
5) The maximum pull rate possible for a 12-cm crystal is approximately 18 cm/h and this assumes semicontinuous growth in which the melt level is maintained constant relative to the crucible lip.

Crystal Slicing

Experiments in the multiblade slurry-sawing of Czochralski ingots have produced several encouraging results. Two different runs in which three 5-cm crystals were sawed simultaneously have indicated that multiple crystals can be sawed at the same rate as a single crystal. The fastest cutting rate to date has been obtained using 400-grit boron carbide abrasive. With a 240-g/blade cutting force at 54-cm/s blade speed, a single 7.6-cm crystal was sawed in 6.2 hours. This corresponds to a slice production rate of about 40 slices/h, which is considerably higher than the rate of conventional ID sawing of semiconductor-quality slices. Multiple-crystal sawing offers the potential of doubling or tripling this production rate.

Crystal slicing determinations made thus far under this contract can be summarized as follows:

1) Sawing rate is directly proportional to blade load.
2) For a given blade load, the sawing rate is proportional to blade speed.
3) Sawing rate is independent of kerf length, i.e., multiple crystals can be sliced at the same rate as a single crystal.
4) As the blade load increases, parameter control (bow, taper, etc.) appears to decrease.
5) Boron carbide sawing is 2.5 times faster than silicon carbide sawing for a given particle size and blade load.
6) Initial scanning electron micrographs of the new and used silicon carbide indicate particle wear and fragmentation.

7) Initial damage-depth measurements indicate damage to a depth of approximately 15 microns.
8) Efforts to date to saw thin slices by utilizing thin blade spacing (0.038 cm, 15 mils) have resulted in excessive slice breakage.
9) Multiblade slurry sawing yields with the thicker slices are in excess of 95%.

Cost Projection

The economic model of the Czochralski wafering process has been updated since the last quarterly report. The impacts of lowering the maximum pull rate to 15 cm/h (from a theoretical 28 cm/h) and decreasing sawing cycle time to 20 h (from 39.8 h) have been included. These changes tend to offset each other, with the result that the final wafer cost is still projected as being in the $\$30\text{-}36/m^2$ range. (This cost projection is unchanged from calculations reported by Texas Instruments in the previous quarter.) At the higher value, the sheet cost of a solar cell fabricated on a 12-cm wafer with an AM1 efficiency of 12.5% would be about $0.29/W.

PART V

DEVELOPMENT, PROCUREMENT, AND EVALUATION OF SOLAR ARRAYS

The objective of the Development, Procurement, and Evaluation of Solar Arrays (DPESA) activity is to stimulate industry to produce larger quantities of improved, less expensive silicon solar arrays in support of the ERDA Photovoltaic Test and Demonstration Project. This involves the periodic purchase of increasing quantities of solar arrays at decreasing unit prices, using the latest state-of-the-art technology. The arrays will be procured from industry on a commercial basis to meet performance specifications and environmental requirements for use in numerous and diverse ERDA tests and demonstrations.

These activities are expected to bring about improved designs in order to achieve production and cost improvements. The arrays will be manufactured by production contractors, under Project sponsorship. In addition, whenever and wherever practical, technology improvements achieved in other tasks of the Project will be applied to contemporary array production. This will aid in the achievement of task objectives, and also in testing the new technology in the context of actual commercial manufacturing conditions.

A. BACKGROUND

At the inception of the LSSA program in January 1975, the solar cell manufacturing industry in the United States was in decline. A solar cell production capacity of about 10 kilowatts per year, for use in space, had been reached in 1970, at the peak of the NASA program. Production of solar cells for spacecraft has been declining since. By comparison, the rate of production of cells for terrestrial application was very low and was increasing only very slowly. A few small companies were making terrestrial modules. These companies could be considered offshoots of the large U.S. semiconductor industry. Silicon solar cells were made of semiconductor-grade silicon, which has been expensive for large-scale terrestrial use. Large variations in availability and price of pure

silicon have been a feature of the dynamic semiconductor industry. In terms of the total production of silicon, the solar cell manufacturers are small consumers. Having limited resources, these companies have been occasionally subjected to strong economic forces, resulting in some instability.

The intervention of the LSSA Project in this market should provide a strong stabilizing force and large cost reductions. An assured and growing market for solar modules should provide the incentives for private capital investment, process development, improved availability of raw materials at lower prices, and lower product costs from increased scale of production. Additional cost reductions will result when the developments generated by the technology development tasks of the LSSA Project are incorporated into the final product during the coming decade.

B. ORGANIZATION AND COORDINATION OF THE DPESA EFFORT

The Project state-of-the-art solar array activities involve the efforts associated with planning, acquiring, evaluating, and interfacing required by the Project/Program with regard to contemporary modules/arrays. These activities are performed by the following Project tasks: engineering, large scale production, quality assurance and reliability, and operations. The Engineering Task defines module/array design, performance, and test requirements in conjunction with appropriate personnel in and out of the Project. The Large Scale Production Task is responsible for the array procurement activities and the interfaces with the array manufacturers. The Quality Assurance and Reliability Task defines and verifies module/array hardware quality including inspection of the manufacturing activities. The Operations Task coordinates and controls module test planning, testing, performance analysis, and liaison with users.

Contracts have been awarded to industry through competitive bidding processes for the production of large quantities of solar cell modules. A summary schedule is shown in Fig. 5-1; a plan for future procurements is given in Fig. 5-2. The contracts will be awarded on essentially an annual basis for progressively increasing quantities of hardware. Beginning with the 130-kilowatt procurement, small business concerns were solicited through a set-aside

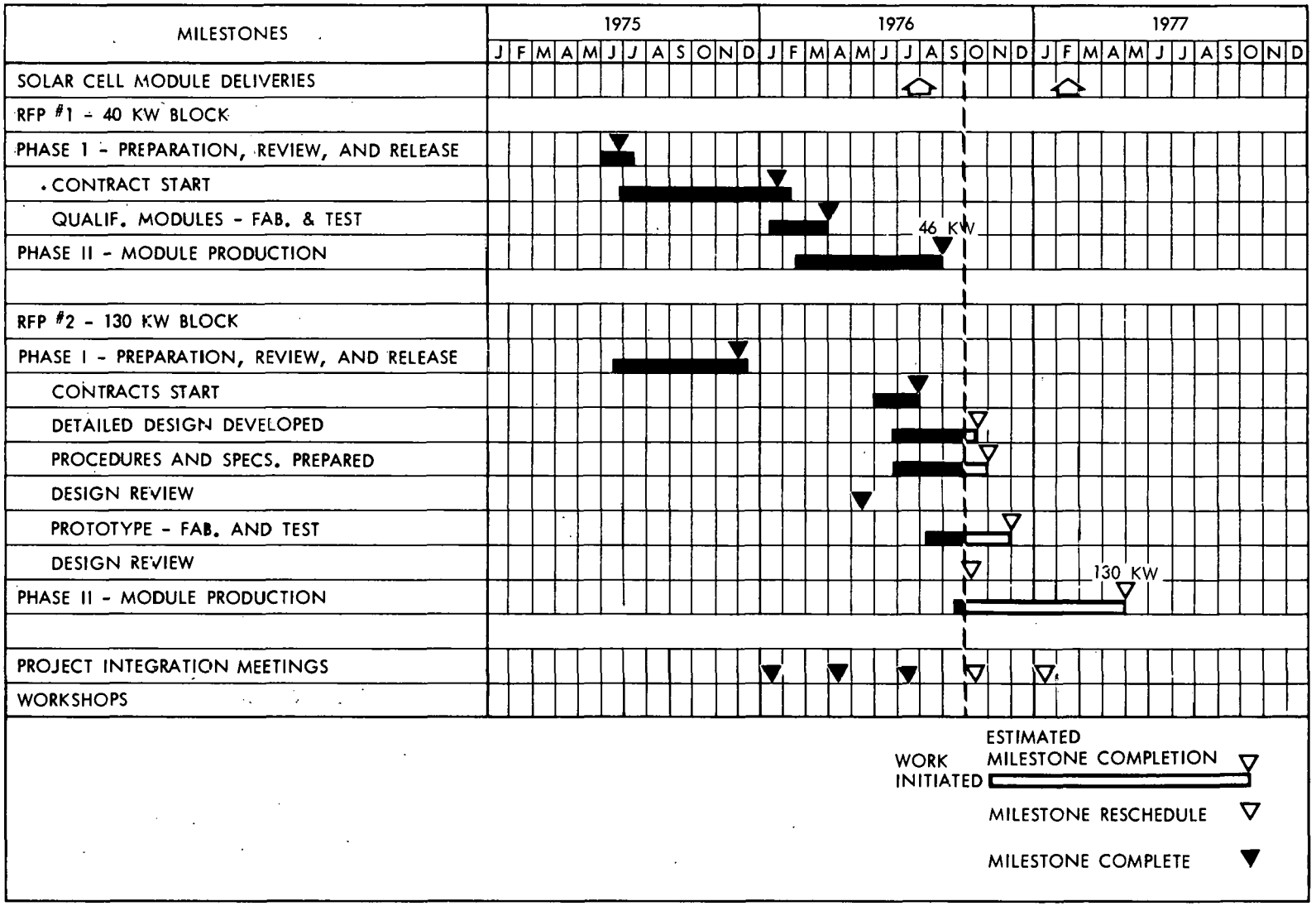

Fig. 5-1. Large-Scale Production Task schedule

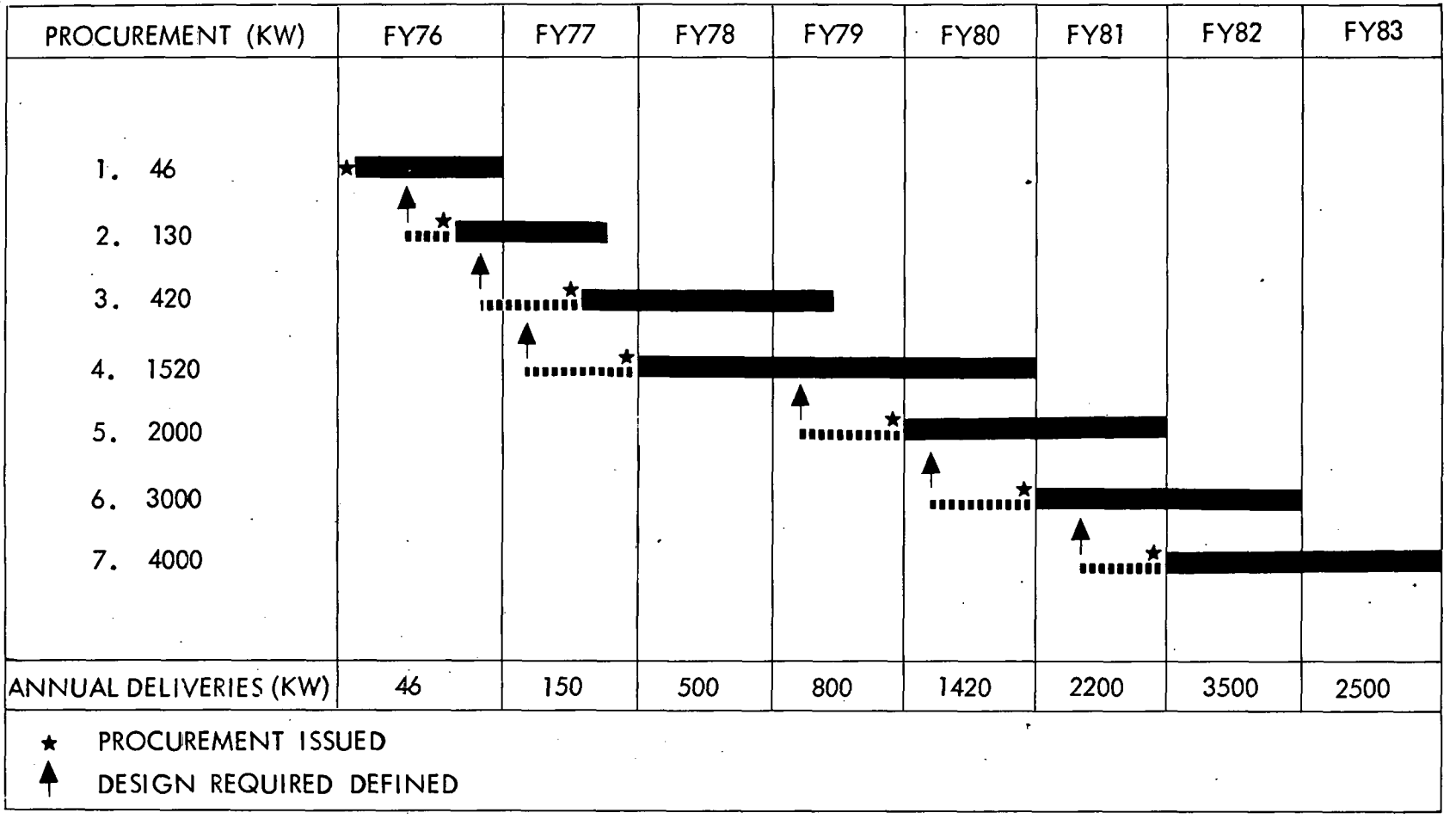

Fig. 5-2. Solar array procurement plan

procedure. The initial modules produced will be used in applications requiring low power, such as for isolated installations of the Department of Defense. Future modules will be for systems testing of a photovoltaic power source tie-in to a commercial power grid.

The purchase of 130 kilowatts of solar arrays will incorporate changes to obtain a more uniform design, to provide greater flexibility in the demonstrations while encouraging further cost reductions. Participation in this procurement was more widely solicited and will involve the many companies presently preparing or extending manufacturing capability.

The RFP for the initial (46 kilowatt) procurement specified the temperature cycling and humidity requirements that the modules must meet. Qualifying the modules to these requirements is the responsibility of the supplier. At JPL, sample modules were subjected to these environments and their performance was evaluated. In addition, the modules were exposed to other environments they are likely to meet during the ERDA demonstration program. These are humidity-freezing, rain-heat, salt fog, and fungus. Also, samples were set up in racks at JPL as a field test in the Pasadena, California environment.

The 130 kilowatt procurement is not limited to state-of-the-art modules of existing design. A contract period for design upgrading is provided and design criteria are given. Module designs are specified that will fit into a 4 x 4-foot subarray. Other requirements of this purchase are:

1) A minimum of 60 watts of power based on the 4 x 4-foot array.
2) Fifty thermal cycles from -40° to $+ 90^{\circ}$C.
3) Five temperature cycles at high relative humidity (RH).
4) One-hundred cyclical applications of structural loads.

A comparison between the procurement specifications for the 46 kilowatt purchase and those for the 130 kilowatt purchase is shown in Table 5-1.

Table 5-1. Key specifications for the LSSA 46 kilowatt and 130 kilowatt solar array purchases

Specification	46 Kilowatt Purchase	130 Kilowatt Purchase
Electrical Performance	100 milliwatts/cm^2, 28°C	100 milliwatts/cm^2, 60°C
Temperature Cycling	100 cycles, -40 to + 90°C at less than 100°/hr	50 cycles, -40 to + 90°C
Humidity	168 hours, 95% RH, 70°C	5 cycles, 95% RH, 23 to 41°C
Wind Loading	N/R	100 cycles, ± 50 lb/ft^2
Insulation Resistance	N/R	100 MΩ, 1000 vdc
High Voltage Breakdown	N/R	1500 vdc, 1 minute
Packaging Envelope	N/R	Envelope of 4 x 4 ft frame
Redundancy	N/R	Terminal and in some cases cell-to-cell redundancy

C. DPESA TECHNICAL ACTIVITY

1. Large-Scale Production Activity

46 Kilowatt Procurement

Contracts to procure 46 kilowatts of terrestrial state-of-the-art silicon solar cell modules were awarded to five contractors in early 1976. The objective of the procurement was to purchase production quantities of existing solar cell module designs for use in practical demonstration programs of photovoltaic solar arrays. Four of the contractors completed delivery of modules on their contract; one was unable to manufacture modules at a reasonable production rate because of technical difficulties, and his contract was terminated (Table 5-2). The contractors produced modules for a total power slightly in excess of 43 kilowatts.

Table 5-2. Module production for 46 kilowatt procurement

Contractor	Number of Modules Delivered	Power of Modules Delivered (kW)
Solar Power Corp.	1037	15.0 (completed)
M7 International	52	0.26 (terminated)
Solarex Corp.	1046	10.0 (completed)
Sensor Technology	1600	8.0 (completed)
Spectrolab, Inc.	2000	10.0 (completed
TOTAL	6735	43.26

Solar Power Corporation began delivery of production modules in mid-May and completed module production in mid-August 1976. A total of 1037 modules were produced which included prototype modules used for evaluation testing. During the report period a contract add-on of 15 kilowatts was negotiated, to provide spares and support additional system-test needs.

M7 International produced a total of 52 modules over a 5-month period. Technical difficulties in solar cell manufacturing limited module production. The contract was terminated when it became evident that a reasonable module production rate could not be sustained.

Solarex Corporation completed their contract for 10 kilowatts of solar cell modules in September 1976. Power per module was an average of 9.46 watts and a total of 1046 modules were produced over a 6-month period.

Sensor Technology completed delivery of production modules in August 1976. A total of 1600 modules were produced over a 5-month period.

Spectrolab produced 2000 5-watt modules over a 6-month period and completed the contract for 10 kilowatts of solar cell modules in October 1976.

130 Kilowatt Procurement

Preliminary design reviews were held with each of the four contractors, Sensor Technology, Solar Power Corporation, Solarex, and Spectrolab. After the design requirements had been met, each contractor was instructed to start production of prototype modules. The basic requirements for the modules of the 130 kilowatt purchase include the following items:

1) Module power to be determined at 15.8 volts at 60°C cell temperature and 100 mw/cm^2 sunlight intensity equivalent.
2) A 4 x 4-foot subarray to produce a minimum power of 60 watts when measured at 60°C and 100 mw/cm^2.
3) Modules to withstand 50 thermal cycles from -40°C to +90°C.
4) Modules to withstand 5 cycles of 95% relative humidity, from 23°C to 41°C.
5) Modules to withstand a simulated wind loading test of 100 cycles of plus and minus 50 lb/ft^2.
6) Modules to withstand 1500 vdc when applied between the solar cell series string and the module grounding terminal.
7) Modules to have an insulation resistance of 100 megohms or greater between the solar cell series string and the grounding terminal.

The Sensor Technology module design is a stamped aluminum substrate. Forty-two cells are connected in series to meet the voltage and power requirements. Eight modules of 11.375 by 22.90 inches fit into a 4 x 4-foot subarray. The encapsulation used in the module is RTV-615; this material is also used to provide insulation between the cell series string and the aluminum substrate. Sensor Technology is contracted to produce 40 kilowatts of modules for this procurement.

Solar Power Corporation will use a molded substrate design for modules produced for the 130 kilowatt procurement. The solar cells and interconnections will be encapsulated in Sylgard 184 with a smooth, harder outer coating bonded to the encapsulant. The module size is 15.29 by 46 inches. Three modules make

up a standard 4 x 4-foot subarray. A total of 15 kilowatts of modules is scheduled for production under the fixed-price purchase order.

The Solarex Corporation module design will use a polyester substrate supported by an aluminum frame. The solar cell series string will be protected by a silicon rubber encapsulant. Four modules 22.875 by 22.97 inches make up a 4 x 4-foot subarray. Thirty kilowatts of solar cell modules will be supplied by Solarex under this procurement.

Spectrolab will employ a glass-laminate module design supported at the edges by an aluminum frame. The module measures 15.26 by 46 inches and three modules make up a 4 x 4-foot subarray. When prototype module testing is successfully completed it is anticipated that an option to procure 46 kilowatts of this type module will be exercised.

2. Engineering Activities

Engineering activities during the quarter centered in two areas: 1) the completion and documentation of previously reported activities in preparation for the start of the new fiscal year in October and 2) support of the start-up of the 130 kilowatt large-scale procurements. Specific activities associated with previously reported work include completion of the first phase of solar cell module thermal evaluation tests, structural cyclic loading tests, and electrical connector environmental qualification tests. The results of these activities are summarized below and described in detail in reports in publication.

Development of requirements for the next large-scale procurement was initiated during the quarter and will be the subject of considerable activity in FY1977. General thoughts on future array requirements were recently presented in a paper at the 1976 International Solar Energy Society Conference in Winnipeg, Canada.*

*Ross, R. G. Jr., "Design Considerations of Solar Arrays for Terrestrial Applications," Proceedings of the 1976 Solar Energy Society Conference, Winnipeg, Canada, Aug. 15-20, 1976, Vol. 6, pp. 48-56.

Thermal Evaluation Testing

Thermal testing of the modules of the 46 kilowatt purchase was briefly described in the first LSSA project quarterly report (JPL Document No. 5101-7, Oct. 8, 1976, pp. 5-12 through 5-15). During the past quarter the testing has continued; current activities are directed toward improved understanding of the effects of wind. In addition, a number of complementary analytical studies have been conducted to extend the test results and understand the module thermal design features responsible for improved thermal performance.

Two of the more interesting test results are presented in Figs. 5-3 and 5-4. Figure 5-3 illustrates the variation in cell temperature above the local air temperature as a function of total intensity for the hottest and coolest of the modules of the 46 kilowatt purchase. The data represent no-load measurements made under open-air field test conditions with thermocouples attached directly to the solar cells. From these data one can see that the simple expression

$$T_C = T_A + 0.3S$$

where T_C = cell temperature (°C), T_A = air temperature (°C), and S = solar insolation level (mW/cm^2), provides a good first order approximation for the operating temperature of a typical solar cell module under open-back field mounting conditions.

Figure 5-4 shows the variation in the cell temperature minus the adjacent black reference plate temperature as a function of total intensity for all modules of the 46 kilowatt purchase. The scatter in the data is large and is primarily due to wind effects. Despite the scatter the data indicate that, over the period of a day, the temperature difference ($T_{cell} - T_{ref.}$) averages out to be a linear function of total intensity for an average wind velocity. (The wind velocity for this particular data averages about 3 mph.) The data of Fig. 5-4 are significant in that they suggest that the cell temperature relative to a standard reference device, such as a flat black plate, may prove useful in characterizing the thermal performance of a module.

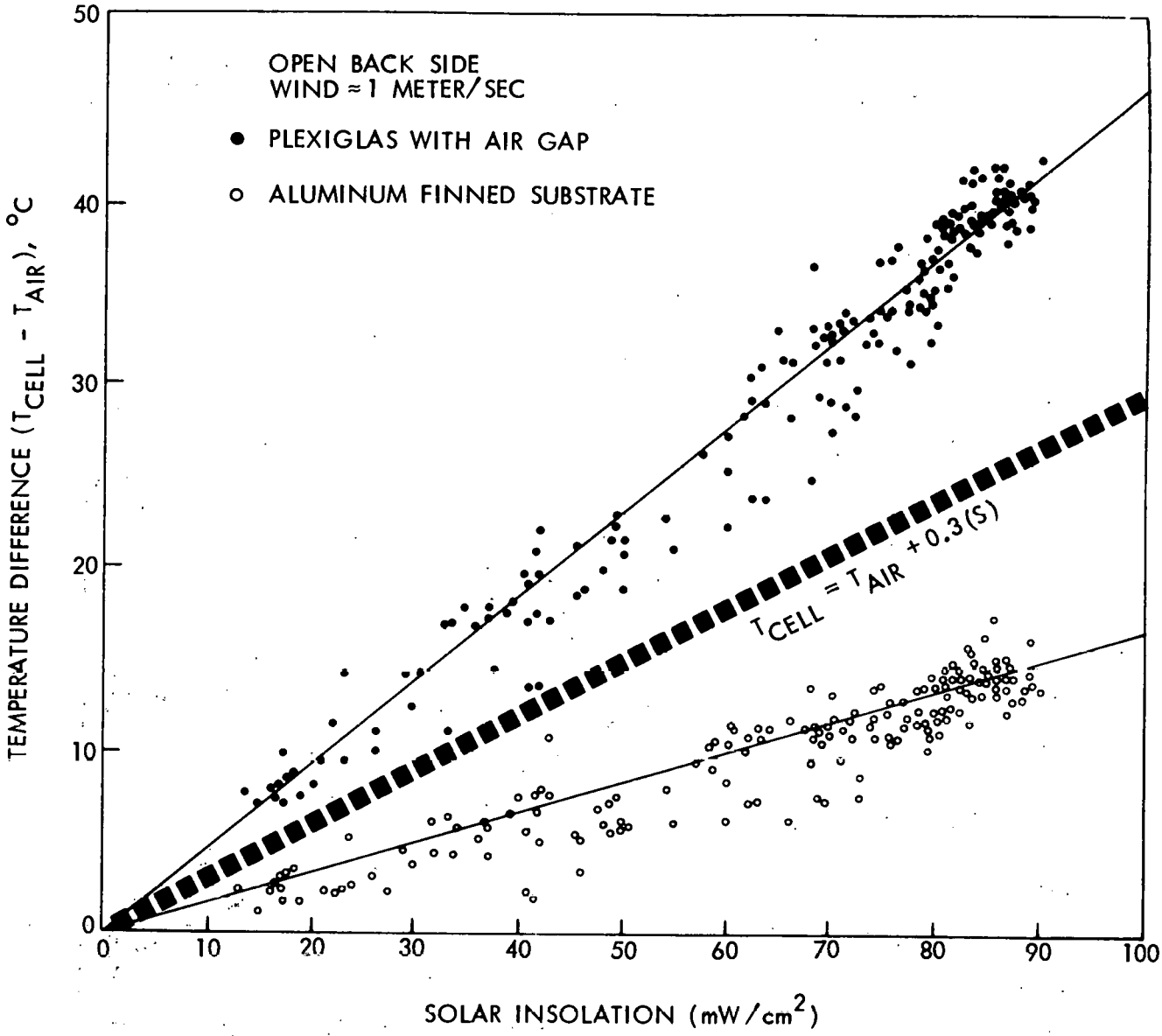

Fig. 5-3. Typical solar cell temperature measurements for hottest and coolest modules -- 46 kilowatt procurement

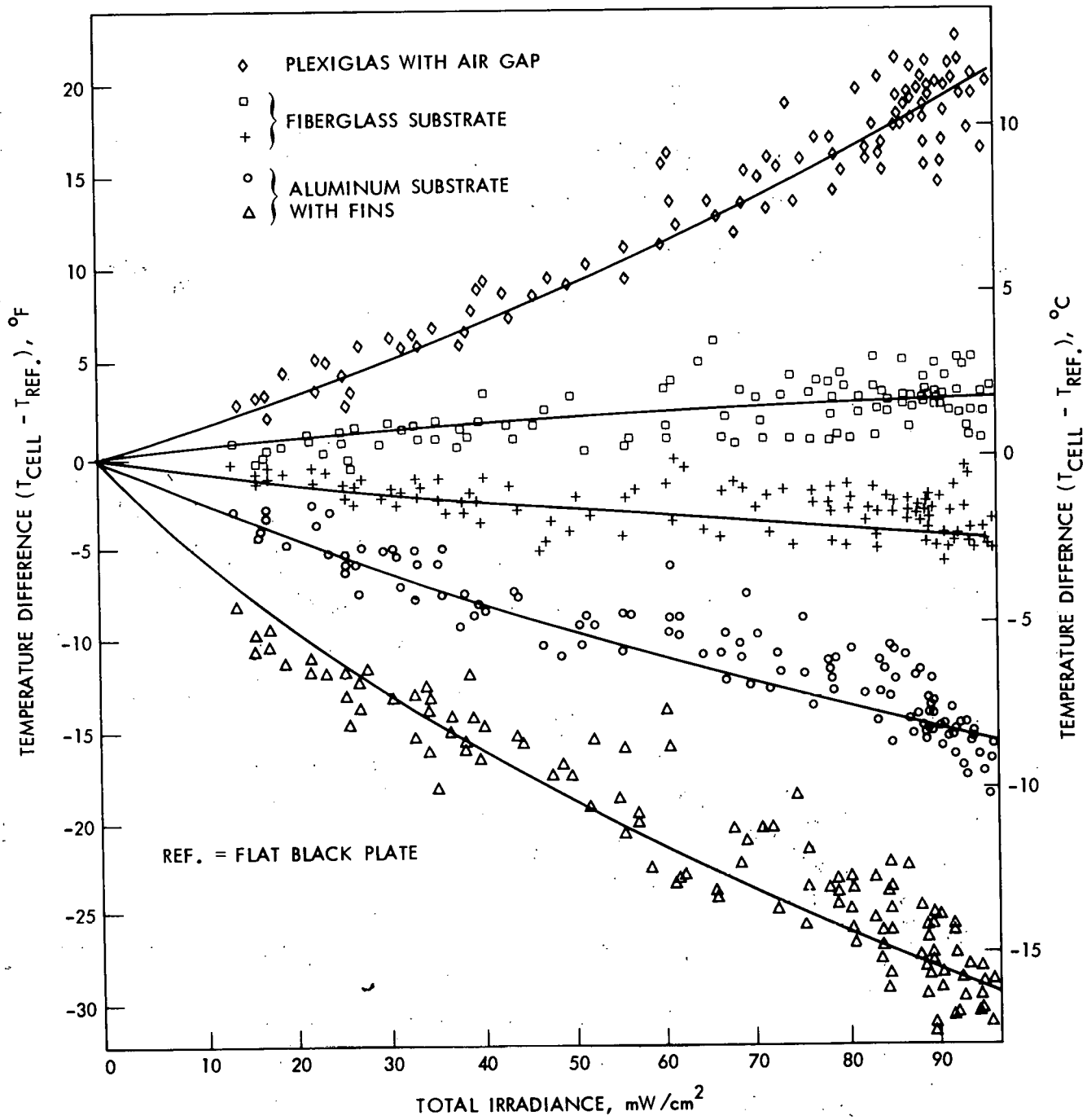

Fig. 5-4. Relative operating temperature of modules — 46 kilowatt procurement

To better understand the effects of the wind, continuous strip chart wind data were measured and analyzed with respect to available theories for convective cooling. The wind is very turbulent at the JPL ground site, which is probably typical of all ground-level sites. This turbulence is indicated by the continuous measurement of its velocity and direction, a representative sample of which is shown in Fig. 5-5. Since convective cooling is, or can be, the dominant mode of heat transfer from a module, an accurate estimate of the convective heat transfer coefficient is very important. The total convective coefficient as reduced from the test data was found to be approximately $H_{total} = 0.42V$ where H is in Btu/hr-ft^2-°F and V is measured in mph. It also appears that, as a first approximation, the coeffficient of heat transfer for the front can be assumed equal to that for the back: $h_f = h_b = 0.21V$. This equation appears to fit the data very well for velocities greater than 3 mph where forced convection is dominating. At lower wind velocities, free convection on both the back and front is significant. For the free convection, it is recommended that $h = 0.22\ (\Delta T \cos \psi)^{1/3}$ and $h = 0.19\ (\Delta T \sin \psi)^{1/3}$ be used for the front and back, respectively. There is always free convection on both sides and, depending on the wind direction, forced convection is applied to one side or the other. If the flow is parallel to the module, a forced convection coefficient ($h = 0.21V$) on both sides appears appropriate.

To determine the key parameters responsible for the operating temperature differences between the modules of the 46 kilowatt purchase, multi-node computer models were constructed for each module type based on its thermal properties, construction geometry, and the heat transfer coefficients just described. Subsequent sensitivity analyses identified the following characteristics as key to reduced cell operating temperature:

1) The presence of good thermal conductance paths from the cell to high emittance external surfaces is the primary requirement for low operating temperatures. Thin transparent material with relatively high thermal conductivity (e.g., glass) should be selected as the material for the front encapsulant. Air gaps between the cell and exterior surfaces create greenhouse effects which are extremely harmful and raise cell temperature by about 15°C. As a result, air spacing should be avoided completely in the module structure.

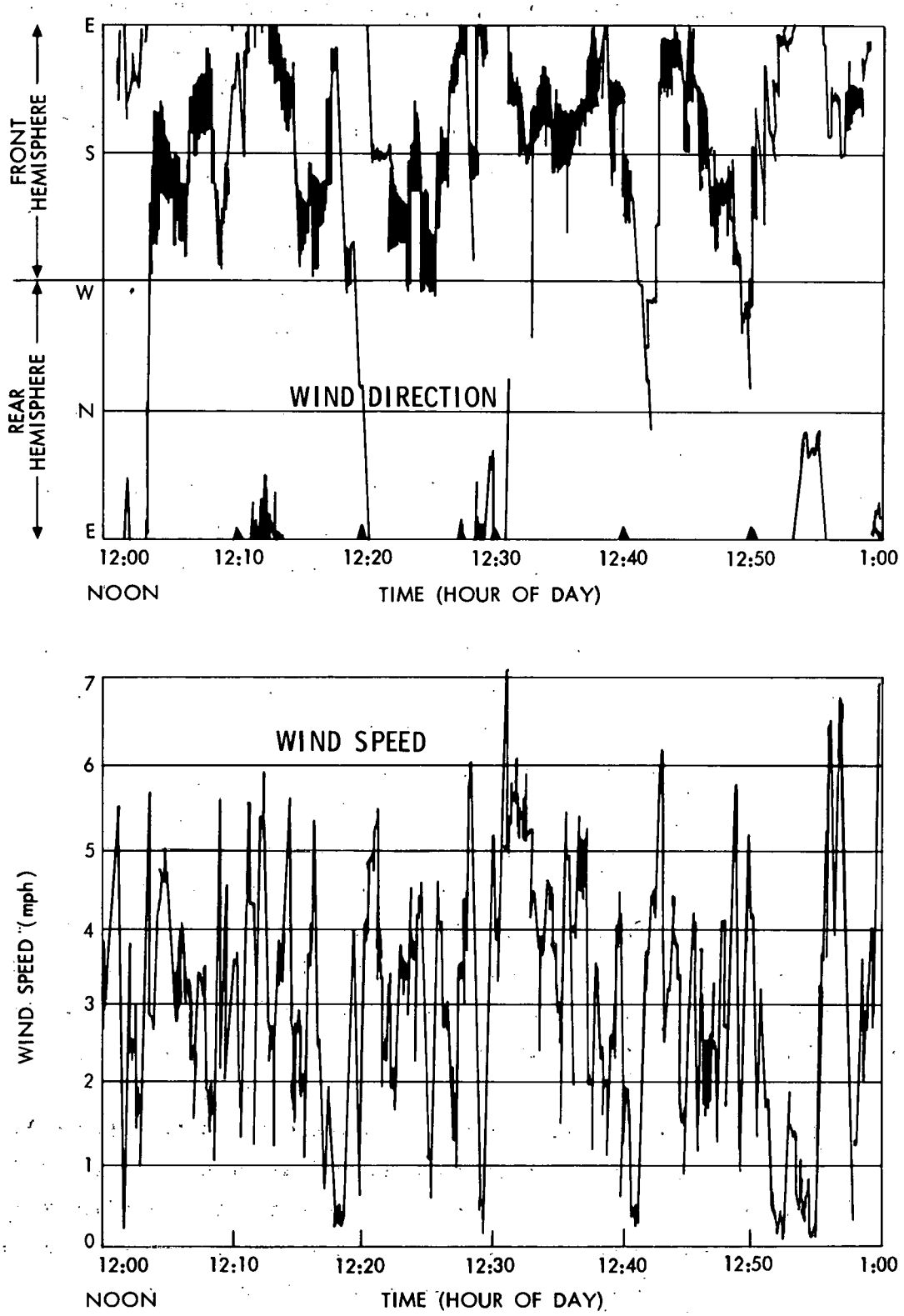

Fig. 5-5. Typical wind data at JPL test site

2) The presence of good lateral conduction from the cell to low absorptance, high emittance surfaces between the cells can reduce cell temperature by as much as 10°C. If material which has poor thermal conductivity is used, the thickness should be kept to a practical minimum. Similarly, for a substrate with poor thermal conductivity, the substrate solar absorptance does not play an important role. Consequently, the substrate solar transmittance should be kept to a minimum. The transparent feature offers negligible advantage in open-frame mounting while allowing reflected solar energy (from the ground or other array surfaces) to impinge on the back surfaces of the cells. For roof-mounting situations, transparent substrates become a major handicap. A nontransparent substrate with high solar reflectance is thus recommended for both types of mounting conditions.

3) The presence of finned rear surfaces to increase convective cooling can reduce cell temperature by about 5°C in open-frame mounting applications. For roof-mounting applications, the effectiveness depends strongly on the "infiltration level" (the amount of air circulation behind the module).

Structural Cyclic Load Testing

Structural testing of the modules of the 46 kilowatt procurement was briefly described in the first LSSA project quarterly report (JPL Document No. 5101-7, Oct. 8, 1976, pp. 5-12 through 4-14). The objective of this testing was to explore the capability of the current module designs to withstand repeated application of 50 lb/ft^2 cyclic pressure loading, particularly with respect to mechanical fatigue of the cell interconnect system, and to evaluate the ease of conducting such tests. The end objective was to obtain data needed to set design and test requirements for future modules.

The cyclic pressure loading apparatus developed as part of this effort performed extremely well and applied more than 130,000 cycles during the test duration. The concept involved pressurizing the module by alternately inflating air mattresses sandwiched between the module and rigid platens on each side of

the module. Cyclic inflation was handled by an automatic control system designed for unattended operation. A continuous electrical continuity check was used to shut down the apparatus in the case of a change in module circuit resistance which would indicate a possible failure.

During the test, nine solar cell modules representing each of the five module types of the 46 kilowatt procurement were subjected to the 50 lb/ft^2 uniform load, which was alternately applied to the front and back sides of the modules. The loading rate was moderately slow (approximately 40 seconds for a complete plus and minus loading cycle) so as to be consistent with the fact that the loading was intended to simulate periodic gust loading of a $\geq$100 mph wind over the lifetime of the module.

The following general comments can be made concerning the test results:

1) All five designs proved to be structurally capable of withstanding the cyclic pressure loading, even though three of them exhibited rather large deflections.

2) All five designs used a clear silicone potting compound as a cell encapsulant. Encapsulant/substrate delamination did not occur during the course of these tests.

3) Three of the five designs exhibited no failures of any sort even though the number of cycles applied to a single panel exceeded 35,000 in two of the designs tested.

4) One design exhibited a tendency to fail at the cell interconnects because of mechanical fatigue. In some cases the failure occurred in the ribbon type interconnect approximately midway between cells, and in other cases the failure occurred where the interconnect was soldered to the top of the cell. This particular design has a very shallow stress relief loop between solar cells, and this is considered to have contributed strongly to the observed failures.

5) Another design exhibited a minor anomaly which was traced to the expanded metal cell interconnects. In a few cases, cutting out the mesh to produce the interconnects produced sharp barbs which were located very close to the edge of a cell. Upon panel flexure these barbs shorted the bottom of a cell to the top of the same cell.

6) A general conclusion from the testing performed here is that it is not difficult to design solar panels to sustain the 50 lb/ft^2 cyclic pressure load. It is also encouraging to note that the cell interconnect anomalies encountered are readily explainable in terms of noticeable differences between these designs and the other designs. These problems are considered easily avoidable in future designs.

Electrical Connector Testing

In support of the Engineering Activities effort to explore alternative approaches to module output electrical terminals, a search was initiated in vendor catalogs and in cabling and connector manufacturing houses for existing electrical connector designs which would fit projected module requirements. Only one company, ITT Cannon Electric, was found to manufacture a promising low cost connector. Cannon's Sure-Seal connector (Fig. 5-6) is presently in use on the automatic-brake-system electrical circuits of large diesel trucks and buses. In this case, the electrical application is at 12 volts, and the advertised insulation resistance for the present production version of this connector is 100 megohms, measured at a low test voltage of 50 Vdc. Working voltages in the solar panel applications are expected to be greater than 250 volts, and possibly as high as 1000 volts. The overall simplicity of the design and construction combined with an attractive low cost make the Cannon Sure-Seal connector a highly viable candidate for use in the solar panel program.

To further understand the capabilities of this particular connector design, 94 mated pairs of three different configurations were purchased and subjected to qualification tests designed to represent the actual environments the connectors would be most likely to experience. The three configurations consisted of

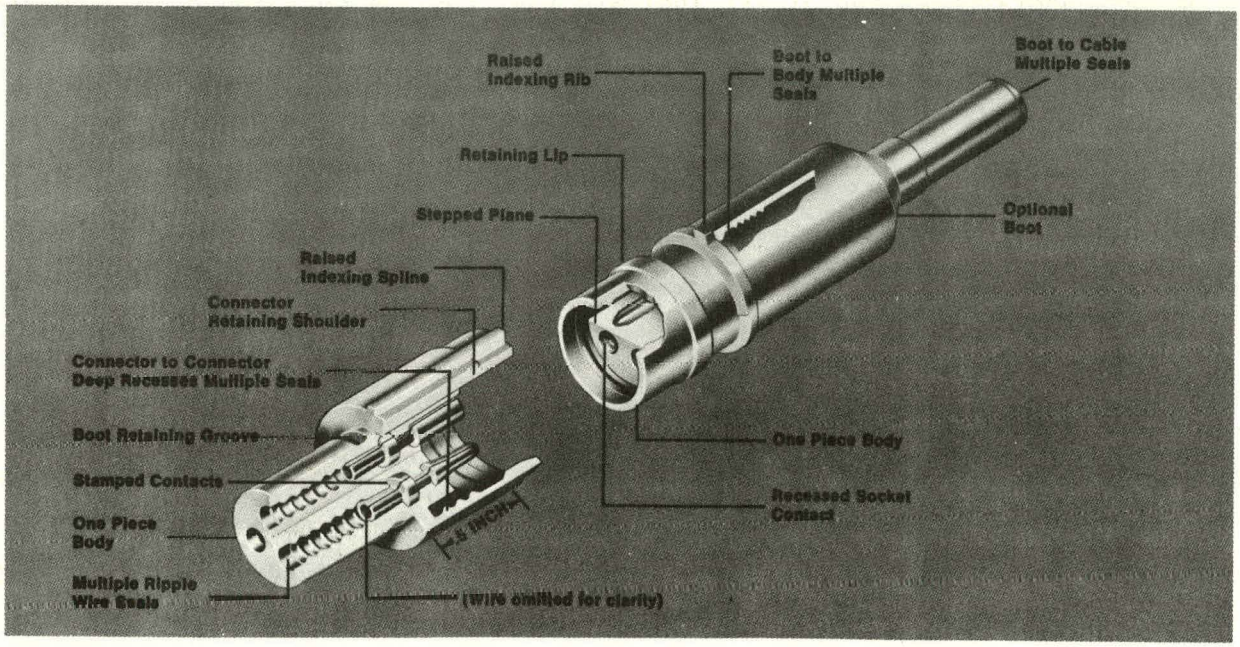

Fig. 5-6. Cannon Sure-Seal connector

two-conductor nitrile rubber connectors, three-conductor nitrile rubber connectors, and a number of prototype three-conductor connectors manufactured from ethylene propylene diene monomer (EPDM). The contacts are a stamped copper-alloy tin-lead plate.

The environmental testing was performed at Delsen Corporation Testing Laboratories in Glendale, California and at JPL as indicated below:

Tests Performed at Delsen Laboratories	Test Performed at JPL
Temperature cycling and humidity	Insulation resistance
Salt spray	Connector/contact retention/ durability
Ozone and ultraviolet exposure	Final connector/contact retention
Insulation resistance at high temperature	Dielectric withstanding voltage (1500 Vac)
Insulation resistance at room temperature prior to and after environmental exposure	Visual (6x microscope)

The results of the test conducted on the ITT Cannon Sure-Seal connector at Delsen Laboratories and at JPL indicate that the low cost connector has great potential in the solar panel interconnect application. The connector performance was better than expected, particularly in view of the application for which it was originally designed. The present production versions of these connectors are made of nitrile rubber and PVC. Of more interest are the EPDM connectors which, on the whole, performed better than the nitrile rubber/PVC connectors. The EPDM connectors were unaffected by ozone and ultraviolet, though the contact resistance of these connectors seemed to increase more than that of the nitrile rubber/PVC connectors upon exposure to moisture. The EPDM configuration tested has since been improved with a longer wire entry barrel. This provides for two additional sealing serrations (six total), which improves the moisture seal. The nitrile rubber/PVC compound connectors were attacked harshly by the ozone and ultraviolet environments. One disadvantage of the EPDM connectors is that they are not as resilient as the nitrile connectors as evidenced by some elongation of the wire entry holes. This condition can be alleviated by prudent wire routing.

The ITT Cannon Sure-Seal connector has been approved by the Underwriters Laboratory for 230 Vac service and is clearly a strong candidate for use on solar array modules. Further evaluation to define possible design improvements and understand the connector's performance in actual field test usage is under way.

As other electrical connectors and alternative electrical terminal designs are identified they will be examined and tested in a similar way.

3. Operations Activities

a. Environmental Testing

46 Kilowatt Procurement Block

By June 30, 1976, qualification testing of the early production modules was nearly complete. A data report covering these results was completed and distributed at the July Project Integration Meeting.

To correct early deficiencies, many minor design changes had been made during production of the modules of the 46 kilowatt procurement; consequently, 20 late production modules from each supplier were shipped to JPL for a new series of qualification tests as well as exploratory environmental and field testing. This late production module testing is called Phase 2 in the data reports. The late production qualification tests were completed on modules from two manufacturers by the end of this quarter. One set of modules showed only minor degradation, but the other showed significant power output reduction (7% and 10%) after humidity tests on two of the four modules tested. (Five percent degradation is acceptable under the terms of the 46 kilowatt procurement contract.) Modules from a third vendor have shown very little degradation to date after 50 temperature cycles.

Two sets of modules from the fourth vender, each of slightly different design, were damaged by a chamber malfunction. The thermal shock of a too-rapid temperature change rate shattered the encapsulant and a number of cells. Temperature cycling of two new sets was completed late in September. One module of the eight showed a temporary 40% electrical degradation, probably due to a cracked cell. Qualification tests will be completed early in October for the remaining modules under test.

Solar Technology Corporation delivered 15 modules late in September, for evaluation testing. These 15 were procured separately from the competitive bidding of the 46 and 130 kilowatt procurements. They will be tested in the same manner as other modules of the 46 kilowatt procurement.

Exploratory tests were initiated during this quarter. Eventually, these tests will include humidity/freezing, humidity/heating, rain/sun, high velocity rain, and salt fog. The humidity/freezing tests are under way and will be completed in early October.

In addition to the testing of late production modules described above, several other activities were undertaken during this quarter. Tests of 200 solar cells with a total of four different contact systems were started with the objective of evaluating each contact system in humidity. Electrical tests will be made before and after the 168 hours of humidity exposure, and the mechanical adherence of cell electrical contacts will be measured using a newly constructed tape puller. A number of module rejects from the Lewis Research Center have also been electrically tested and inspected, and extensive preparations have been made for the increased scope of testing activities for the 130 kilowatt procurement block modules.

130 Kilowatt Procurement Block

The module control and evaluation center at JPL in use at the beginning of this quarter would not accommodate the increased level of effort required for the 130 kilowatt procurement plus residual activity from the 46 kilowatt procurement. Construction of a second floor mezzanine has been started which will nearly double the working space. A decision to test all modules while installed in the 4 x 4-foot subarray frames caused the greatest impact on space requirements. Increased area is needed for test chambers. Rearrangements are under way to provide space for environmental chambers and fixtures.

Test planning for the quarter is summarized in OTP-01, "Environmental Test Plan for the 130 kW Procurement," published September 20, 1976. A number of new tests are being added for the modules of the 130 kilowatt procurement. Figures 5-7 and 5-8 show the qualification and exploratory test flows, respectively. The discussion below follows the test flow path of Fig. 5-7.

Electrical testing with the Large Area Pulsed Solar Simulator (LAPSS) is described in OTP-03. These electrical tests and physical inspection will be performed on all modules upon receipt. Electrical isolation tests will also

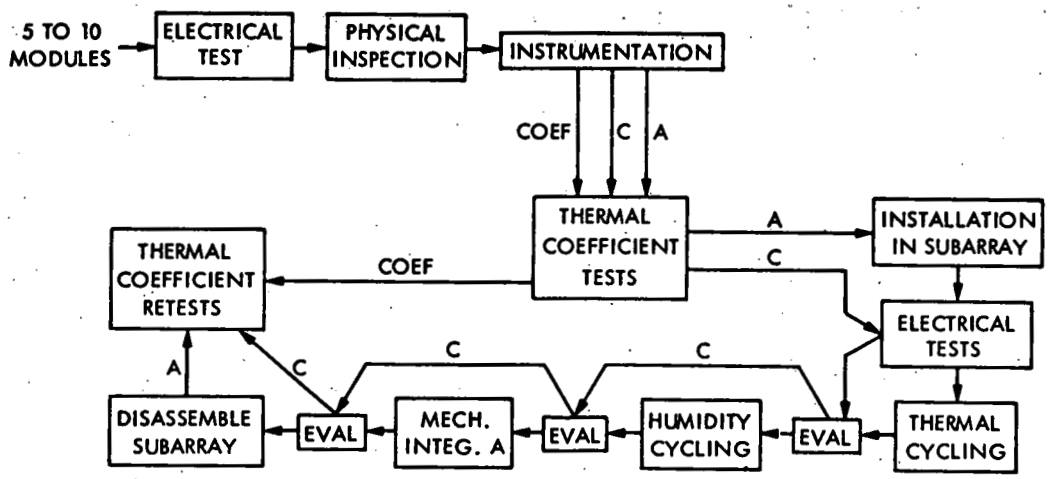

COEF SPECIALLY INSTRUMENTED TEMPERATURE COEFFICIENT TEST MODULE
C CONTROL MODULE
A SET A TEST MODULES (3 TO 8)
EVAL INSPECTION AND ELECTRICAL TEST (INCLUDES FLASH AND INSULATION)

Fig. 5-7. Test flow for Set A modules

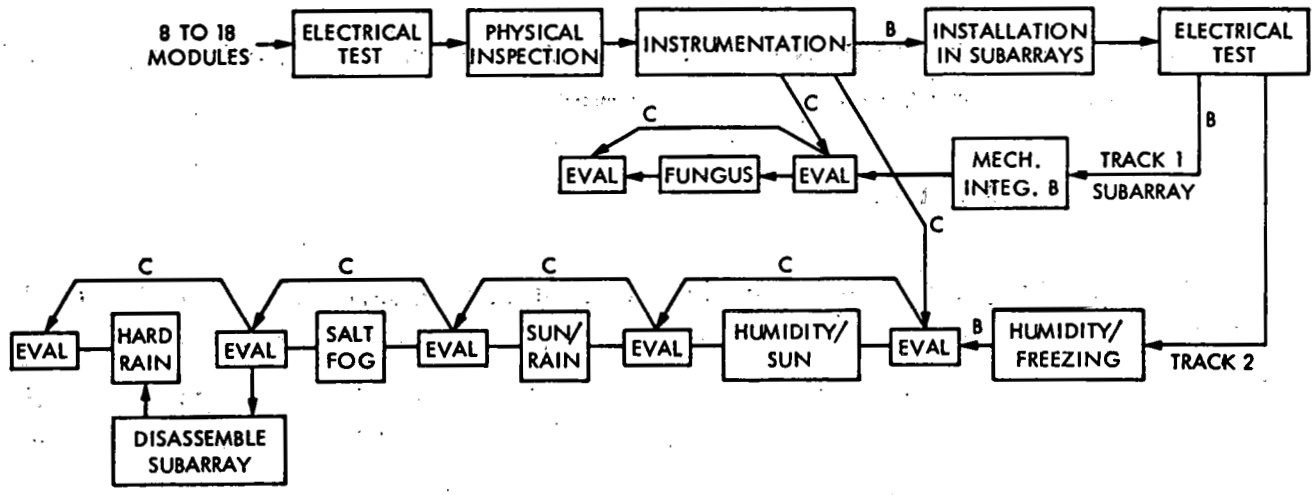

C CONTROL MODULE
B SET B TEST MODULES
EVAL INSPECTION AND ELECTRICAL TEST (INCLUDES FLASH AND INSULATION)

Fig. 5-8. Test flow for Set B modules

be made to verify compliance with the Design and Test Specification, 5-342-1, Rev. A. Two modules will be especially instrumented for thermal coefficient (hot box) tests. Then, the remaining modules will be tested in the hot box. The hot box has been built and will be checked out early in the next quarter.

A special subarray frame has been designed to provide stiff, equally distributed support for all modules in the 46-inch-square module subarray during test. The modules will be mounted in this subarray frame and retested electrically, using the temperature coefficients derived from hot box tests to extrapolate performance 60°C.

Each of the environmental tests required by 5-342-1A will be followed by electrical testing and inspection. Design and fabrication of a mechanical integrity (wind loading) test fixture is underway which will accommodate a complete subarray.

Other items of handling equipment for modules of the 130 kilowatt procurement are in design. These include an adjustable subarray inspection stand, a hand-operated subarray transporter, a support rack for automotive transport, and various other items needed for subarray handling and test.

Twenty Spectrolab prototype modules arrived on the last day of the quarter; qualification tests will start immediately.

b. Field Testing

During this quarter, progress was made in all aspects of the field testing activity. At the JPL Site, plans were finalized and construction started. The area was fenced off, underground data line conduits and utility lines were laid from Building 248 to the Site, post holes for the first 15 test stands were dug, and a concrete trench to carry the data wires from the modules to the trailer was constructed. These 15 stands will be sufficient to accommodate the 46 and 130 kilowatt procurements. Near the end of the quarter a 50-foot trailer was installed in the northwest corner of the Site. The trailer will house the data acquisition equipment, and will contain a working area and a demonstration room.

The first 16 4 x 8-foot test stands were ordered and obtained. Eight of these were installed at the JPL Site (Fig. 5-9) and four at the Table Mountain Site. The remaining four are due to be installed at the Goldstone Site early in the next quarter. The modules will be mounted on 4 x 4-foot frames and these in turn will be mounted on the stands. The plans call for a total of 240 modules from the 46 kilowatt procurement to be under life test in the field before the end of the next quarter.

The distribution will be as follows:

	JPL	Table Mountain	Goldstone
Solar Power	24	6	6
Spectrolab	36	18	18
Solarex	32	8	8
Sensor Tech	56	14	14

In terms of power, these quantities amount to about 1 kilowatt at JPL and about 0.3 kilowatt at the other two sites.

Progress was also made on the procurement of a data acquisition and processing system for the JPL Site. The data system will perform a daily electrical I-V interrogation of each module in order to continually monitor its condition. In addition, the system will have considerable flexibility and will be capable of interrogating selected modules on a more frequent basis. It will be capable of compiling programs for analyses of the modular data, and handle other types of data such as strain gage, thermocouple, and other diagnostic instrumentation. Along with the engineering data, weather data will be simultaneously obtained on a routine basis. A contract for the data system is expected to be awarded early in the next quarter, and the system is expected to be operational 8 months after that.

The method for monitoring the condition of the modules at the Table Mountain and Goldstone Sites is under evaluation. Two alternate approaches are being considered: One method would involve removing the modules and bringing them back to JPL for a LAPSS I-V interrogation every 4 to 8 weeks, and the other

Fig. 5-9. Stands being installed at JPL Site

method would entail taking portable I-V equipment to the sites at about the same frequency and obtaining the data in situ. The two methods will be investigated on a trial basis at the JPL Site during the next quarter, both to select the best technique and to obtain data on the JPL modules while awaiting the automated data system.

c. Performance and Failure Analysis

During the July-September period, the module problem/failure reporting system was implemented. The problem/failure reporting system for the LSSA

Project is patterned after the JPL flight project reporting system, streamlined to accommodate the specific needs of the Project. The goals of the system are:

1) To provide information to the LSSA Project organization on related engineering, test, and environmental test problems or failures.
2) To alert user application centers to testing problems, weaknesses, and corrective actions taken.
3) To feed back JPL test experience to the individual vendors on problems/failures and to understand and resolve problems/failures as production continues.
4) To provide a record of problems/failures in field application and test sites.
5) To provide overall summaries of problems/failures to measure the performance of each vendor product.

In the July-September period, the reporting was mainly centered on the JPL testing effort for the modules of the 46 kilowatt procurement. At present, no solar modules have been received from Lewis Research Center application sites, with the exception of reported voltage breakdown problems with metal substrate modules when attempting to obtain high voltage output (250 vdc). The voltage breakdown problem was studied in detail to ascertain the nature of such failures. The problems were found to be related to both design and workmanship. The workmanship problem, illustrated in Fig. 5-10, shows a sharp point of the interconnect mesh projecting down to the substrate.

The design problem was evidenced on a module which depends on encapsulant for insulation, and was related to inadequate insulation between the substrate and bottom of the solar cells. This was attributed to uneveness in the solder in the area where the interconnect attached to the bottom of the cell. The low insulation resistance allowed a path for a corona discharge to the substrate when the potential difference between the interconnect and the substrate became greater than about 200 volts. Figures 5-11 through 5-15 show details of the underside of the cell at the breakdown site and the corresponding substrate contact point. The following corrective action was instituted by the manufacturer:

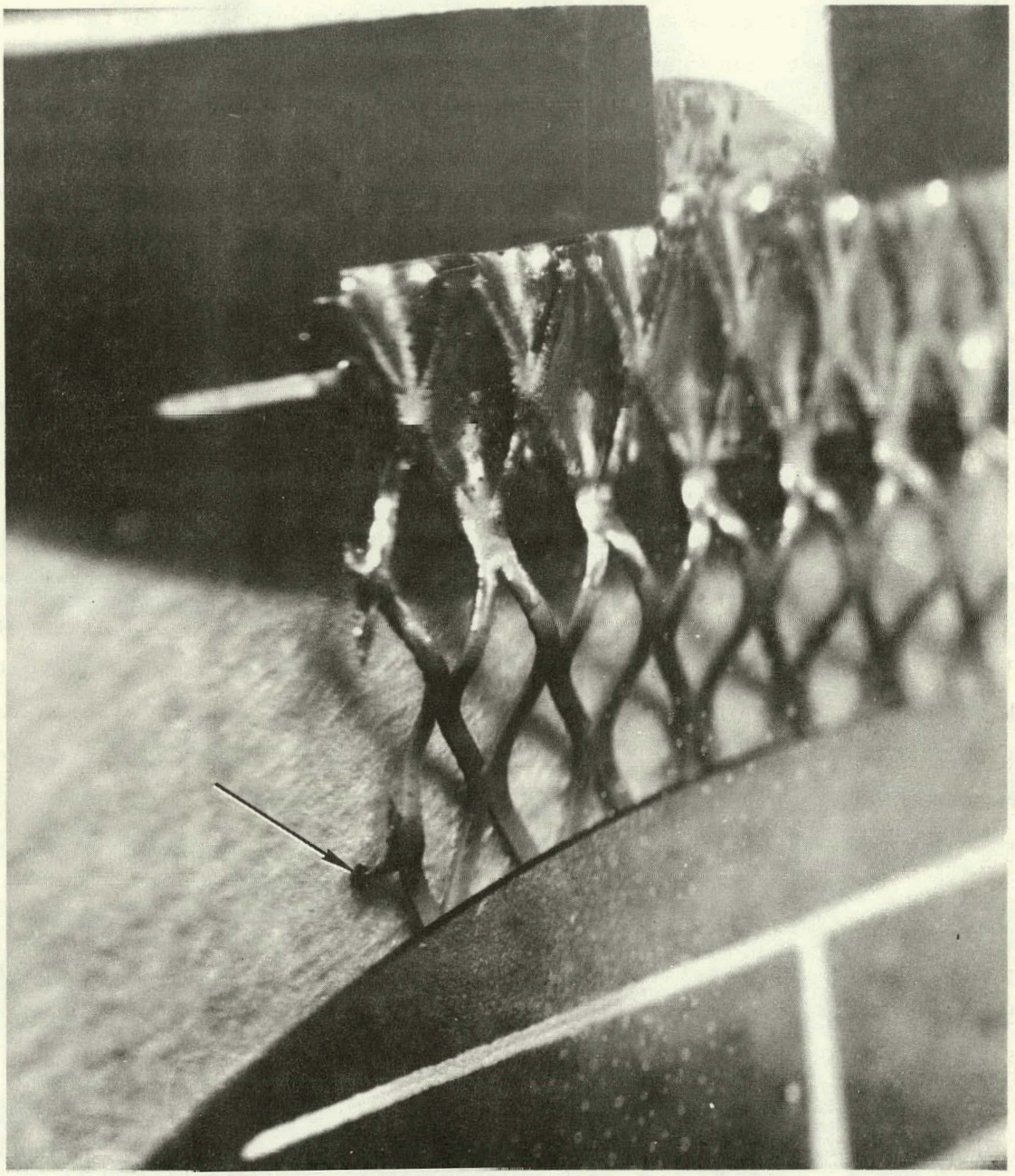

Fig. 5-10. Breakdown site between solar cell and substrate

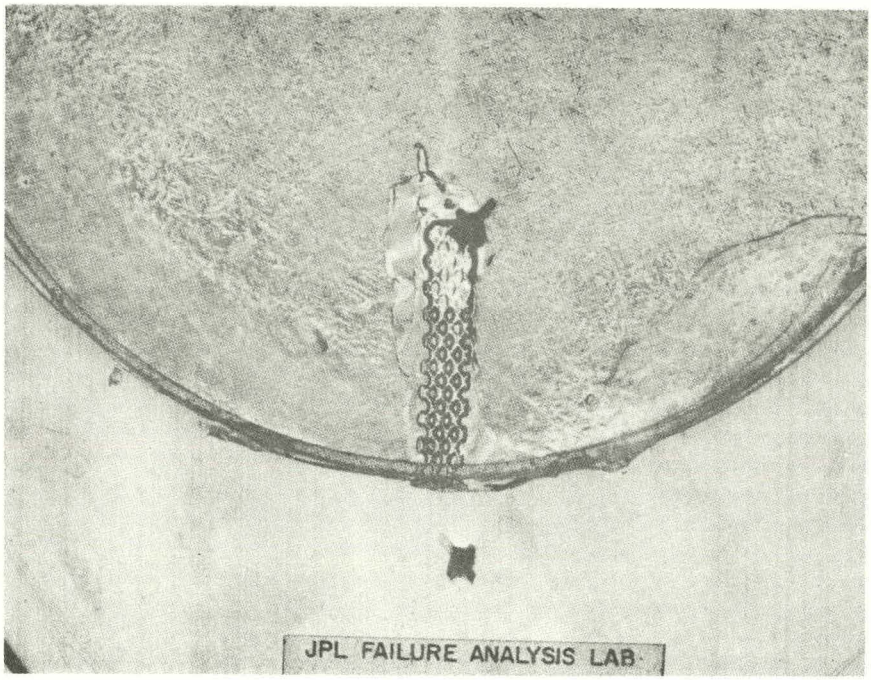

Fig. 5-11. Solar cell No. 16 from module assembly, S/N 13: Macrophoto showing breakdown site on back contact of cell 16 and the corresponding breakdown site on the aluminum substrate. The RTV615 coating is still on in this photo except in the lower right hand side of this cell.

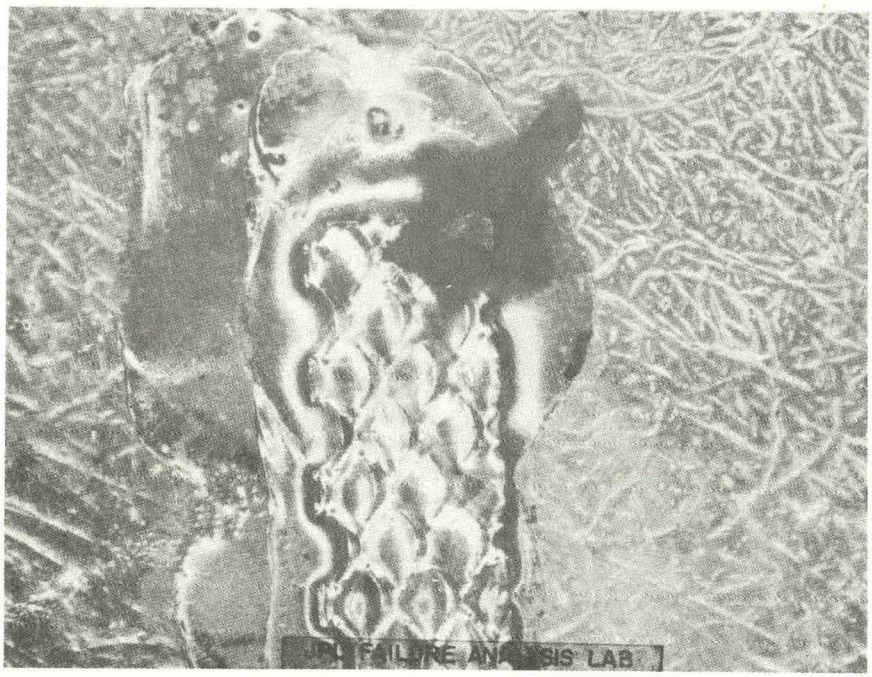

Fig. 5-12. Solar cell No. 16 from module assembly, S/N: Macrophoto showing closer view of breakdown site through the RTV615 coating on the back contact of cell 16.

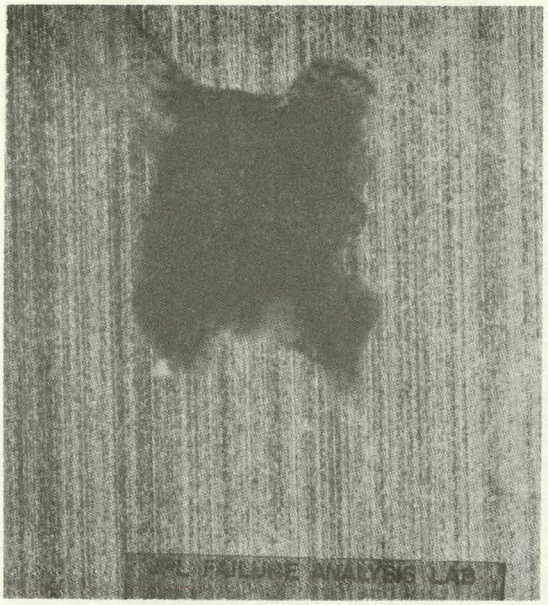

Fig. 5-13. Solar cell module assembly, S/N: Macrophoto showing closer view of corresponding breakdown site on the aluminum substrate.

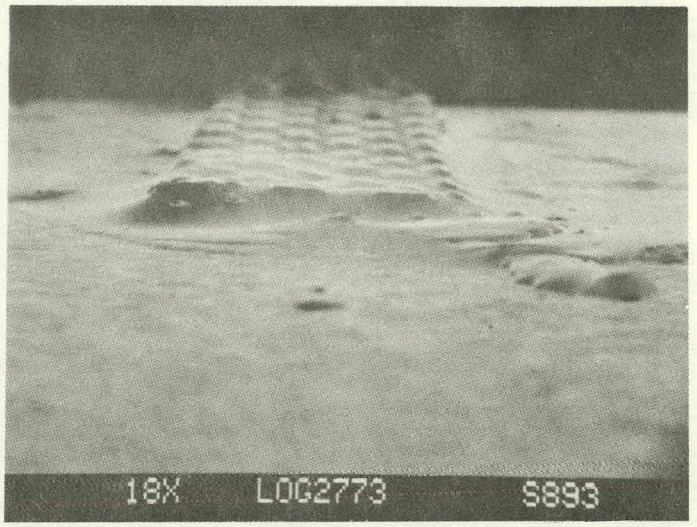

Fig. 5-14. Solar cell No. 16 from module assembly, S/N 13: SEM photo of breakdown site on back contact of cell 16. The RTV615 coating was removed in this photo.

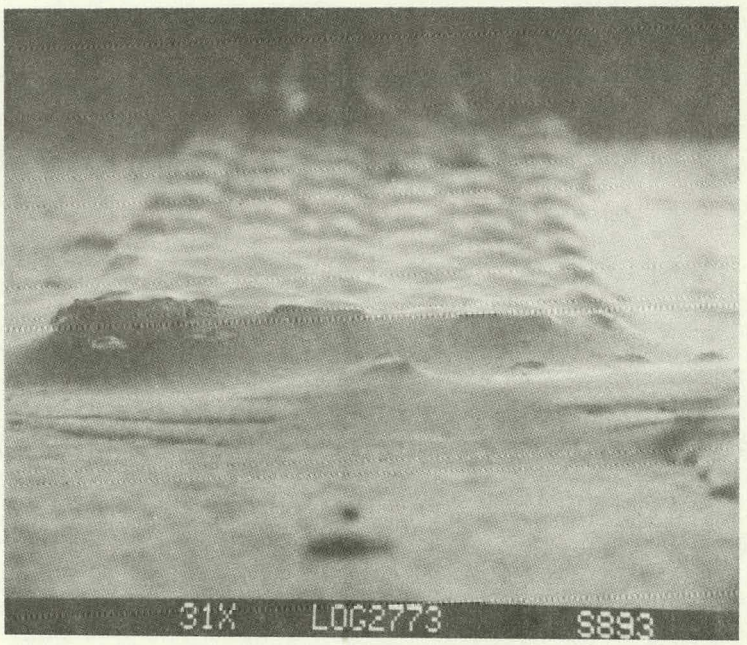

Fig. 5-15. Solar cell No. 16 from module assembly, S/N 13: SEM photo showing closer view of breakdown site on back contact of cell 16.

1) Doubled the insulation thickness beneath the cells.

2) Performed insulation resistance tests.

3) Improved the inspection criteria before final encapsulation.

The formal problem/failure reporting system was implemented in July. In the July/September period, 29 PFRs were initiated and 21 were closed. In addition, 40 PFRs were generated to cover all of the JPL environmental test problems that occurred prior to July in connection with the 46 kilowatt procurement. Verification and analysis are continuing on encapsulation delamination, solar cell discoloration, and the degradation of power output after environmental testing.

d. Performance Measurement Standardization

During this quarter, major emphasis was placed on a cooperative effort with Lewis Research Center (LeRC) directed toward assessing the experience gained in measuring the performance of modules of the 46 kilowatt procurement and toward the development of more stringent procedures for the 130 kilowatt procurement modules. This activity resulted in statements of agreement on "Standards for the Procurement and Evaluation of the ERDA 130 kW Solar Array Modules" and "Analysis of the Standardization and Measurement Process Used for the 45 kW Buy," jointly signed by Henry Brandhorst of LeRC and John Goldsmith of JPL. It was agreed that, in generating and maintaining standard cells, care should be taken to match the spectral response of the standard cells to that of the particular modules being measured and to characterize atmospheric conditions at the time of cell calibration. The process and schedule for generating standard cells for the 130 kilowatt procurement were formulated, and the areas of LeRC and JPL responsibilities were defined. Close coordination of LeRC, JPL, and manufacturers' efforts was seen to be essential; LeRC/JPL coordination meetings have been scheduled at intervals not exceeding 2 months to assure this result.

As a first step in the implementation of this plan, a "round robin" set of standard cell and module measurements was performed by LeRC and JPL. The results were generally encouraging, showing good agreement except for one solar power cell. At the first JPL/LeRC Standards and Calibration Meeting, conducted at

LeRC on September 16th, these data were reviewed and further intercomparisons of measurements were devised to resolve the remaining differences. At the same meeting, a technique of cell-to-module spectral matching based on red/blue ratios obtained from filtered xenon measurements was adopted for primary emphasis.

Standard cell fabrication and calibration are under way at LeRC, using cells procured by JPL from manufacturers of modules in the 130 kilowatt procurement. During the next quarter, standard cells for production measurements will be delivered by JPL to the manufacturers, and consultation on their proper use will be provided.

NASA—JPL—Coml., L.A., Calif.